

**Determination of Design and Operation Parameters  
for Upper Atmospheric Research Instrumentation  
to Yield Optimum Resolution with Deconvolution**

N93-25088

Unclass

G3/46 0157637

(NASA-CR-192833) DETERMINATION OF  
DESIGN AND OPERATION PARAMETERS FOR  
UPPER ATMOSPHERIC RESEARCH  
INSTRUMENTATION TO YIELD OPTIMUM  
RESOLUTION WITH DECONVOLUTION,  
APPENDIX 2 Final Report (New  
Orleans Univ.) 122 p

NASA Grant NAG 1-804

**FINAL REPORT**

**APPENDIX 2**

**Dr. George E. Ioup, Principal Investigator  
Dr. Juliette W. Ioup, Principal Investigator  
Department of Physics  
University of New Orleans  
New Orleans, LA 70148**

*10-1-77  
157637  
P.122*

**Determination of Design and Operation Parameters  
for Upper Atmospheric Research Instrumentation  
to Yield Optimum Resolution with Deconvolution**

**NASA Grant NAG 1-804**

**FINAL REPORT**

**APPENDIX 2**

**Dr. George E. Ioup, Principal Investigator  
Dr. Juliette W. Ioup, Principal Investigator  
Department of Physics  
University of New Orleans  
New Orleans, LA 70148**

Expanded Analysis of Combined Window Spectral  
Estimate Channel Clearing

Submitted to the Graduate Faculty of the  
University of New Orleans in Partial  
fulfillment of the Requirement for the degree of  
Master of Science  
in the  
Department of Physics

by

James Lester Kreamer

B.S., Northern Illinois University, 1980

August, 1988

## ACKNOWLEDGEMENT

The author gratefully acknowledges the patience and guidance of Dr. George Ioup in the completion of this thesis. I would also like to thank my wife, Kathy, and my children for all their support. My appreciation also is extended to my parents for being constant motivators. I am very grateful for the technical support provided by Fran Nash in generating the final draft. Finally, I would like to thank God for providing me the wisdom and knowledge necessary to complete this work.

## TABLE OF CONTENTS

	<u>PAGE</u>
List of Tables .....	iv
List of Figures .....	vi
Abstract .....	x
1. Introduction .....	1
2. Technical Background .....	4
3. Channel Clearing: Theoretical Background and Initial Results .....	13
4. Method and Algorithms for Calculations .....	17
5. Computational Results .....	20
6. Conclusions and Future Considerations .....	28
Tables .....	30
Figures .....	51
Bibliography .....	104
Appendix A .....	105
Vita .....	110

## LIST OF TABLES

TABLE 4.1...FUNCTION DOMAIN WINDOWS

TABLE 5.1...LARGE SPIKE IN CHANNEL 16 WITH HYBRID WINDOW  
USED FOR CLEARING CHANNEL 35 IN PRESENCE OF  
SPIKE IN CHANNEL 31

TABLE 5.2...LARGE SPIKE IN CHANNEL 16 WITH NEW HYBRID WINDOW  
APPLIED TO CLEAR CHANNEL 20

TABLE 5.3...20 PERCENT LAGS INPUT OF LARGE SPIKE IN CHANNEL  
31

TABLE 5.4...INPUT OF 20 PERCENT LAGS CHANNEL 31-CLEAR CHANNEL  
35 USING WINDOWS 1 AND 6

TABLE 5.5...INPUT OF 20 PERCENT LAGS CHANNEL 31-CLEAR CHANNEL  
35 USING WINDOWS 3 AND 7

TABLE 5.6...INPUT OF 20 PERCENT LAGS CHANNEL 31-CLEAR CHAN-  
NELS 33 AND 35 USING WINDOWS (1,6) AND (3,7)

TABLE 5.7...100 PERCENT LAGS INPUT OF LARGE SPIKE IN CHANNEL  
31

TABLE 5.8...HYBRID WINDOW COMBINATIONS FOR CLEARING CHANNEL  
36 IN PRESENCE OF SPIKE IN CHANNEL 31-100 PERCENT  
LAGS

TABLE 5.9...INPUT OF 100 PERCENT LAGS CHANNEL 31-CLEAR CHAN-  
NEL 35 USING WINDOWS 1 AND 6

TABLE 5.10...INPUT OF 100 PERCENT LAGS CHANNEL 31-CLEAR CHAN-  
NEL 35 USING WINDOWS 1 AND 7

TABLE 5.11...INPUT OF 100 PERCENT LAGS CHANNEL 31-CLEAR CHAN-  
NEL 35 USING WINDOWS 4 AND 5

TABLE 5.12...INPUT OF 100 PERCENT LAGS CHANNEL 31-CLEAR CHAN-  
NEL 35 USING WINDOWS 3 AND 8

TABLE 5.13...INPUT OF 100 PERCENT LAGS CHANNEL 31-CLEAR CHAN-  
NEL 35 USING WINDOWS 7 AND 10

TABLE 5.14...INPUT OF 100 PERCENT LAGS CHANNEL 31-CLEAR CHAN-  
NELS 35 AND 36 USING WINDOWS (3,8) AND (7,10)

TABLE 5.15...INPUT OF 100 PERCENT LAGS CHANNEL 31-CLEAR CHAN-  
NELS 35 AND 44 USING WINDOWS (1,6) AND (4,5)

TABLE 5.16..INPUT OF 100 PERCENT LAGS CHANNEL 31 AND SMALL  
PEAK IN CHANNEL 35-CLEAR CHANNELS 35 AND 44  
USING SAME WINDOW COMBINATION AS IN TABLE 5.15

TABLE 5.17..INPUT OF 100 PERCENT LAGS CHANNEL 31 AND SMALL  
PEAK IN CHANNEL 35-CLEAR CHANNELS 35 AND 44  
USING RECALCULATED WINDOWS (1,6) AND (4,5)

TABLE 5.18..INPUT OF 100 PERCENT LAGS CHANNEL 31-CLEAR CHAN-  
NELS 35,39, AND 44 USING WINDOWS (1,6), (4,5),  
AND (7,10)

TABLE 5.19..INPUT SMALL PERCENT LAGS SPIKES IN CHANNELS  
30,35, AND 40 WITH SMALL SPIKE IN 33-CLEAR  
CHANNEL 33 WITH WINDOW COMBINATION USED FOR  
TABLE 5.19

## LIST OF FIGURES

- FIG 1.1...AMPLITUDE PLOT WITH SINGLE SPIKE IN  
CHANNEL 31
- FIG 1.2...INVERSE FOURIER TRANSFORM OF FIG 1.1
- FIG 1.3...AMPLITUDE PLOT OF FOURIER TRANSFORM  
OF FIGURE 1.2
- FIG 3.1...AMPLITUDE PLOT OF LARGE SPIKE IN CHANNEL  
16 AND 1/20TH AMPLITUDE SPIKE IN CHANNEL  
20
- FIG 3.2...AMPLITUDE PLOT OF LARGE SPIKE IN CHANNEL  
16 AND 1/20TH AMPLITUDE SPIKE IN CHANNEL  
20 WITH A SINGLE WINDOW SCALED TO UNITY  
APPLIED
- FIG 4.1...FUNCTION DOMAIN RESPONSE OF WINDOW 1
- FIG 4.2...FUNCTION DOMAIN RESPONSE OF WINDOW 2
- FIG 4.3...FUNCTION DOMAIN RESPONSE OF WINDOW 3
- FIG 4.4...FUNCTION DOMAIN RESPONSE OF WINDOW 4
- FIG 4.5...FUNCTION DOMAIN RESPONSE OF WINDOW 5
- FIG 4.6...FUNCTION DOMAIN RESPONSE OF WINDOW 6
- FIG 4.7...FUNCTION DOMAIN RESPONSE OF WINDOW 7
- FIG 4.8...FUNCTION DOMAIN RESPONSE OF WINDOW 8
- FIG 4.9...FUNCTION DOMAIN RESPONSE OF WINDOW 9
- FIG 4.10...FUNCTION DOMAIN RESPONSE OF WINDOW 10
- FIG 4.11...FUNCTION DOMAIN RESPONSE OF WINDOW 11
- FIG 5.1...AMPLITUDE PLOT OF SPIKE IN CHANNEL 31  
ONLY-CLEAR CHANNEL 35 BY DUPLICATING  
SMITH'S(1985) WINDOW COMBINATION
- FIG 5.2...dB-DOWN PLOT OF FIGURE 5.1
- FIG 5.3...AMPLITUDE PLOT OF SPIKE IN CHANNEL 31  
AND 1/20TH SPIKE IN CHANNEL 35-CLEAR  
CHANNEL 35 USING SAME WINDOW COMBINATION  
AS FIG 5.1



FIG 5.4...dB-DOWN PLOT OF FIG 5.3

FIG 5.5...AMPLITUDE PLOT OF GAUSSIAN CENTERED IN  
CHANNEL 31-CLEAR CHANNELS 35 AND 36  
USING SMITH'S(1985) WINDOW COMBINATION

FIG 5.6...dB-DOWN PLOT OF FIG 5.5

FIG 5.7...AMPLITUDE PLOT OF GAUSSIAN IN CHANNEL 31  
WITH 1/20TH AMPLITUDE GAUSSIAN CENTERED  
IN CHANNEL 35-CLEAR CHANNEL 35 USING  
WINDOW COMBINATION OF FIG 5.5

FIG 5.8...dB-DOWN PLOT OF FIG 5.7

FIG 5.9...AMPLITUDE PLOT OF INPUT OF SPIKE IN CHAN-  
NEL 16-CLEAR CHANNEL 20 USING HYBRID USED  
TO CLEAR CHANNEL 35IN PRESENCE OF SPIKE  
IN CHANNEL 31

FIG 5.10...dB-DOWN PLOT OF FIG 5.9

FIG 5.11...AMPLITUDE PLOT OF INPUT OF SPIKE IN CHAN-  
NEL 16 WITH 1/20TH AMPLITUDE SPIKE IN  
CHANNEL 20-CLEAR CHANNEL 20 USING WINDOW  
COMBINATION OF FIG 5.9

FIG 5.12...dB-DOWN PLOT OF FIG 5.11

FIG 5.13...AMPLITUDE PLOT OF INPUT OF SPIKE IN CHAN-  
NEL 16-CLEAR CHANNEL 20 WITH RECALCULATED  
WINDOWS 3 AND 9

FIG 5.14...dB-DOWN PLOT OF FIG 5.13

FIG 5.15...FUNCTION DOMAIN WINDOW REPRESENTING 20  
PERCENT LAGS

FIG 5.16...FUNCTION DOMAIN WINDOW REPRESENTING 100  
PERCENT LAGS

FIG 5.17...AMPLITUDE PLOT OF 20 PERCENT LAGS INPUT  
OF SPIKE IN CHANNEL 31

FIG 5.18...dB-DOWN PLOT OF FIG 5.17

FIG 5.19...dB-DOWN PLOT OF 20 PERCENT LAGS CHANNEL  
31-CLEAR CHANNEL 35 USING WINDOWS 1 AND 6

FIG 5.20...dB-DOWN PLOT OF 20 PERCENT LAGS CHANNEL  
31 WITH 1/20TH SPIKE IN CHANNEL 35-CLEAR  
CHANNEL 35 USING WINDOW COMBINATION OF  
FIG 5.19

- FIG 5.21..dB-DOWN PLOT OF 20 PERCENT LAGS CHANNEL  
31-CLEAR CHANNEL 35 USING WINDOWS 3 AND 7
- FIG 5.22..dB-DOWN PLOT OF 20 PERCENT LAGS CHANNEL  
31 WITH 1/20TH SPIKE IN CHANNEL 35-CLEAR  
CHANNEL 35 USING WINDOW COMBINATION OF  
FIG 5.21
- FIG 5.23..dB-DOWN PLOT OF 20 PERCENT LAGS CHANNEL  
31 WITH 1/20TH SPIKE IN CHANNEL 35-CLEAR  
CHANNELS 33 AND 35 WITH WINDOWS (1,6)  
AND (3,7)
- FIG 5.24..AMPLITUDE PLOT OF 100 PERCENT LAGS INPUT  
OF SPIKE IN CHANNEL 31
- FIG 5.25..bB-DOWN PLOT OF FIG 5.24
- FIG 5.26..dB-DOWN PLOT OF 100 PERCENT LAGS CHANNEL  
31-CLEAR CHANNEL 35 USING WINDOWS 1 AND 6
- FIG 5.27..dB-DOWN PLOT OF 100 PERCENT LAGS CHANNEL  
31-CLEAR CHANNEL 35 USING WINDOWS 1 AND 7
- FIG 5.28..dB-DOWN PLOT OF 100 PERCENT LAGS CHANNEL  
31-CLEAR CHANNEL 35 USING WINDOWS 4 AND 5
- FIG 5.29..dB-DOWN PLOT OF 100 PERCENT LAGS CHANNEL  
31-CLEAR CHANNEL 35 USING WINDOWS 3 AND 8
- FIG 5.30..dB-DOWN PLOT OF 100 PERCENT LAGS CHANNEL  
31-CLEAR CHANNEL 35 USING WINDOWS 7 AND 10
- FIG 5.31..dB-DOWN PLOT OF 100 PERCENT LAGS CHANNEL  
31-CLEAR CHANNELS 35 AND 36 USING WINDOWS  
(3,8) AND (7,10)
- FIG 5.32..dB-DOWN PLOT OF 100 PERCENT LAGS CHANNEL  
31-CLEAR CHANNELS 35 AND 44 USING WINDOWS  
(1,6) and (4,5)
- FIG 5.33..dB-DOWN PLOT OF 100 PERCENT LAGS CHANNEL  
31 WITH 1/20TH SPIKE IN CHANNEL 35-CLEAR  
CHANNELS 35 AND 44 USING SAME COMBINATION  
USED FOR FIG 5.32
- FIG 5.34..dB-DOWN PLOT OF 100 PERCENT LAGS CHANNEL  
31 WITH 1/20TH SPIKE IN CHANNEL 35-CLEAR  
CHANNELS 35 AND 44 USING RECALCULATED  
COMBINATION OF WINDOWS (1,6) AND (4,5)

FIG 5.35..dB-DOWN PLOT OF 100 PERCENT LAGS CHANNEL  
31-CLEAR CHANNELS 35, 39, AND 44 USING  
WINDOWS (1,6), (4,5), AND (7,10)

FIG 5.36..dB-DOWN PLOT OF SMALL PERCENT OF LAGS  
CHANNELS 30, 35, AND 40-CLEAR CHANNEL  
33 USING WINDOWS 3 AND 8

FIG 5.37..dB-DOWN PLOT OF SMALL PERCENT OF LAGS  
CHANNELS 30, 35, AND 40 WITH 1/20TH  
AMPLITUDE SPIKE IN CHANNEL 33-CLEAR  
CHANNEL 33 USING WINDOW COMBINATION  
USED FOR FIG 5.36

## ABSTRACT

This thesis reviews the technique established to clear channels in the Power Spectral Estimate by applying linear combinations of well known window functions to the autocorrelation function. The need for windowing the autocorrelation function is due to the fact that the true autocorrelation is not generally used to obtain the Power Spectral Estimate. When applied, the windows serve to reduce the effect that modifies the autocorrelation by truncating the data and possibly the autocorrelation has on the Power Spectral Estimate.

It has been shown in previous work that a single channel has been cleared, allowing for the detection of a small peak in the presence of a large peak in the Power Spectral Estimate.

The utility of this method is dependent on the robustness of it on different input situations. We extend the analysis in this paper, to include clearing up to three channels. We examine the relative positions of the spikes to each other and also the effect of taking different percentages of lags of the autocorrelation in the Power Spectral Estimate.

This method could have application wherever the Power Spectrum is used. An example of this is beam forming for source location, where a small target can be located next to a large target. Other possibilities extend into seismic data processing. As the method becomes more automated other applications may present themselves.

## CHAPTER 1

### INTRODUCTION

Autocorrelation estimates are adversely effected when truncated data sets are used (Blackman and Tukey, 1958). To overcome the bias due to the data truncation, the autocorrelations are themselves often truncated, producing sidelobes around peaks and the corresponding power spectral estimates. Figures 1.1 thru 1.3 demonstrate this effect. Figure 1.1 is a power spectrum with a single spike residing in channel 31. When inverse Fourier transformed this spike produces a function domain time series shown in Figure 1.2. This function domain time series is modified by taking only a limited number of samples from the original series corresponding to the multiplication by a rectangular window. This modified or truncated time series is Fourier transformed so that we witness the effect of this modification (Figure 1.3). The spike remains prevalent in channel 31 but now the "ringing" sidelobes pervade throughout the spectrum. These side lobes can override and mask smaller peaks in the vicinity of the dominant peak. The application of windows also has the general effect of smoothing the power spectral estimate which may also have a deleterious effect on a small peak in the vicinity of a larger peak in the spectrum.

There has been much work done with the utilization of window functions to reduce the effects of truncation. Harris (1978) details the use of windows in harmonic analysis, and describes a number of variables with which to measure the performance of each. Specific application of these windows has been used to modify an autocorrelation

function prior to power spectral estimation. This technique is described by Blackman and Tukey (1958) and Robinson (1980). The autocorrelation being windowed is modified such that when transformed the effects of this modification are seen in the power spectrum. These effects are typically seen as reduced sidelobes associated with dominant peaks in the power spectrum. Still there remains sidelobes, although they are much smaller than when no window used.

Because of these effects, Smith (1985) developed a technique in which a linear combination of window functions were implemented to clear a single channel in the power spectral estimate. Although the technique was established, its implementation was limited to two input data situations, which will be reviewed. As a consequence, this thesis expands on the work done by Smith by examining the performance of this method on different input data sets. A review of the mathematical background and theory of the technique is given in order to establish a foundation for this work. To understand the procedures involved in utilizing this method, it is beneficial to understand the theory it is based on. In light of this, a review of the techniques and algorithms used in performing these calculations is presented. Finally, the input data and results of the calculations performed on these data are presented and analyzed.

This method has potential applicability in a number of fields which involve power spectral estimation. Among these is beam forming, where the objective is to locate a small target in the presence of a larger target. In seismic data processing we will, in future research, investigate the influence of a dominant signal in the power spectrum,

specifically 60 Hz noise. The purpose of this is to determine by channel clearing whether we can detect reflection signals near a dominant event such as 60 Hz noise.

The mathematical notations used in this paper will be similar to those Smith (1985) used in his work. The symbol  $w$  with or without subscripts will refer to a weighting function or a window in the function domain  $(t)$ . The Fourier transform of  $w(t)$  is represented by  $W(s)$  where  $(s)$  is the transform domain variable. Likewise, the function domain autocorrelation is represented by  $g(t)$  and its Fourier transform by  $G(s)$ .

## CHAPTER 2

## TECHNICAL BACKGROUND

In order to understand the need for channel clearing in the Power Spectral Estimate, we need to review the concept and purpose of the autocorrelation function and windows. Given a discrete input time series with  $M$  terms

$$(x(0), x(1), x(2), \dots, x(M-1))$$

where

$$x(j)=0 \text{ for } j<0 \text{ and } j>M-1,$$

the autocorrelation is defined as follows:

$$g(jT) = \sum_{k=0}^{M-j-1} x(k+j)x(k) \quad (1)$$

where  $j$  is a lag index and  $T$  is the sample increment. The autocorrelation function, as described by equation (1), is a shift, multiply and add operation which has the property of being non-negative definite (Robinson 1980). It is also commutative, which is expressed by the following equality:

$$\sum_{k=0}^{M-j-1} x(k+j)x(k) = \sum_{k=0}^{M-j-1} x(k)x(k-j) \quad (2)$$



We can show this easily by expanding the summation operation as follows. We write the input series

$$x(0) \ x(1) \ x(2) \ x(3) \ \dots\dots\dots x(m-1)$$

$$x(0) \ x(1) \ x(2) \ x(3) \ \dots\dots\dots x(m-1) \quad (3)$$

where in this case  $j=0$ , meaning there is no time shift or we are calculating the zero lag value of the autocorrelation. The result of applying (2) to (3) gives

$$g(0)=x^2(0)+x^2(1)+x^2(2)+x^2(3)+\dots\dots\dots x^2(m-1). \quad (4)$$

We recognize equation (4) as the total energy of the series given in (3), because by definition (Robinson (1980) the total energy of a signal is given by

$$E=\sum_{n=0}^{m-1} |x|^2. \quad (5)$$

The lag value will now be shifted by 2 units to the right.

$$x(0) \ x(1) \ x(2) \ x(3) \ \dots\dots\dots x(m-1) \quad (6a)$$

$$x(0) \ x(1) \ \dots\dots\dots x(m-3) \ x(m-2) \ x(m-1) \quad (6b)$$

or

$$g(2)=(x(0)x(2))+(x(1)x(3))+\dots(x(m-1)). \quad (7)$$

Similarly a shift of 2 units to the left yields

$$x(0) \ x(1) \ \dots\dots\dots x(m-3) \ x(m-2) \ x(m-2) \quad (8a)$$

$$x(0) \ x(1) \ x(2) \ x(3) \ \dots\dots\dots x(m-1) \quad (8b)$$

therefore

$$g(-2)=(x(2)x(0))+(x(3)x(1))+\dots(x(m-1)x(m-3)) \quad (9)$$

Now we can see from equations (7) and (9) that

$$g(-2)=g(2)$$

and in general,

$$g(j)=g(-j) \quad (10)$$

showing the autocorrelation function is symmetric about the zero lag ( $j=0$ ).

It was shown earlier that the zero lag value of the autocorrelation of a signal was equivalent to the total energy of the signal. Another quantity calculated from the autocorrelation is based on the interrelation of the autocorrelation function and the power spectral estimate and the effects windowing has on each. Bracewell (1978), through the use of the Autocorrelation Theorem and associated derivation, defines the relationship between the autocorrelation function and the power spectrum. These two quantities are Fourier transform pairs where the Fourier transform of a function  $f(x)$  is defined as

$$F(s) = \int_{-\infty}^{\infty} f(x) e^{-i2\pi s x} dx. \quad (11)$$

Similarly, the Fourier transform of  $F(s)$  is defined as

$$f(x) = \int_{-\infty}^{\infty} F(s) e^{i 2 \pi s x} ds. \quad (12)$$

The quantity given in equation 11 is the result of what Harris (1978) refers to as a decomposition of a signal over a basis set. The Fourier transform specifically decomposes the signal set  $(f(x))$  into the sums of sines and cosines. This complex arithmetic transform is defined for the discrete functions by the following:

$$F(s) = T/T(0) \sum f(x) \cos(2 \pi s x/M) - \quad (13)$$

$$i T/T(0) \sum f(x) \sin(2 \pi s x/M)$$

where

$M$  - the total number of samples

$T$  - the sample interval

$s$  - a multiple of the harmonic frequency counter, a multiple of  $1/T(0)$

$T(0)$  - the length of the data set

$x$  - the sample counter

$f(x)$  - input data samples

Using the Euler relation

$$e^{i\theta} = \cos\theta - i\sin\theta \quad (14)$$

we can rewrite equation 13 as

$$F(s) = \sum f(x) \exp(-2\pi s x / M). \quad (15)$$

A discussion of the applicability of equations 11 and 15 will be given later in this chapter. The sums in equation 13 are over the aforementioned basis set. Through this decomposition or Fourier transform we obtain a representation of the signal in terms of frequency based on the component of each monotonic cosine and sine. The  $f(x)$  and  $F(s)$  in equations 11 and 12 are referred to as Fourier transform pairs and are represented by the following notation

$$f(x) \supset F(s).$$

Therefore, in agreement with the notation given in the introduction, the Fourier pair, autocorrelation and power spectrum, are represented by the following.

$$g(x) \supset G(s).$$

The calculation of the Fourier transform as defined in equation 11 is for a continuous function of  $x$ , evaluated from minus infinity to plus infinity. Due to the reality of not being able to measure an infinite signal, we are confined to analyzing a finite data set. Also, we are not interested here in evaluating a continuous function but rather, a sampled function. The above discussion suggests the relationship between equations 11 and 15, i.e., equation 15 is the finite sampled function domain equivalent of equation 11. Brigham (1974) extensively discusses sampling theory as related to the Fourier transform and also discusses the algorithms developed for the Fast Fourier Transform, which is implemented in the work presented in this paper. Inherent in the transform of this sampled-finite data set, are artifacts of the numeric process. These artifacts of the transform process can cause the deleterious consequences shown in Figure 1.3. Specific to this, Harris

(1978) discusses the concept of spectral leakage. When sampling a finite data set with  $T$  sample interval, we obtain a total length  $nT$ , where  $n$  is the number of samples. If there are frequencies contained in the signal not contained in the basis set then these signals will not be periodic in the total sample interval. These signals which are not commensurate with the natural period exhibit discontinuities at their periodic extension. These discontinuities contribute to the spectral content of the signal calculated by the Fourier transform. The phenomenon just described is a particular case of Gibbs phenomenon (Bracewell 1978), which refers to the sidelobe or ripple effect in the function produced by the discontinuity in the transform. It is this behavior in the transform, due to truncation of the autocorrelation, which prompts us to perform windowing.

Because of the reasons stated above, Blackman and Tukey (1958) developed a technique whereby an autocorrelation function is modified by multiplying a weighting function in order to obtain a Power Spectral Estimate. This weighting function, which multiplies the autocorrelation in the function domain, is equivalent to the convolution of the Fourier transforms of the weighting function and the autocorrelation in the transform domain. The Fourier transform of the weighting function is called a window. The expression for the above relationship is the following:

$$W(s) = \int_{-\infty}^{\infty} w(x) \exp(-i2\pi sx) dx. \quad (16)$$

To avoid a convolution in the power spectral estimate calculation, Blackman and Tukey presented the method for windowing in the continuous case by multiplying the autocorrelation with the weighting function. The product of the above was then Fourier transformed to obtain the power spectral estimate. For the discrete case the convolution in the transform domain is not difficult. Therefore convolution of the window with the transform of the autocorrelation is an alternative. Robinson (1980) also elaborates on the above method. The specific methodology used in this work will be reviewed later.

A number of windows have been introduced in the literature (Geckinli and Yavuz 1983). Harris (1978) elaborates on several of these and presents quantitative measurements which measure the performance of each. Table 1 of Harris's paper lists these parameters. As with the truncated input autocorrelation, the windows themselves will exhibit spectral leakage. This leakage is measured in Harris's work by the peak sidelobe level and the asymptotic rate of falloff of the sidelobes. These quantities are illustrated in Harris's Figure 5. Though the ratings of these quantities given by Harris are a measure of the performance quality of the window, they may not accurately reflect the usefulness of the windows in this work. The sidelobes play a critical role in the work presented here, because through these we will be determining the proper combinations to clear channels in the power spectral estimate.



## CHAPTER 3

## CHANNEL CLEARING: THEORETICAL BACKGROUND AND INITIAL RESULTS

In 1985 Smith introduced the technique of channel clearing. This method is based on the ability to apply weighting functions alone or in linear combinations to the autocorrelation function in order to clear channels or domain segments in the power spectral estimate.

A specific problem as stated by Smith is the location of a small spike near a large spike in the power spectrum. In this case application of a window along with its sidelobes effect on the power spectrum has masked the smaller spike. Figure 3.1 shows the spectrum with a spike in channel 16 and a spike of 1/20th amplitude in channel 20. Figure 3.2 shows the same spectrum with a single window applied. The influence of the larger spike combined with the window has masked the smaller spike in channel 20. The idea behind the technique is to combine windows linearly and apply to the spectrum containing the large spike only in order to clear or bring to zero the channel in which the smaller spike resides. When this combination is established, it is applied to the spectrum which contains both spikes. Subsequent to this the smaller spike would be detected.

This combination of windows is called a hybrid window. We are allowed to make this construction because scalar addition and multiplication by a constant are preserved through the Fourier transform. This is shown in the following relationship

$$\sum a_i w_i(t) \supseteq \sum a_i W_i(s).$$

where  $a$  is a coefficient such that the sum of all  $a$ 's for a particular hybrid window equals unity. This normalization is recommended due to the fact that the zero lag of the autocorrelation is a maximum and amplification of this value can occur if the weighting is not normalized. Another result that is related to this normalization is that the hybrid window  $w(x)$  is bounded by the windows of which it is composed. A consequence of this bounding is that it prevents amplification in any of the sidelobes. The proof of this bounding is given in Smith's thesis (1985). This proof extends to the case where the hybrid window is constructed of  $n$  component windows. In this case an envelope is constructed with an upper limit window comprised of greatest components of all the input windows and a lower limit window comprised of the least magnitude components of the input windows. The analogy here results in the following statement: that for any  $x$  there are two component windows such that

$$w_l(x) \leq w_h(x) \leq w_u(x)$$

where  $u$  = the upper bound window,  $l$  = the lower bound window and

$$\sum_{i=1}^n a(i) = 1$$

and

$$0 \leq a(i) \leq 1.$$

The last property discussed in this section is the combination process and the use of hybrid windows as component windows in subsequent hybrid windows. It was shown that a linear combination of any number of windows, with normalized coefficients, produces a hybrid window. This hybrid window can be used in the construction of a new hybrid window, again with proper normalization of the coefficients. This property is important in the calculation of hybrid windows when attempting to clear more than one channel simultaneously. The technique used in determining the coefficients for the windows will demonstrate this.

The initial results of this technique showed that a single channel can be cleared within  $10^{-7}$  of the normalized peak value. The use of double precision may result in clearing within  $10^{-15}$ . The experiment was conducted by putting a unit spike in channel 31 and a spike of 1/20th amplitude in channel 35. The purpose of the experiment was to see if a combination of windows could be calculated to eliminate the effects of the spike in channel 31 at channel 35. A combination of three windows were used in order to eliminate channel 35 from the spectrum with only the spike in channel 31 present. Windows 3, 6 and 9 of Table 4.1 with respective coefficients of .0000016, .0000074, .9999910 were the choices. This hybrid window was then applied to the spectrum with the two spikes and clearly the spike in channel 35 was detected (Figure 5.3 and 5.4). The exact procedure for calculating the coefficients will be detailed in the next chapter.

The second experiment involved replacing the spikes with Gaussians centered at channels 31 and 35. Again the maximum amplitude of each was 1.0 and .05 respectively. The purpose of this experiment is to

attempt to clear a finite extent or more than one channel and to treat peaks which are not spikes in the power spectral estimate. In this experiment a combination of two hybrid window were used to clear channels 35 and 36. The final hybrid window was constructed from windows 2, 6 and 9 from Table 4.1. The respective coefficients were .3533488, .0501631, and .5965287. The clearing of channels 35 and 36 was successful (Figure 5.6). A similar result is achieved in this work and is shown in chapter 5.

## CHAPTER 4

## METHOD AND ALGORITHMS FOR CALCULATIONS

The method, at this time, is based on the assumption that we have some knowledge of the type of power spectral estimate and that portion relative to a large peak in which we need to consider the effects of windowing. For example, in the results reviewed in chapter 3 we set up the spectrum such that we knew channel 31 contained a dominant peak. We can model this response independently and design the appropriate hybrid windows to clear certain channels relative to the peak from the effect of this response.

The exact method employed here utilizes a combination of hand and computer calculation. The first step in the method involves creating the model spectrum. For example, in the first experiments we placed a unit spike in a channel. Upon the creation of the model input each window is scaled to unity and applied to the model data. This is done by a program of the type listed in Appendix 1. These windows are listed in Table 4.1 and graphically represented in Figures 4.1 thru 4.11. The numeric output is listed for each window result. The actual calculation by the algorithm is as follows:

- 1) Input window number (based on Table 4.1)
- 2) Input of coefficients
- 3) Algorithm multiplies windows by coefficients
- 4) Algorithm inverse Fourier Transform of input
- 5) Algorithm multiplies windows by inverse transformed input

# 6) Algorithm Fourier transform result to frequency domain.

The output represents the numeric value for each frequency domain channel. From this a certain channel will be selected to extinguish. This selection requires for the window combination that there is a negative and a positive result in that particular channel. This restriction is due to the fact we are limiting the value of the coefficients to being positive and less than unity (Smith 1985). With the window and the associated values in the specific channel chosen we can use the following formula to calculate the coefficients.

$$w(\text{hybrid}) = (1/(a(1)+a(2)))(a(1)W(2)+a(2)W(1)) \quad (17)$$

where

$$(1/(a(1)+a(2))) = \text{normalization.}$$

Therefore the coefficient applied to window

$W(1) = a(2)/(a(1)+a(2))$ , and for

$W(2) = a(1)/(a(1)+a(2))$ .

The following is a numeric example of this calculation. Suppose from the initial output we have values for channel 35 of -.0004536 and .0658214 from windows 1 and 2 respectively. Then in the formula  $a(1) = .0004536$  and  $a(2) = .0658214$ . These values can be inserted into equation 17. The normalization factor is equal to

$$1/ (.0004536 + .0658214) = 15.0886457.$$

Therefore the coefficient for window 1 is equal to

$$a(2)15.0886457 - (.0004536)(15.0886457) = .0068442$$

and for window 2 is equal to

$$a(1)15.0886457 - (.0658214)(15.0886457) = .9931558.$$

These coefficients can then be applied to a spectrum with a response in the channel cleared other than the response resulting from the model input. This hybrid window along with another hybrid window clearing the same channel may be utilized in the construction of new hybrid windows to extinguish further channels. We are able to do this because we know that for the first channel cleared there are zeroes or relatively small numbers resident in this channel. So when we add and then apply by multiplying these hybrid windows, the first channel will remain extinguished. The same process for clearing as outlined above, in which we can utilize the numeric output from the first hybrids to identify a channel with a positive and negative value, is used.

## CHAPTER 5

## COMPUTATIONAL RESULTS

The first experiment conducted was to duplicate the results obtained by Smith (1985) in his work, which was reviewed in Chapter 3. The purpose for this exercise was twofold. 1) The algorithm utilized by Smith was transported from a mainframe environment to a personal computer. The Fortran used by the two systems is different. As a consequence of this, some conversion was necessary. 2) The plots produced in the original work displayed the resultant Power Spectral Estimate with the normalized amplitude values from the calculation. In keeping with the literature, a dB-down representation of the results is generated for this work. We wanted to present Smith's results in this manner also.

Figure 5-1 duplicates the result of the window combination used to extinguish channel 35 with the unit spike in channel 31 only. Notice from this scale the extinction of channel 35 is not observable. The rescaling to dB-down (Figure 5.2) clearly shows the extinction at channel 35. Figures 5.3 and 5.4 show the results of the applied hybrid window to the spectrum consisting of spikes in both channels 31 and 35. The spike located in channel 35 is 1/20th the amplitude of the spike in channel 31. Restating the conclusions from the original results, it appears that the spike in channel 35 suffered no adverse effects generated by the spike in channel 31 subsequent to windowing.



Figures 5.5 through 5.8 duplicate the results for the Gaussian input introduced in chapter 3. The numeric objective in this experiment was to clear channels 35 and 36. Again in the amplitude plot of Figure 5.5, the extinction of these channels is not detectable. In Figure 5.6 channels 35 and 36 are obviously down from their adjacent channels. Figures 5.7 and 5.8 show the results of application of the same hybrid window to the two Gaussian input. Notice the increase of amplitude in channel 34 when comparing Figures 5.6 and 5.8. This increase in amplitude is attributed to the application of the hybrid window to clear 35 and 36 but not 34 and presence of the smaller Gaussian centered in channel 35.

As explained in the methodology in chapter 4, it is necessary to examine the actual numeric output in order to calculate the coefficients for the windows. In the subsequent experiments these lists of values will be given as tables.

The main purpose of the experimental work is to introduce new data input to this technique in order to examine the robustness thereof.

The first computation is to investigate, for the same magnitude input spikes used in the above, whether the channel clearing is affected by the location of the spikes in the spectrum. The first data set was constructed by placing the large spike in channel 16 and the smaller spike in channel 20. Application of the same scaled windows were applied to these data with the intent of clearing channel 20 from the effects of the spike in channel 16. The results are displayed in figures 5.9 through 5.12. From analyzing figure 5.10 it is evident that the extinction at channel 20 is not significant relative to its two

adjacent channels. This is borne out in the output run listed in table 5.1. Although the extinction was not as complete as it was in channel 31-35 case, the sidelobe level of the spike in channel 16 generated by the windowing did not mask the smaller spike in channel 20 (Figure 5.11 and 5.12). The technique was then applied to these same input data with windows 3 and 9 applied with respective coefficients of .000002279 and .999997736. Table 5.2 lists the results of the application of these windows to the input of a spike in channel 16 only. Comparing channels 19 through 21 in tables 5.1 and 5.2 demonstrates that the new calculated windows performed better. Figures 5.13 and 5.14 also show that channel 20 has been better cleared relative to its adjacent channels, but once again, it does not appear that the sidelobe effect of the spike in channel 16 is greatly influential out to channel 20. Because of this the application of the windows to the input of spikes in both channels 16 and 20 was not performed, knowing the smaller spike in 20 would be detectable.

The second experiment involves taking different percentages of possible lag values of the autocorrelation as represented in the input power spectral estimate. By placing spikes in the spectrum, as we have in the first experiments, we have represented an autocorrelation function from a very small percentage of total possible lags (re. Chapter 2). Typically in the use and application of the autocorrelation function a greater percentage of lags are used to represent the function. In this work we will examine the effect of taking 20 and 100 percent of the lags. The effect of taking different percentages of lags in itself is a type of windowing. Figures 5.15 and 5.16 show the function domain

weightings representing 20 and 100 percent lags respectively. These weightings are multiplied times the input similar to the other function domain windows to give the effect of using 20% or 100% of available lags.

The first analysis was performed with a single spike in channel 31 using 20 percent of the lags. Again the windows will be designed to extinguish channel 35. Figures 5.17 and 5.18 show the smoothing of the spectrum from a larger number lags. It should be noted here that, when adding the smaller spike to the spectrum, the smoothing effect of taking 20 percent of the lags is present as a result of the presence of the smaller spike also. Consequently, there is a larger effect in channel 35 (Table 5.3). The clearing of channel 35 was accomplished twice using two different combinations of windows. At this point, for the remaining analysis, the dB-down representations will only be shown with the exception of Figure 5.24. The first result used windows 1 and 6 (Table 4.1) with respective coefficients of .312745355 and .687254645. Figure 5.19 and Table 5.14 give the results of this calculation. The extinction of channel 35 was accomplished along with channel 27. It should be stated that the calculations were not intended to clear channel 27, but the clearing appears to be the result of symmetry. Figure 5.20 shows the result of applying the above window combination with the input consisting of the smaller spike in channel 35. The spike in channel 35 is now detectable apparently with the correct relative amplitude. The second combination of windows applied to this data set was 3 and 7 with respective coefficients of .450843611 and .549156389. Figures 5.21 and 5.22 along with Table 5.5 show a similar result as for window

combination 1 and 6. The last part of this experiment was to attempt to clear a channel closer to the main peak. The input is the 20 percent lags of the autocorrelation with the spectrum containing the large spike in channel 31 and the smaller spike in channel 35. In the previous part of this experiment two window combinations were given to clear channel 35. In order to clear the second channel the method of chapter 4 will be used in conjunction with the fact that the combination of existing hybrid windows can be used as a new hybrid window. An important aspect of methodology stems from this analysis and will be shown in detail in another experiment. It is important when calculating the coefficients for the extinction of the second channel that the presence of the other spike, which may be detected due to the clearing of the first channel, be taken into account. The two hybrid windows used consisted of windows 1, 6, 3 and 7 with coefficients .1325286, .291230213, .259794658, and .316446529 respectively. Figure 5.23 and Table 5.6 show that this combination cleared channel 33 and channel 35, resulting in the preservation of the small spike.

The second experiment involves the use of 100 percent of the lags of the input data. This input is shown in Figures 5.24, 5.25, and Table 5.7. The smoothing effect from using all the lags is greater. Because of this broadening of the main lobe, this data set was used more extensively in this analysis. It is felt that this broadening effect can better demonstrate the robustness of the method. The experiments performed this on this data set required the use of many different window combinations. Therefore, in like manner to the 20 percent lag case, several window combinations were used to clear a single channel.

Table 5.8 gives a list of window combinations and their respective coefficients which clear channel 35. This table also provides the Figure and Table numbers associated with the results of these calculations. The five window combinations utilized were all successful in clearing channel 35 to at least -70 db. The first four combinations show symmetry in their spectra. The fifth window combination is anomalous in this regard. This variability in symmetry should be investigated but was not in this analysis.

The second a part of this analysis was to clear two consecutive channels or in effect clear a small domain segment. For this we utilized the window combinations of (3,8) and (7,10). The coefficients are as follows:  $a(3)=-.201309972$ ,  $a(8)=-.193117857$ ,  $a(7)=-.494649063$ ,  $a(10)=-.110862395$ . Figure 5.31 and Table 5.14 demonstrate the successful results of this combination. The concept of clearing domain segments or successive channels has more importance in considering broad lobed input spectra (e.g. broad Gaussians, Smith 1985).

The third part of this analysis refers back to the first experiment. It demonstrates the importance of the methodology of the technique when clearing more than one channel after detecting an event in the first channel cleared. The combination of hybrid windows (1,6) and (4,5) will be used to clear channel 44 after clearing of channel 35. Figure 5.32 and Table 5.15 show the extinction of channels 35 and 44 in the presence of a spike in channel 31 with 100 percent of lags. The following coefficients were used:  $a(1)=-.517188658$ ,  $a(6)=-.007515903$ ,  $a(4)=-.307604029$ ,  $a(5)=-.16769141$ . Figure 5.33 and Table 5.16 show the results of using the same windows and coefficients applied to the input

spectrum including the smaller spike in channel 35. The presence of this spike has adversely affected the ability of these specific coefficients to clear channel 44. Recalculation of the coefficients, utilizing the same window combinations, produces the results shown in Figure 5.34 and Table 5.17. These recalculated coefficients are  $a(1)=-.5290774$ ,  $a(6)=-.007688673$ ,  $a(4)=-.29979798$ ,  $a(5)=-.163435915$ . This procedure has more importance as the second channel to be cleared comes nearer to the secondary peak. Also, the magnitude of the secondary peak influences this result proportionally. The next experiment extends this technique to clearing three channels simultaneously without the presence of a secondary or tertiary response in any of the previously cleared channels. The hybrid window combinations of (1,6) (4,5) (7,10) are used in this case with the following coefficients:

$$\begin{aligned}a(1) &= -.661751704 \\a(6) &= -.009616726 \\a(4) &= -.198866131 \\a(5) &= -.108412565 \\a(7) &= -.017443401 \\a(10) &= -.003909473\end{aligned}$$

Figure 5.35 and Table 5.18 show the success of clearing channels 35, 39, and 44. Any further extension of this to more channels or larger domain segments will necessitate the automation of the method. This is due to the number of computations to be made.

The last experiment considers three large spikes in the input spectrum at channels 30, 35, and 40. In this case we considered a small percentage of lags. Using windows 3 and 8 with respective coefficients .785292479 and .214707521, the attempt to clear channel 33 was made. Figure 5.36 and Table 5.19 show the extinction of channel 33 greater than -70 dB. Figure 5.37 and Table 5.20 show the results of the same window combination with a 1/20th amplitude spike placed in channel 33. The smaller spike is detected despite the proximity of the two large spikes.

## CHAPTER 6

## CONCLUSIONS AND FUTURE CONSIDERATIONS

The purpose for and technique of channel clearing, in the power spectral estimate by application of linearly combined window functions, has been reviewed. It has been established in previous work, that this method is effective in clearing up to two channels. This work extends the applicability of this method to different input data.

The first calculation demonstrated that the location of the spike in the input spectrum varied the result of channel clearing calculations relative to an equivalent valued spike used in the previous work. Part of this effect could be the result of the transform wrap-around.

The second investigation involved the use of varied percentages of lags relative to the input autocorrelation and its associated power spectral input. It was demonstrated that the effect of broadening the main lobe did not effect the channel clearing capabilities of the method. Several calculations were performed using the greater percentage lag input. It was shown that three channels could be cleared simultaneously. Two consecutive channels or a small domain segment were cleared. The importance of the methodology in the calculations was demonstrated by clearing two channels simultaneously with and without the presence of a smaller spike in the first channel cleared. The final calculation demonstrated the effectiveness of the technique when three large spikes are relatively close together. A single channel between two of the large spikes was cleared.



The method of channel clearing in the power spectral estimate needs further evaluation. Specific to this is the need to examine varying input data, different windows, more arithmetic precision and further clearing of more channels or larger domain segments. In light of the latter it is important that the technique become more automated. This automation could include the capability of channel marching, whereby each channel is cleared successively. Lastly, the implementation of this technique to solve real data situations needs to be investigated.

TABLE 4.1

WINDOW NUMBER	$w(x)$ for $-1/2 < x < +1/2$
1	1
2	$1 - 4x^2$
3	$\cos(\pi x)$
4	$\sin(2\pi x)/2\pi x$
5	$1 + 2 x $
6	$.5 + .5\cos(2\pi x)$
7	$.54 + .46\cos(2\pi x)$
8	$1 - 2 x \cos(2\pi x) + (1/\pi) \sin(2\pi x) $
9	$.42 + .5\cos(2\pi x) + .08\cos(4\pi x)$
10	$1 - 2 x $
11	$.5 + .5\cos(2\pi( x  - .15))/.7$

TABLE 5.1

CHANNEL	AMPLITUDE	CHANNEL	AMPLITUDE
1	0.0000000168	33	0.0000000013
2	0.0000000108	34	0.0000000088
3	0.0000000044	35	0.0000000253
4	-0.0000000199	36	0.0000000008
5	0.0000000009	37	0.0000000061
6	0.0000000029	38	0.0000000138
7	-0.000000017	39	0.0000000143
8	-0.0000000442	40	0.0000000207
9	-0.0000000046	41	-0.0000000074
10	-0.0000000176	42	0.0000000047
11	0.0000000126	43	0.0000000039
12	-0.0000000458	44	0.0000000121
13	0.0000000537	45	0.0000000048
14	0.079999164	46	0.0000000053
15	0.49999979	47	0.0000000133
16	0.8400017	48	-0.0000000037
17	0.49999982	49	0.0000000296
18	0.079999164	50	0.0000000596
19	0.0000001012	51	0.0000000447
20	0.0000000184	52	0.0000000075
21	0.0000000308	53	-0.0000000034
22	-0.0000000187	54	0.0000000006
23	0.0000000334	55	0.0000000173
24	0.0000000531	56	0.0000000086
25	0.0000000201	57	0.0000000068
26	0.0000000086	58	0.0000000138
27	0.0000000143	59	0.0000000102
28	0.0000000107	60	0.0000000103
29	0.0000000075	61	0.0000000187
30	-0.0000000085	62	-0.0000000102
31	-0.0000000024	63	0.0000000017
32	-0.0000000034	64	-0.0000000201

TABLE 5.2

CHANNEL	AMPLITUDE	CHANNEL	AMPLITUDE
1	0.0000000042	33	0.0000000033
2	-0.0000000003	34	-0.0000000119
3	0.000000001	35	0.0000000155
4	-0.0000000158	36	-0.0000000069
5	9.3563823E-11	37	0.0000000132
6	-0.0000000035	38	0.0000000119
7	-0.0000000124	39	0.0000000216
8	-0.0000000043	40	0.0000000132
9	0.0000000006	41	0.0000000066
10	-0.0000000174	42	-0.0000000004
11	0.0000000009	43	0.0000000079
12	-0.0000000006	44	0.0000000118
13	0.00000000751	45	0.0000000102
14	0.079999648	46	0.0000000046
15	0.49999976	47	0.0000000123
16	0.64000081	48	0
17	0.49999976	49	0.0000000298
18	0.079999611	50	0
19	0.0000001086	51	0.0000000298
20	0.0000000042	52	0.0000000186
21	0.0000000399	53	0.0000000021
22	-0.0000000152	54	0.0000000069
23	0.0000000415	55	0.0000000212
24	0.0000000408	56	0.0000000042
25	0.0000000204	57	0.0000000117
26	0.0000000044	58	0.0000000097
27	0.0000000016	59	-0.0000000013
28	0.0000000065	60	0.0000000147
29	-0.0000000057	61	0.0000000143
30	-0.0000000011	62	0.0000000019
31	-0.0000000135	63	-0.0000000091
32	0.0000000003	64	-0.0000000174

TABLE 5.3

CHANNEL	AMPLITUDE	CHANNEL	AMPLITUDE
1	0	33	0.0032585
2	0	34	0.0080555
3	0	35	0.0032575
4	0	36	0.0049645
5	0	37	0.0032585
6	0	38	0.0041285
7	0	39	0.0032575
8	0	40	0.0037895
9	0	41	0.0032575
10	0	42	0.0036195
11	0	43	0.0032585
12	0	44	0
13	0	45	0
14	0	46	0
15	0	47	0
16	0	48	0
17	0	49	0
18	0	50	0
19	0.0032585	51	0
20	0.0036195	52	0
21	0.0032575	53	0
22	0.0037895	54	0
23	0.0032575	55	0
24	0.0041285	56	0
25	0.0032585	57	0
26	0.0049645	58	0
27	0.0032575	59	0
28	0.0080555	60	0
29	0.0032585	61	0
30	0.0473235	62	0
31	1	63	0
32	0.0473235	64	0

TABLE 5.4

CHANNEL	AMPLITUDE	CHANNEL	AMPLITUDE
1	-0.0087503614	33	0.014556956
2	0.0087503623	34	0.02156426
3	-0.0087503213	35	0.0000000596
4	0.0087503623	36	0.017506585
5	-0.0087503539	37	-0.0013481798
6	0.008750366	38	0.016409133
7	-0.0087503577	39	-0.0017531442
8	0.0087503577	40	0.015963767
9	-0.0087503418	41	-0.0019281537
10	0.0087503688	42	0.015740924
11	-0.0087503558	43	-0.0032289964
12	0.0087503623	44	0.0098700784
13	-0.0087503716	45	-0.0087503511
14	0.0087503595	46	0.0087503549
15	-0.0087503456	47	-0.0087503772
16	0.0087503605	48	0.0087503623
17	-0.0087503577	49	-0.0087503707
18	0.0098700728	50	0.0087503605
19	-0.0032290181	51	-0.0087503623
20	0.015740927	52	0.0087503623
21	-0.001928166	53	-0.0087503614
22	0.015963722	54	0.0087503521
23	-0.0017533107	55	-0.0087503381
24	0.016409073	56	0.0087503679
25	-0.0013481884	57	-0.0087503623
26	0.017506564	58	0.0087503521
27	-0.0000000758	59	-0.0087503642
28	0.021564264	60	0.0087503688
29	0.014556956	61	-0.0087503502
30	0.41562104	62	0.0087503726
31	1.336518	63	-0.0087503688
32	0.41562104	64	0.0087503688

TABLE 5.5

CHANNEL	AMPLITUDE	CHANNEL	AMPLITUDE
1	-0.0015726413	33	-0.010477018
2	0.0015736328	34	0.027609587
3	-0.0015765488	35	0
4	0.0015815215	36	0.014808223
5	-0.0015885813	37	0.0026072514
6	0.0015980169	38	0.011388922
7	-0.0016099884	39	0.0038268473
8	0.0016247729	40	0.010008626
9	-0.0016428066	41	0.0042828671
10	0.0016647036	42	0.0093892235
11	-0.0016910387	43	0.0031106449
12	0.0017228881	44	0.0034286149
13	-0.0017615802	45	-0.0020691007
14	0.0018091003	46	0.0019359596
15	-0.001869089	47	-0.001854112
16	0.0019456677	48	0.0017926926
17	-0.0020815721	49	-0.0017436622
18	0.0034399191	50	0.0017033712
19	0.0031004637	51	-0.0016697475
20	0.0093984222	52	0.0016414967
21	0.0042746561	53	-0.0016175528
22	0.010015843	54	0.001597214
23	0.0038203243	55	-0.0015799081
24	0.011394353	56	0.0015652351
25	0.0028025657	57	-0.0015527973
26	0.01481205	58	0.0015423286
27	-0.0000031461	59	-0.001533656
28	0.027611868	60	0.0015265713
29	-0.010478545	61	-0.00152091
30	0.49984768	62	0.0015166529
31	1.2078092	63	-0.0015136404
32	0.49984694	64	0.0015118601

TABLE 5.6

CHANNEL	AMPLITUDE	CHANNEL	AMPLITUDE
1	-0.0048152702	33	-0.0000000021
2	0.0048158318	34	0.045683905
3	-0.0048175207	35	0.055507839
4	0.0048205	36	0.036541209
5	-0.0048246789	37	0.0011355346
6	0.0048302528	38	0.014625136
7	-0.0048373439	39	0.0014689919
8	0.004846076	40	0.013229766
9	-0.0048567597	41	0.0016927826
10	0.0048696799	42	0.01266754
11	-0.0048852339	43	0.0004212931
12	0.0049040862	44	0.0064487387
13	-0.0049268967	45	-0.0051310528
14	0.0049549919	46	0.0050476063
15	-0.0049903756	47	-0.0049959356
16	0.0050380644	48	0.0049571553
17	-0.0051163761	49	-0.0049262699
18	0.0064271176	50	0.0049009654
19	0.0004415293	51	-0.0048799003
20	0.012593273	52	0.0048622494
21	0.0017247929	53	-0.0048473151
22	0.013049007	54	0.0048346845
23	0.0015342634	55	-0.0048238523
24	0.014043696	56	0.0048148078
25	0.0011129705	57	-0.004807068
26	0.016499601	58	0.0048006219
27	0.0000582112	59	-0.0047951946
28	0.025635593	60	0.0047908537
29	0.0001712512	61	-0.0047873775
30	0.46480489	62	0.0047847191
31	1.2619438	63	-0.0047829049
32	0.46447843	64	0.0047817547



TABLE 5.7

CHANNEL	AMPLITUDE	CHANNEL	AMPLITUDE
1	0	33	0.0000915
2	0	34	0.0456595
3	0	35	0.0000935
4	0	36	0.0163905
5	0	37	0.0000945
6	0	38	0.0083305
7	0	39	0.0000955
8	0	40	0.0050195
9	0	41	0.0000965
10	0	42	0.0033475
11	0	43	0.0000975
12	0	44	0
13	0	45	0
14	0	46	0
15	0	47	0
16	0	48	0
17	0	49	0
18	0	50	0
19	0.0000975	51	0
20	0.0033475	52	0
21	0.0000965	53	0
22	0.0050195	54	0
23	0.0000955	55	0
24	0.0083305	56	0
25	0.0000945	57	0
26	0.0163905	58	0
27	0.0000935	59	0
28	0.0456595	60	0
29	0.0000915	61	0
30	0.4115925	62	0
31	1	63	0
32	0.4115925	64	0

TABLE 5.8

HYBRID WINDOW	WINDOW NUMBER	COEFFICIENT	FIGURE	TABLE
1	1	0.985675934	5.26	5.9
	6	0.014324066		
2	1	0.984430441	5.27	5.10
	7	0.015569559		
3	4	0.647184896	5.28	5.11
	5	0.352815104		
4	3	0.51030626	5.29	5.12
	8	0.48969374		
5	7	0.816911152	5.30	5.13
	10	0.183088848		

TABLE 5.9

CHANNEL	AMPLITUDE	CHANNEL	AMPLITUDE
1	-0.000630172	33	0.0028264243
2	0.000630194	34	0.091296464
3	-0.0006300242	35	-0.00000001788
4	0.0006301731	36	0.033177733
5	-0.0006301632	37	-0.0002654514
6	0.0006301354	38	0.017173227
7	-0.0006301847	39	-0.0003448348
8	0.0006301642	40	0.010598686
9	-0.0006301193	41	-0.0003786089
10	0.0006301703	42	0.00727861
11	-0.0006301042	43	-0.0004125431
12	0.0006301827	44	0.0006308775
13	-0.0006301479	45	-0.0006301322
14	0.0006301561	46	0.0006301564
15	-0.0006301106	47	-0.0006301673
16	0.0006301499	48	0.0006301616
17	-0.000630165	49	-0.0006301492
18	0.0006308669	50	0.0006301531
19	-0.000412513	51	-0.0006301033
20	0.0072785877	52	0.0006301809
21	-0.0003786093	53	-0.0006301597
22	0.010598592	54	0.0006301677
23	-0.0003450355	55	-0.0006301397
24	0.017173154	56	0.0006301698
25	-0.0002654459	57	-0.0006301646
26	0.03317773	58	0.0006301806
27	-0.0000001369	59	-0.0006301446
28	0.091296434	60	0.0006301526
29	0.0028264024	61	-0.0006301355
30	0.82508206	62	0.0006301415
31	1.990941	63	-0.0006300947
32	0.82508206	64	0.0006301437

TABLE 5.10

CHANNEL	AMPLITUDE	CHANNEL	AMPLITUDE
1	-0.0006301599	33	0.0028263982
2	0.0006301828	34	0.091296464
3	-0.000630054	35	-0.0000001192
4	0.0006301713	36	0.033177733
5	-0.0006301547	37	-0.0002654495
6	0.0006301391	38	0.017173231
7	-0.0006301939	39	-0.0003448291
8	0.0006301592	40	0.010598685
9	-0.0006301318	41	-0.0003786082
10	0.0006301683	42	0.0072786137
11	-0.0006300929	43	-0.0004125502
12	0.0006301932	44	0.0006308747
13	-0.0006301431	45	-0.0006301298
14	0.0006301478	46	0.000630154
15	-0.0006301464	47	-0.0006301718
16	0.0006301695	48	0.0006301422
17	-0.000630149	49	-0.0006301503
18	0.0006308607	50	0.0006301635
19	-0.0004125077	51	-0.0006300971
20	0.0072785863	52	0.0006301824
21	-0.0003786138	53	-0.0006301414
22	0.010598598	54	0.0006301624
23	-0.0003450263	55	-0.0006301602
24	0.017173145	56	0.0006301712
25	-0.0002654413	57	-0.0006301574
26	0.033177722	58	0.0006301671
27	-0.0000001421	59	-0.0006301196
28	0.091296449	60	0.0006301573
29	0.0028263789	61	-0.0006301436
30	0.82508206	62	0.0006301451
31	1.990941	63	-0.0006301208
32	0.82508206	64	0.0006301316

TABLE 5.11

CHANNEL	AMPLITUDE	CHANNEL	AMPLITUDE
1	-0.0008334196	33	0.030994404
2	0.0000694477	34	0.063495696
3	-0.0008376982	35	0
4	0.0000603489	36	0.022702038
5	-0.000851211	37	-0.0006930614
6	0.000041149	38	0.011676647
7	-0.0008749869	39	-0.0006569907
8	0.0000099249	40	0.0071865907
9	-0.0009114152	41	-0.0005918291
10	-0.0000371338	42	0.0049963323
11	-0.0009647381	43	-0.0008982156
12	-0.0001066394	44	-0.0006964591
13	-0.0010418404	45	-0.0013124065
14	-0.0002110194	46	-0.0003632295
15	-0.0011546231	47	-0.0011379927
16	-0.0003783755	48	-0.0001928792
17	-0.0013262827	49	-0.0010219279
18	-0.0007090171	50	-0.0000849636
19	-0.0009096047	51	-0.0009410232
20	0.0049861227	52	-0.000011332
21	-0.0006009785	53	-0.0008832853
22	0.0071784561	54	0.0000406222
23	-0.000664284	55	-0.0008414645
24	0.01167044	56	0.0000777696
25	-0.0006982649	57	-0.000811311
26	0.022697762	58	0.0001041191
27	-0.0000034742	59	-0.0007900024
28	0.063493118	60	0.0001222219
29	0.030992692	61	-0.0007757854
30	0.88186336	62	0.0001335811
31	1.9435923	63	-0.0007676826
32	0.88186419	64	0.0001390325

TABLE 5.12

CHANNEL	AMPLITUDE	CHANNEL	AMPLITUDE
1	-0.0006275484	33	-0.0041795401
2	0.0006295493	34	0.10816383
3	-0.0006271469	35	0.0000001192
4	0.0006292728	36	0.034976363
5	-0.0006263803	37	-0.0001949549
6	0.0006283546	38	0.017589815
7	-0.0006246361	39	-0.0003095506
8	0.000626748	40	0.010751481
9	-0.0006214118	41	-0.0003990322
10	0.0006237291	42	0.0073398859
11	-0.0006154042	43	-0.0003448787
12	0.0006179126	44	0.0005664784
13	-0.0006037591	45	-0.0005002396
14	0.0006057019	46	0.0005773117
15	-0.0005778007	47	-0.000577857
16	0.0005774596	48	0.0006055641
17	-0.0005003061	49	-0.0006037398
18	0.0005665833	50	0.00061777
19	-0.0003449189	51	-0.0006154683
20	0.0073399711	52	0.0006236124
21	-0.0003990874	53	-0.0006214893
22	0.01075148	54	0.0006266517
23	-0.000309806	55	-0.000624793
24	0.017589815	56	0.0006283118
25	-0.0001949752	57	-0.0006267225
26	0.034976389	58	0.0006292514
27	-0.0000001007	59	-0.0006278249
28	0.10816382	60	0.0006297429
29	-0.0041795578	61	-0.0006284985
30	0.80595249	62	0.000630028
31	2.0041552	63	-0.0006287869
32	0.80595243	64	0.0006302231

TABLE 5.13

CHANNEL	AMPLITUDE	CHANNEL	AMPLITUDE
1	-0.01612797	33	0.30148342
2	-0.013706565	34	0.07438153
3	-0.0089507475	35	0
4	-0.006047863	36	-0.022786975
5	-0.0080551067	37	-0.01013279
6	-0.012974271	38	0.01270414
7	-0.016506637	39	0.020290535
8	-0.01492344	40	0.0096400874
9	-0.0096571175	41	-0.01097194
10	-0.0052116001	42	-0.023223832
11	-0.0061881421	43	-0.021978475
12	-0.011894779	44	-0.0098132491
13	-0.017562045	45	0.001688648
14	-0.017429573	46	0.0017857002
15	-0.011094769	47	-0.0087619368
16	-0.003588052	48	-0.020197598
17	-0.0021740822	49	-0.023196142
18	-0.0089588314	50	-0.015668012
19	-0.017194647	51	-0.0048406716
20	-0.018569034	52	0.0002371874
21	-0.010338039	53	-0.0046547656
22	0.0057766885	54	-0.014672683
23	0.015224451	55	-0.021393139
24	0.010702341	56	-0.019007541
25	-0.0074134166	57	-0.010122581
26	-0.017665148	58	-0.0022388194
27	0.0032037748	59	-0.002312514
28	0.072982423	60	-0.0098404614
29	0.29667765	61	-0.018509429
30	1.0420661	62	-0.020614322
31	1.618788	63	-0.014695399
32	1.0462196	64	-0.0056453291

TABLE 5.14

CHANNEL	AMPLITUDE	CHANNEL	AMPLITUDE
1	-0.010013235	33	0.18090288
2	-0.0080511672	34	0.087708324
3	-0.0056672352	35	-0.0000000596
4	-0.0034138164	36	-0.0000000298
5	-0.0051245769	37	-0.0062124208
6	-0.0076082028	38	0.01463151
7	-0.010241373	39	0.012164063
8	-0.0087890709	40	0.010078562
9	-0.0060926247	41	-0.0068010194
10	-0.0029096408	42	-0.01116678
11	-0.0039897766	43	-0.013444284
12	-0.0069586877	44	-0.0057185646
13	-0.010872209	45	0.0008251369
14	-0.01031487	46	0.0013090034
15	-0.0069459821	47	-0.0055334438
16	-0.0019447953	48	-0.01199099
17	-0.0015138001	49	-0.014283719
18	-0.0052011646	50	-0.0092434743
19	-0.01054764	51	-0.0031738635
20	-0.0083482042	52	0.0003896314
21	-0.0064172242	53	-0.0030636846
22	0.0077392296	54	-0.0086372625
23	0.009096385	55	-0.013200269
24	0.013419379	56	-0.011261439
25	-0.0045658275	57	-0.0063766045
26	0.0031013507	58	-0.0011074292
27	0.001939863	59	-0.0016479371
28	0.086861067	60	-0.0057100602
29	0.17799297	61	-0.011455595
30	0.94892192	62	-0.012233658
31	1.7708108	63	-0.009146275
32	0.951437	64	-0.0031696965



TABLE 5.15

CHANNEL	AMPLITUDE	CHANNEL	AMPLITUDE
1	-0.0007267897	33	0.016214548
2	0.0003636213	34	0.078082889
3	-0.0007288065	35	0.0000000596
4	0.000359321	36	0.028198689
5	-0.0007352171	37	-0.0004686741
6	0.0003502349	38	0.014560707
7	-0.0007465136	39	-0.0004932102
8	0.0003353361	40	0.0089769382
9	-0.0007638502	41	-0.0004799398
10	0.0003129798	42	0.006193867
11	-0.0007891749	43	-0.0006433618
12	0.0002799801	44	0.0000000065
13	-0.0008258244	45	-0.0009544246
14	0.0002303424	46	0.0001579961
15	-0.0008794409	47	-0.0008715394
16	0.0001508033	48	0.0002389747
17	-0.0009610341	49	-0.0008163354
18	-0.0000059596	50	0.0002902792
19	-0.0006487506	51	-0.0007779046
20	0.0061890148	52	0.0003252768
21	-0.0004842821	53	-0.0007504617
22	0.0089730266	54	0.0003499581
23	-0.0004967653	55	-0.0007305867
24	0.01455773	56	0.000367618
25	-0.0004711586	57	-0.0007162648
26	0.02819664	58	0.0003801139
27	-0.0000016817	59	-0.0007061326
28	0.078081675	60	0.0003887031
29	0.016213726	61	-0.0006994074
30	0.85206997	62	0.0003940842
31	1.9684365	63	-0.0006955029
32	0.85207033	64	0.0003967483

TABLE 5.16

CHANNEL	AMPLITUDE	CHANNEL	AMPLITUDE
1	-0.0007717316	33	0.017002968
2	0.0003937155	34	0.12062502
3	-0.0007738003	35	0.098383486
4	0.0003893094	36	0.070738912
5	-0.0007804257	37	0.0003068298
6	0.0003798906	38	0.018410794
7	-0.0007920204	39	-0.0005344908
8	0.0003645715	40	0.010318644
9	-0.0008099162	41	-0.0005498171
10	0.0003415833	42	0.0068389936
11	-0.0008359729	43	-0.0007362581
12	0.0003076236	44	-0.0000175606
13	-0.0008735884	45	-0.0010287495
14	0.0002566777	46	0.0001623952
15	-0.0009285968	47	-0.0009356655
16	0.0001751472	48	0.0002527031
17	-0.0010121401	49	-0.0008743219
18	0.0000147671	50	0.00030931
19	-0.0006910345	51	-0.0008320084
20	0.0063565653	52	0.0003476706
21	-0.0005224662	53	-0.000801898
22	0.0091902679	54	0.0003746022
23	-0.0005352072	55	-0.0007801768
24	0.014859481	56	0.000393806
25	-0.0005119497	57	-0.0007646617
26	0.028640091	58	0.000407364
27	-0.0000409718	59	-0.000753648
28	0.07880754	60	0.0004166873
29	0.016175929	61	-0.0007463881
30	0.85347605	62	0.0004224689
31	1.9684162	63	-0.0007421259
32	0.85596037	64	0.0004253136

TABLE 5.17

CHANNEL	AMPLITUDE	CHANNEL	AMPLITUDE
1	-0.0007692082	33	0.016646266
2	0.000400869	34	0.12092602
3	-0.000771243	35	0.098412037
4	0.0003965298	36	0.070831031
5	-0.0007777035	37	0.0002950793
6	0.0003873242	38	0.018493826
7	-0.0007890451	39	-0.0005306772
8	0.0003724316	40	0.010366028
9	-0.0008064367	41	-0.0005469068
10	0.00035002	42	0.0068696984
11	-0.0008317996	43	-0.0007297598
12	0.000316902	44	-0.0000000289
13	-0.0008685358	45	-0.0010197775
14	0.0002672436	46	0.0001753429
15	-0.0009220879	47	-0.0009290504
16	0.0001877873	48	0.0002633152
17	-0.0010035612	49	-0.0008692722
18	0.0000314856	50	0.0003185329
19	-0.000684932	51	-0.00082797
20	0.0063850107	52	0.0003559383
21	-0.0005197326	53	-0.0007986321
22	0.0092325676	54	0.0003822021
23	-0.0005312714	55	-0.0007774544
24	0.014927295	56	0.0004009211
25	-0.0005066058	57	-0.0007623264
26	0.02876861	58	0.0004141744
27	-0.0000407096	59	-0.0007515688
28	0.079146251	60	0.0004232136
29	0.015836433	61	-0.0007444961
30	0.85279739	62	0.000428871
31	1.968987	63	-0.0007403872
32	0.85529232	64	0.0004316319

TABLE S.18

CHANNEL	AMPLITUDE	CHANNEL	AMPLITUDE
1	-0.0010235459	33	0.017859034
2	0.0001317812	34	0.082392663
3	-0.0008715268	35	0
4	0.0003125338	36	0.028763741
5	-0.0008565909	37	-0.0006075463
6	0.0001587073	38	0.015388817
7	-0.0010444112	39	-0.0000001227
8	0.0001074481	40	0.009529734
9	-0.0009093343	41	-0.0006703536
10	0.00030038	42	0.0059259632
11	-0.0008516007	43	-0.001022293
12	0.0001363355	44	-0.0000000149
13	-0.0011182111	45	-0.0007902887
14	-0.0000139704	46	0.0003495659
15	-0.0010147353	47	-0.0009598439
16	0.0002301898	48	-0.000067477
17	-0.0008770221	49	-0.0012323714
18	0.0000143998	50	0.000062424
19	-0.000923537	51	-0.0008154805
20	0.0060222498	52	0.0004247015
21	-0.0006596057	53	-0.000793864
22	0.0094446745	54	0.0001222414
23	-0.0001106963	55	-0.001138442
24	0.015344099	56	0.0000411073
25	-0.0005510989	57	-0.0008885158
26	0.028871795	58	0.0004072865
27	0.0000672724	59	-0.0007151581
28	0.082362019	60	0.0002504764
29	0.017755866	61	-0.0010566916
30	0.84716296	62	0.0000239295
31	1.9684452	63	-0.0009726973
32	0.84725189	64	0.0003452739

TABLE 5.19

CHANNEL	AMPLITUDE	CHANNEL	AMPLITUDE
1	0.014027503	33	-0.0000000121
2	-0.014028227	34	0.1903618
3	0.014034309	35	1.6371415
4	-0.014041785	36	0.19035983
5	0.014055185	37	0.0000033304
6	-0.014070335	38	-0.03625989
7	0.014092386	39	0.22756466
8	-0.014116675	40	1.5972935
9	0.014149866	41	0.23479062
10	-0.01418641	42	-0.057561494
11	0.014234834	43	0.039812744
12	-0.014288335	44	-0.026918059
13	0.014359378	45	0.02237111
14	-0.014438513	46	-0.019405698
15	0.014545067	47	0.017918076
16	-0.014665774	48	-0.016825864
17	0.014832503	49	0.016180804
18	-0.01502596	50	-0.01567018
19	0.015304765	51	0.015338654
20	-0.015639521	52	-0.015063119
21	0.01615287	53	0.014873258
22	-0.016800832	54	-0.014710286
23	0.017895328	55	0.014594066
24	-0.019385239	56	-0.014492093
25	0.022352934	57	0.014418321
26	-0.026902139	58	-0.014352719
27	0.039798617	59	0.01430596
28	-0.057549331	60	-0.014264372
29	0.23478037	61	0.014236153
30	1.597302	62	-0.01421174
31	0.2275579	63	0.014198057
32	-0.036255151	64	-0.014187049

TABLE 5.20

CHANNEL	AMPLITUDE	CHANNEL	AMPLITUDE
1	0.013326434	33	0.07948482
2	-0.013327075	34	0.20233938
3	0.013332912	35	1.6340945
4	-0.01334006	36	0.19246924
5	0.013352912	37	-0.0014325902
6	-0.013367363	38	-0.035073802
7	0.013388529	39	0.226541
8	-0.013411701	40	1.5982311
9	0.013443629	41	0.23391546
10	-0.013478592	42	-0.056725346
11	0.01352516	43	0.039006829
12	-0.013576454	44	-0.026132951
13	0.013644673	45	0.021602863
14	-0.013720875	46	-0.018649761
15	0.013823727	47	0.017172426
16	-0.013939913	48	-0.01608807
17	0.014101386	49	0.015449688
18	-0.014268158	50	-0.01494433
19	0.014559092	51	0.014617335
20	-0.014863511	52	-0.014345434
21	0.015384625	53	0.014158753
22	-0.016015731	54	-0.013998368
23	0.017089425	55	0.013884398
24	-0.018549023	56	-0.013784283
25	0.021477759	57	0.013712084
26	-0.025964499	58	-0.013647805
27	0.038774937	59	0.013602111
28	-0.056363199	60	-0.013561386
29	0.23334444	61	0.013533884
30	1.5994115	62	-0.013510015
31	0.22451079	63	0.013496719
32	-0.024277404	64	-0.013485905

FIGURE 1.1

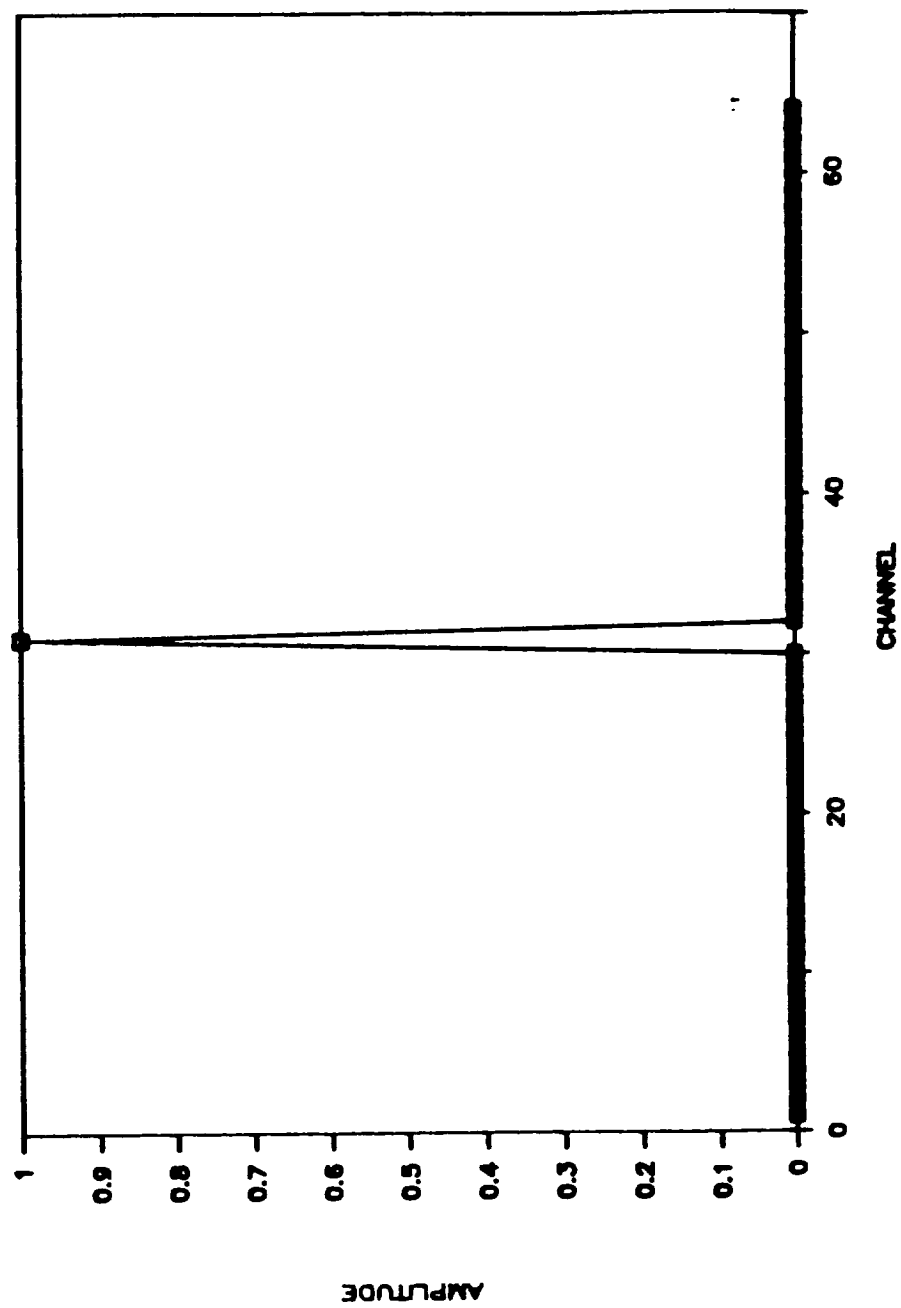


FIGURE 1.2

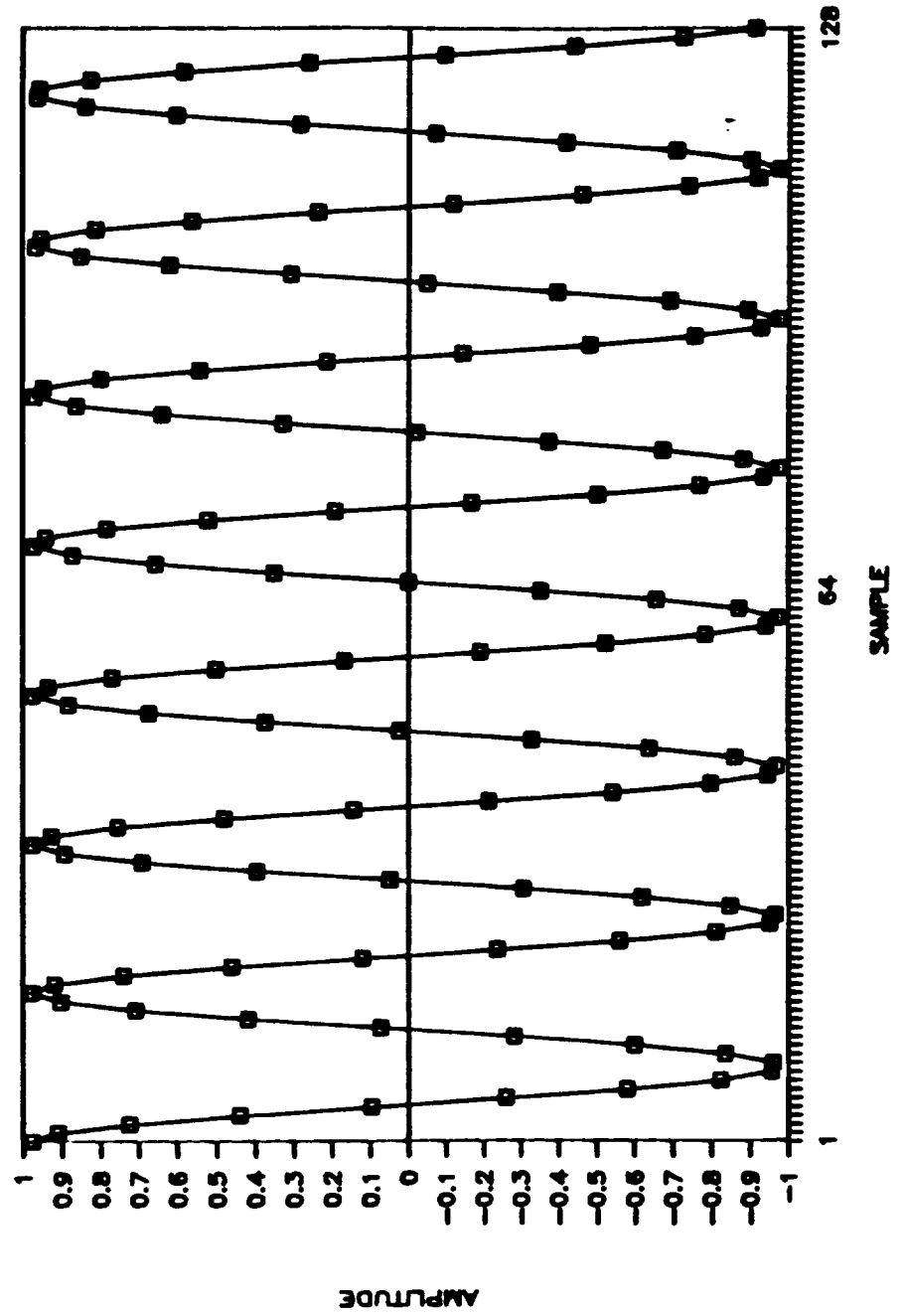
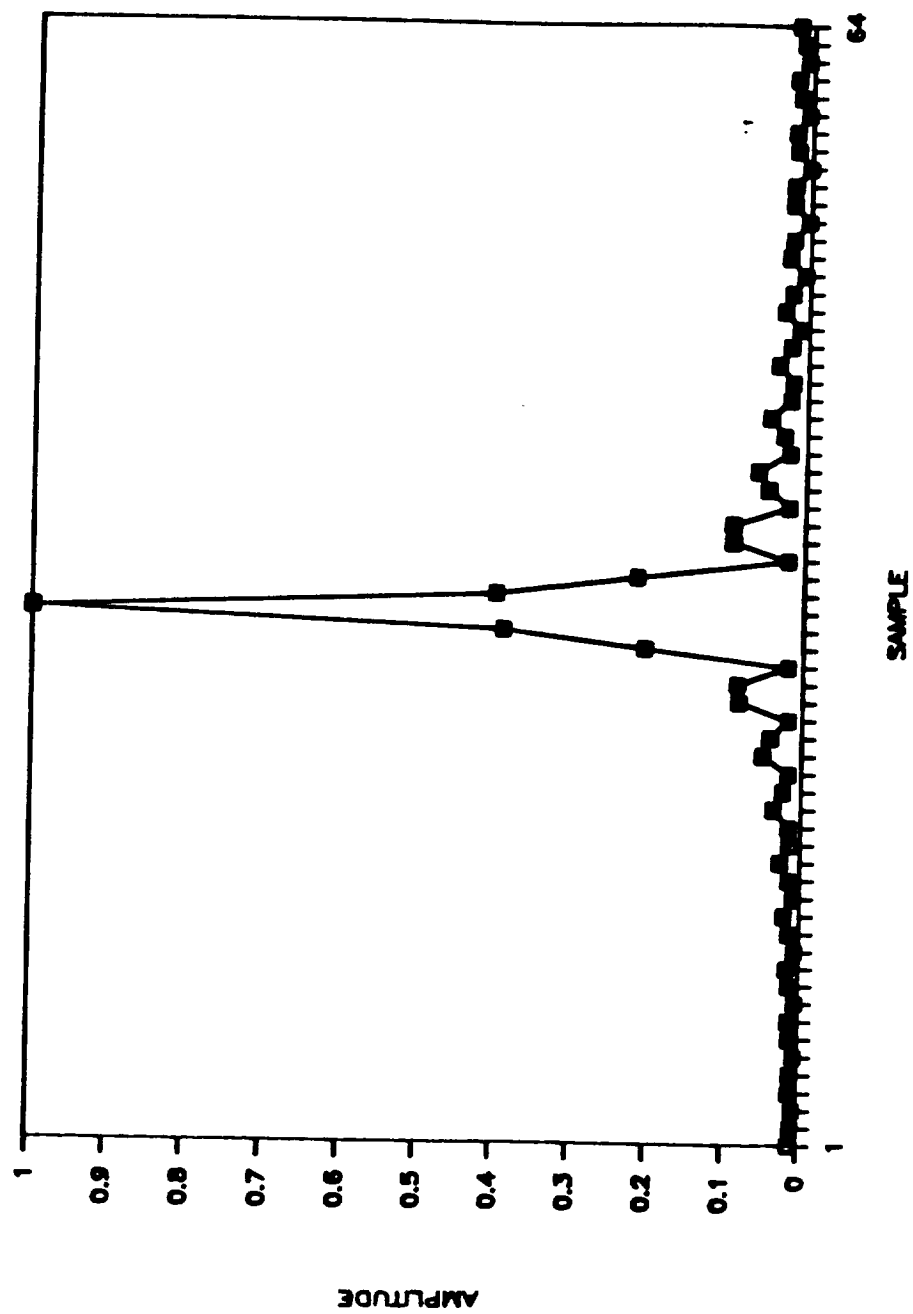




FIGURE 1.3



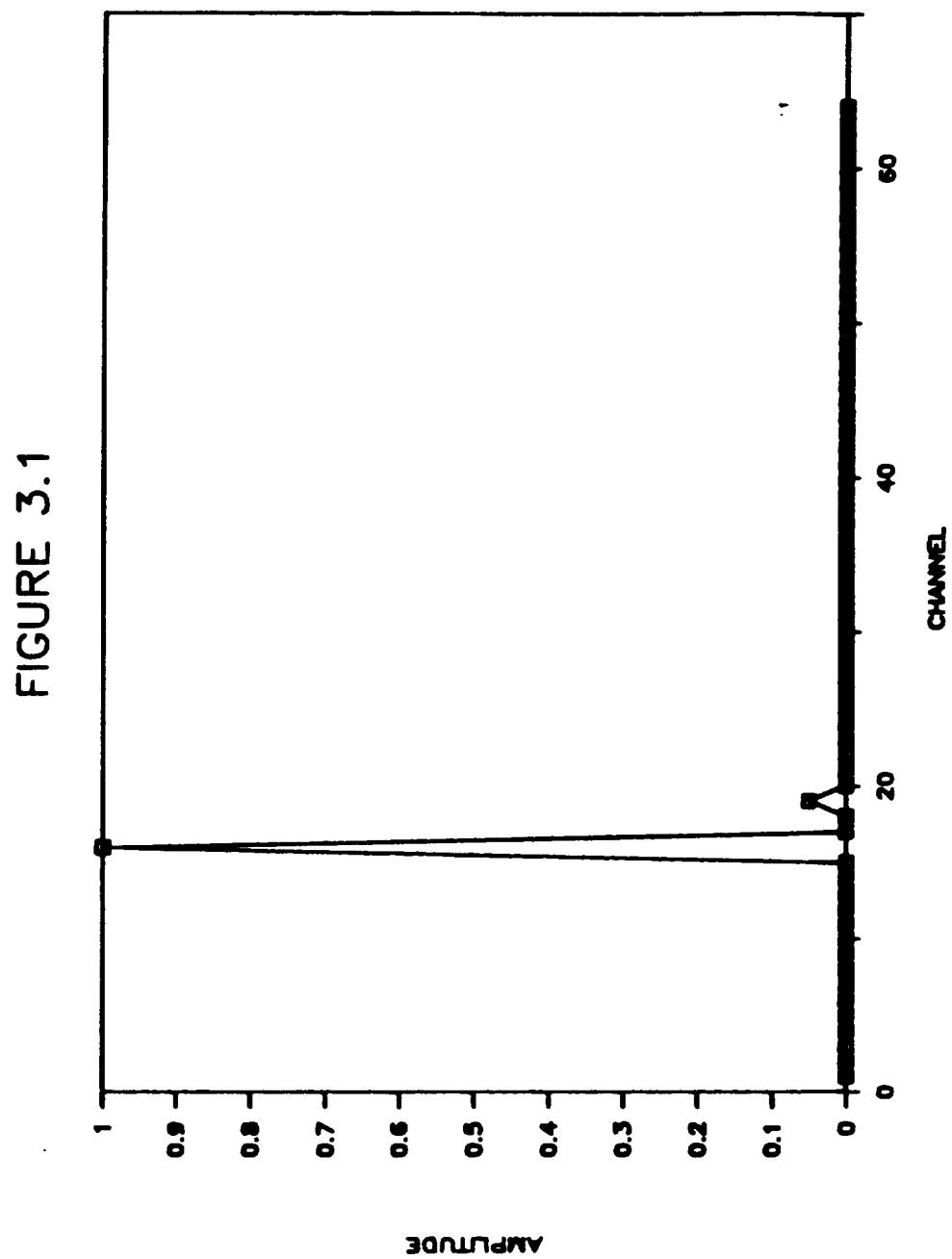
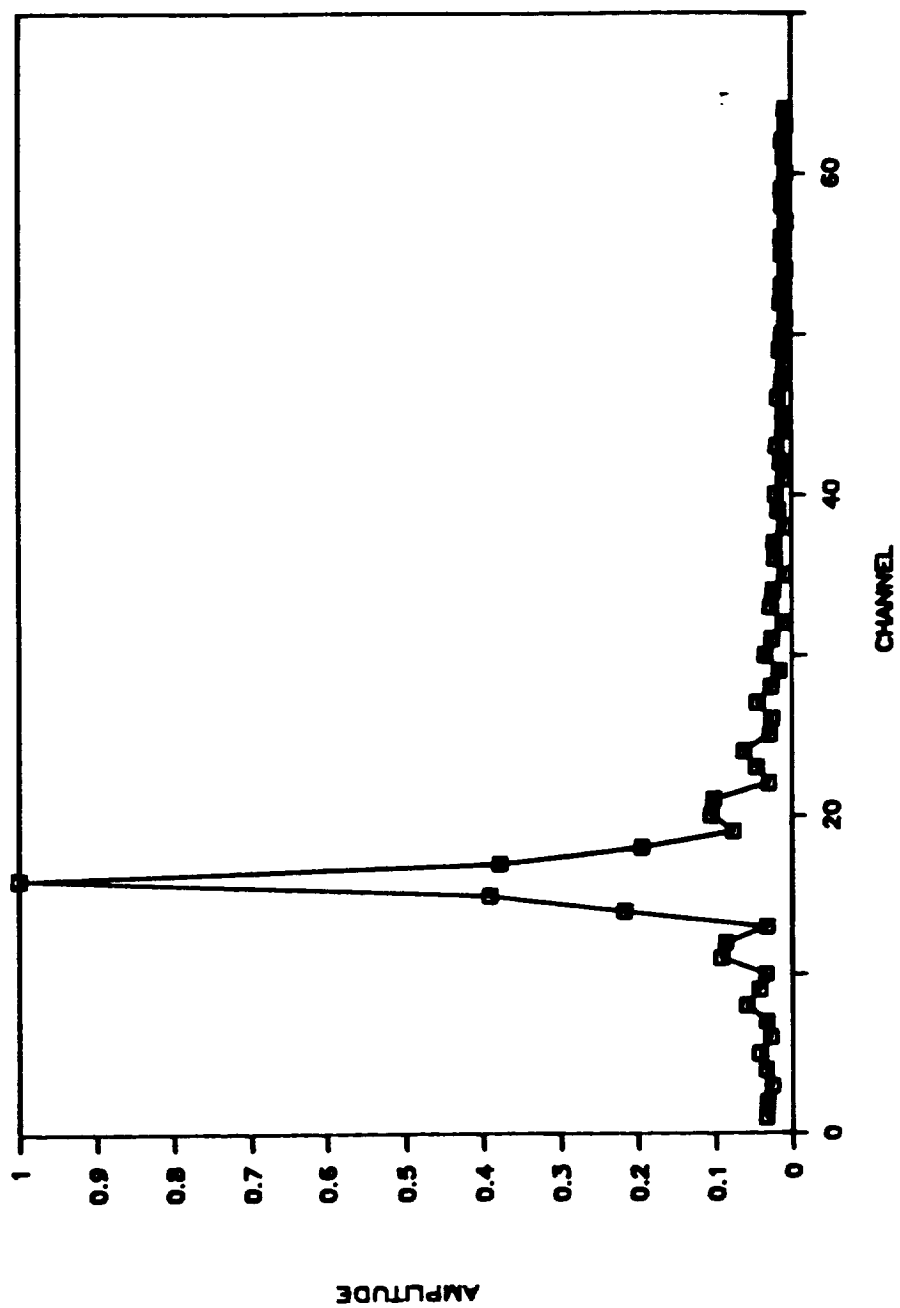
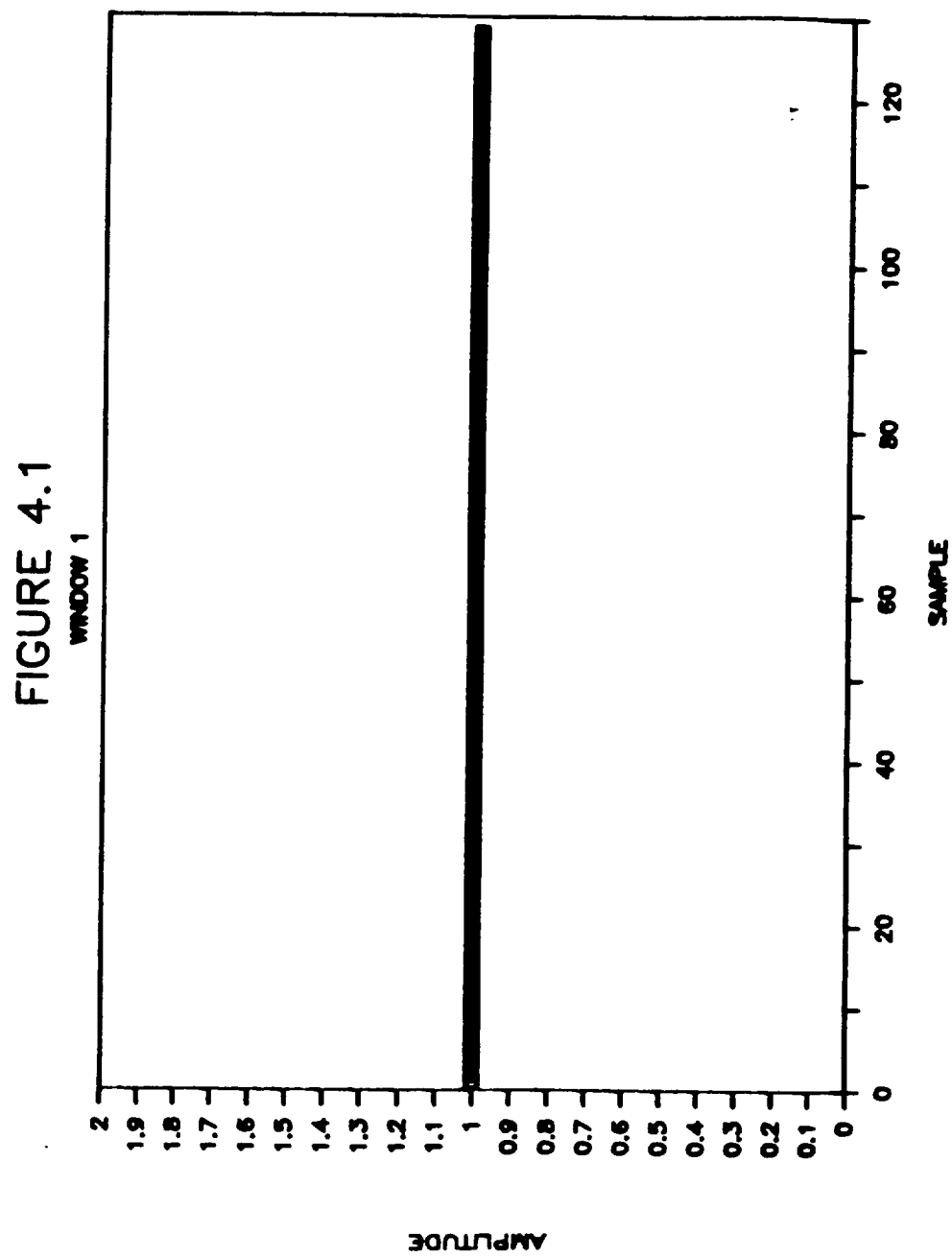
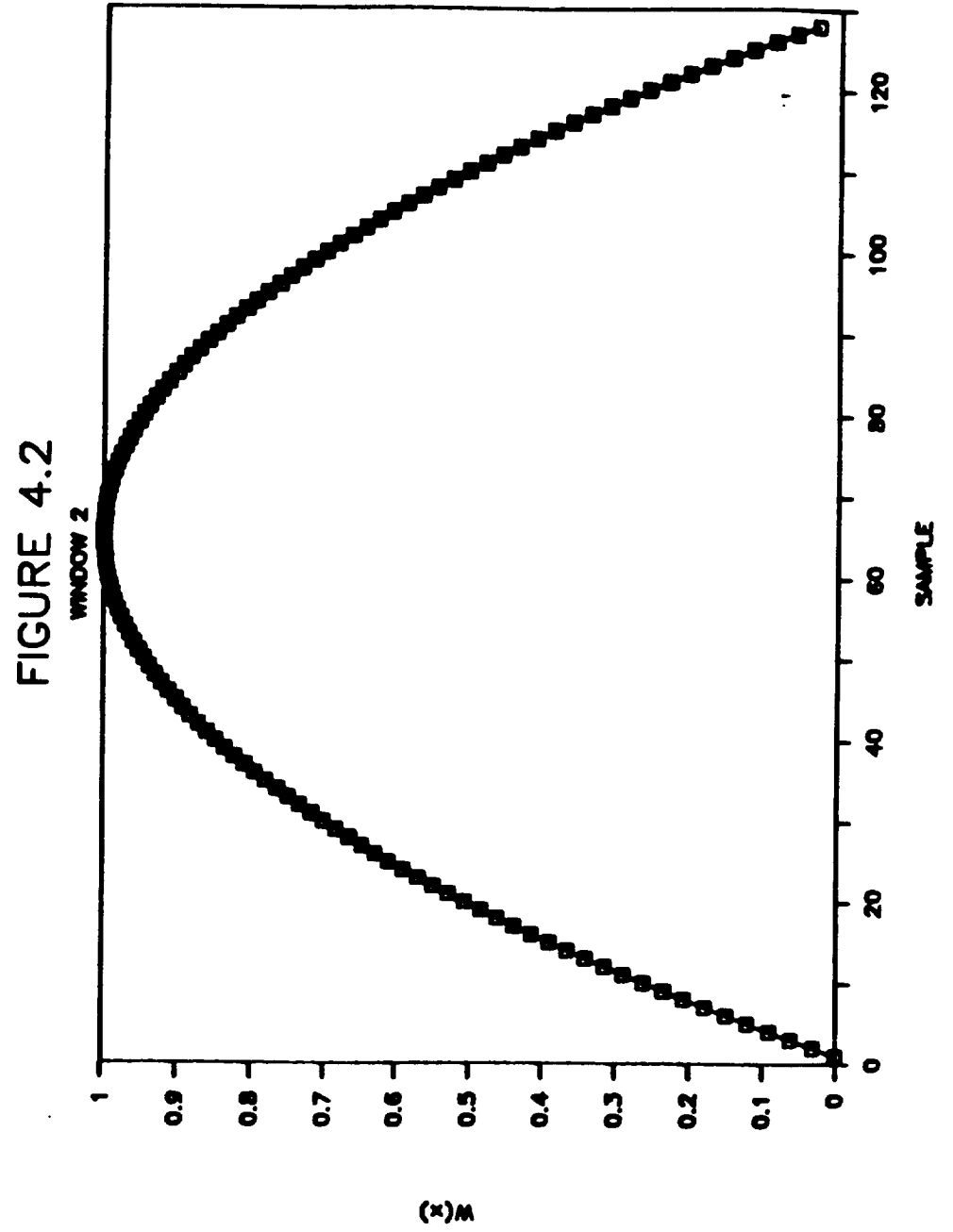
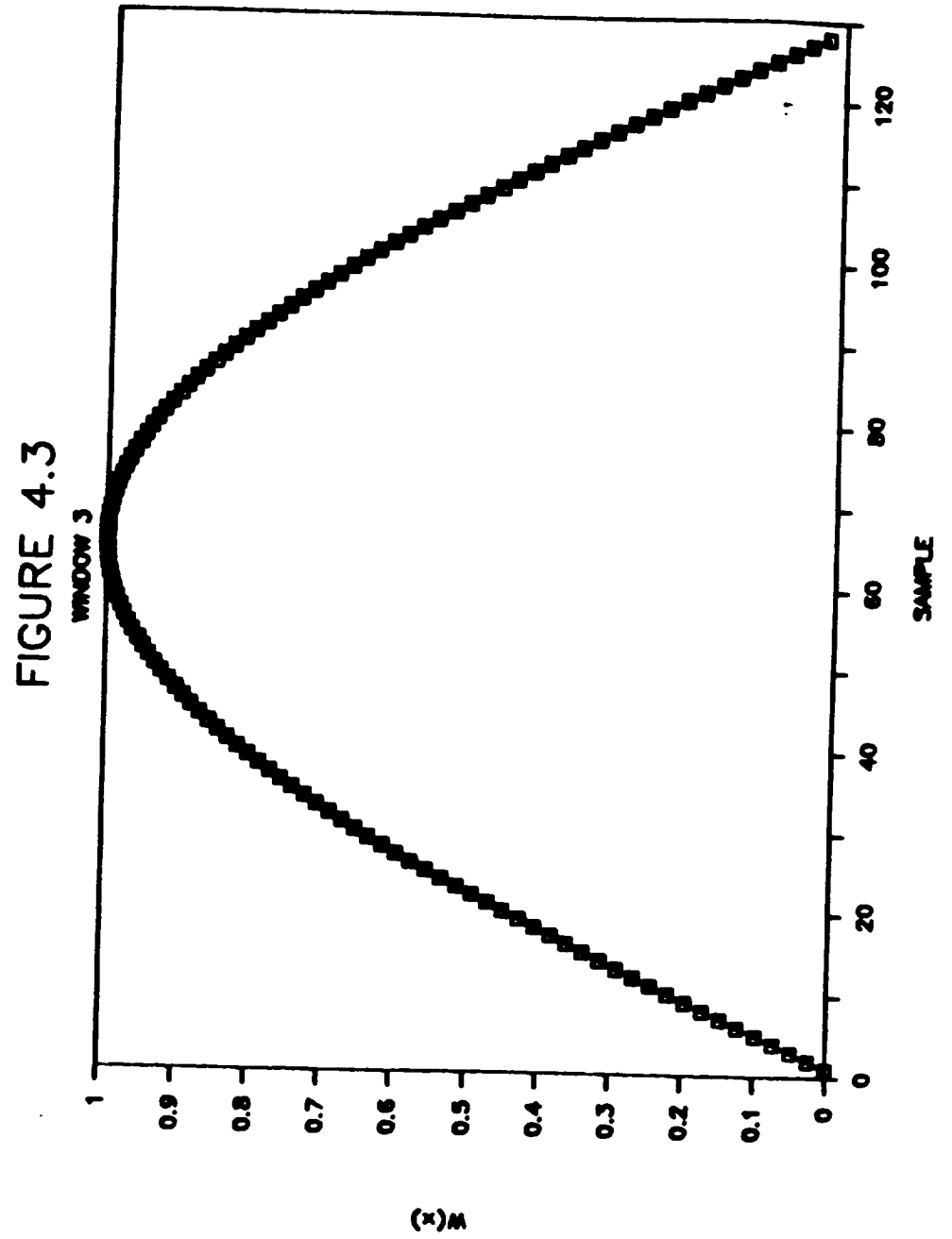


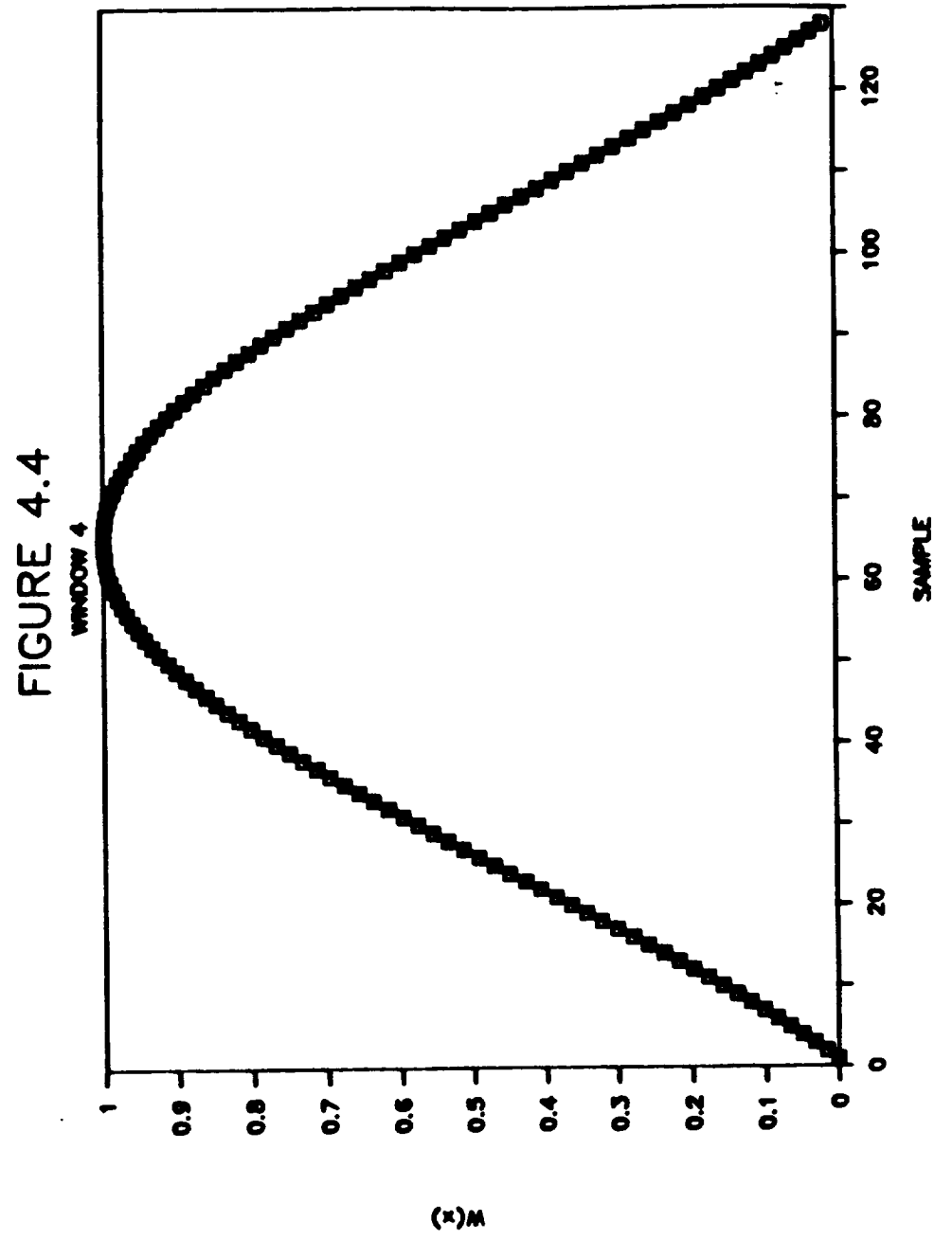
FIGURE 3.2

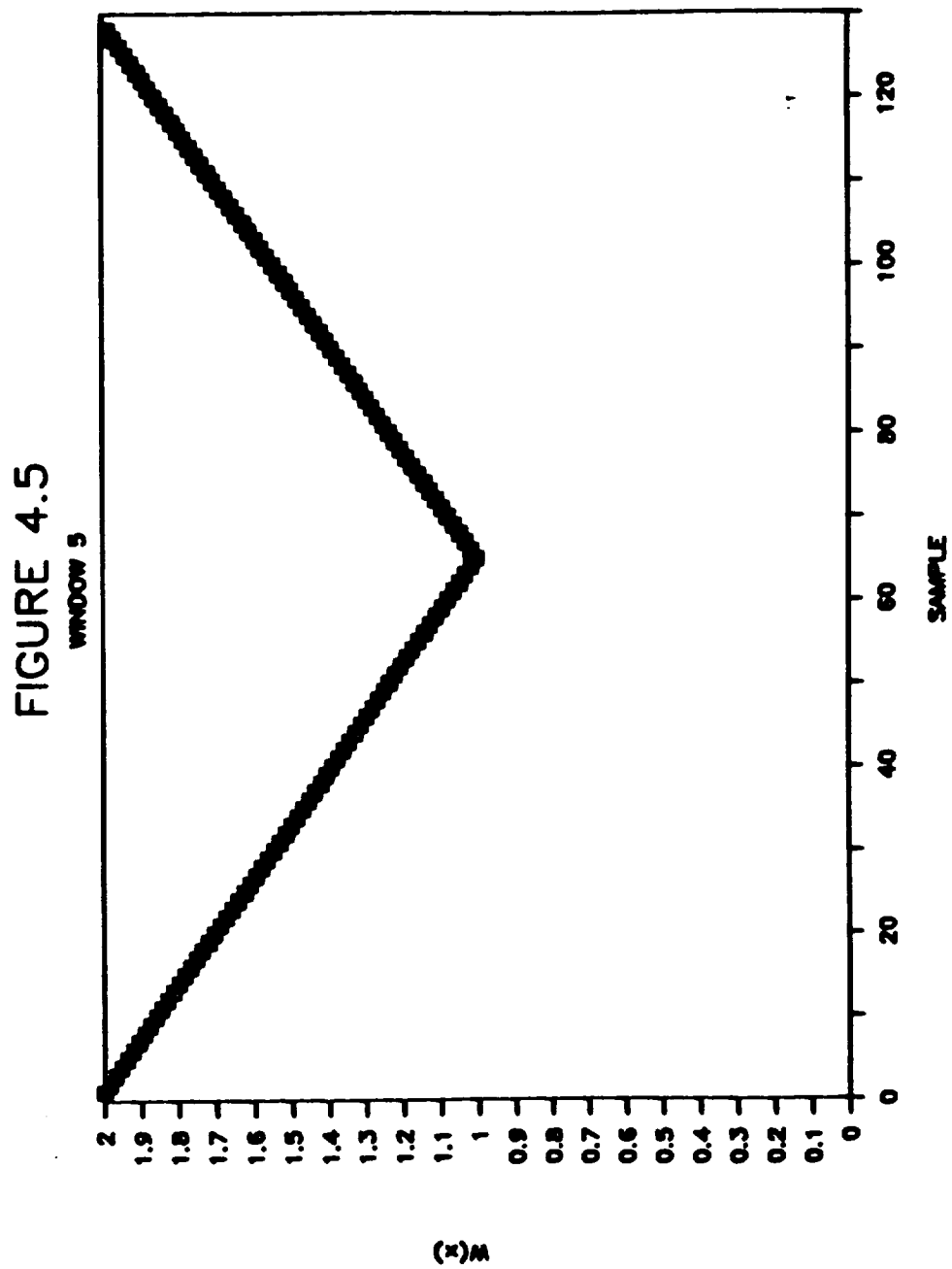




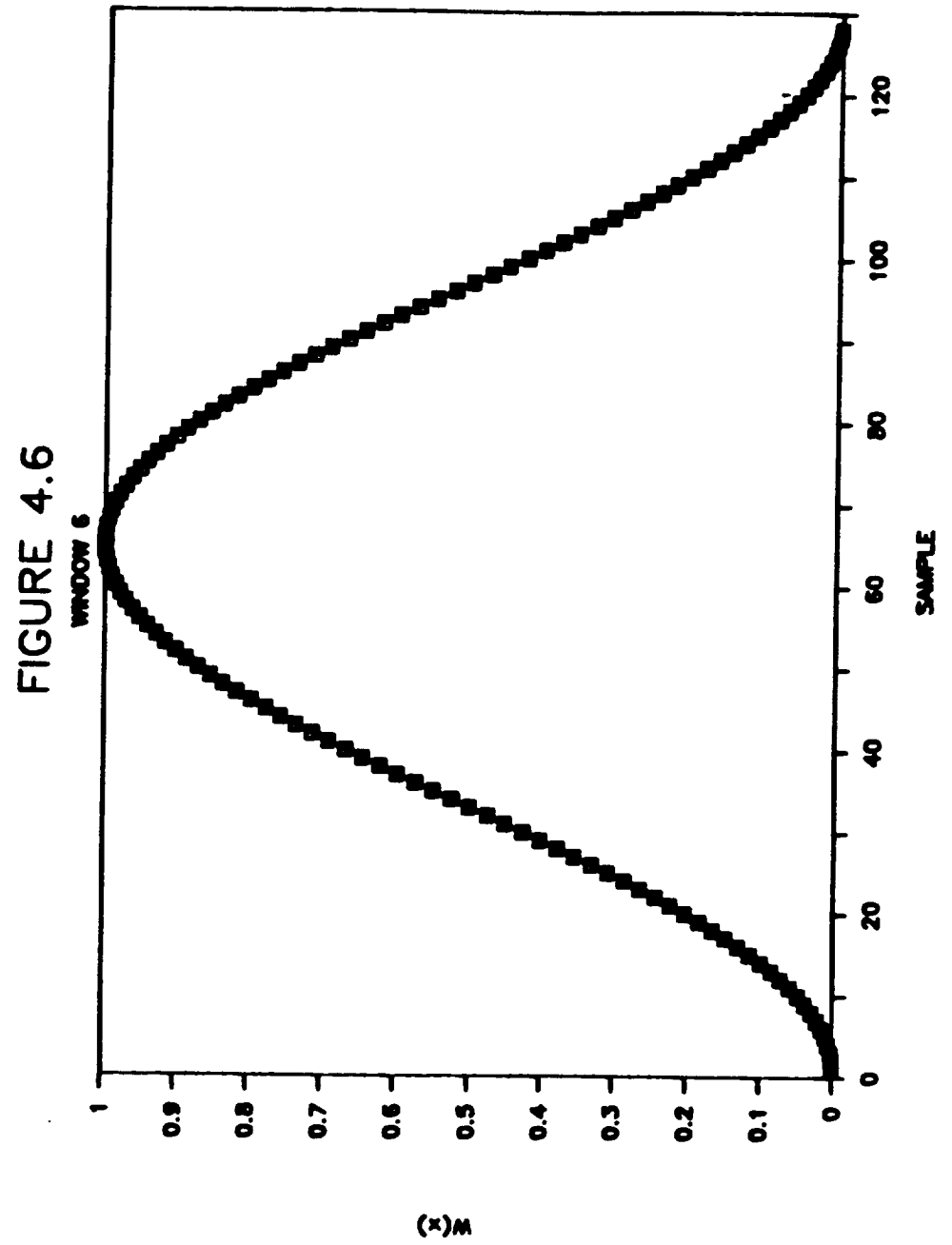












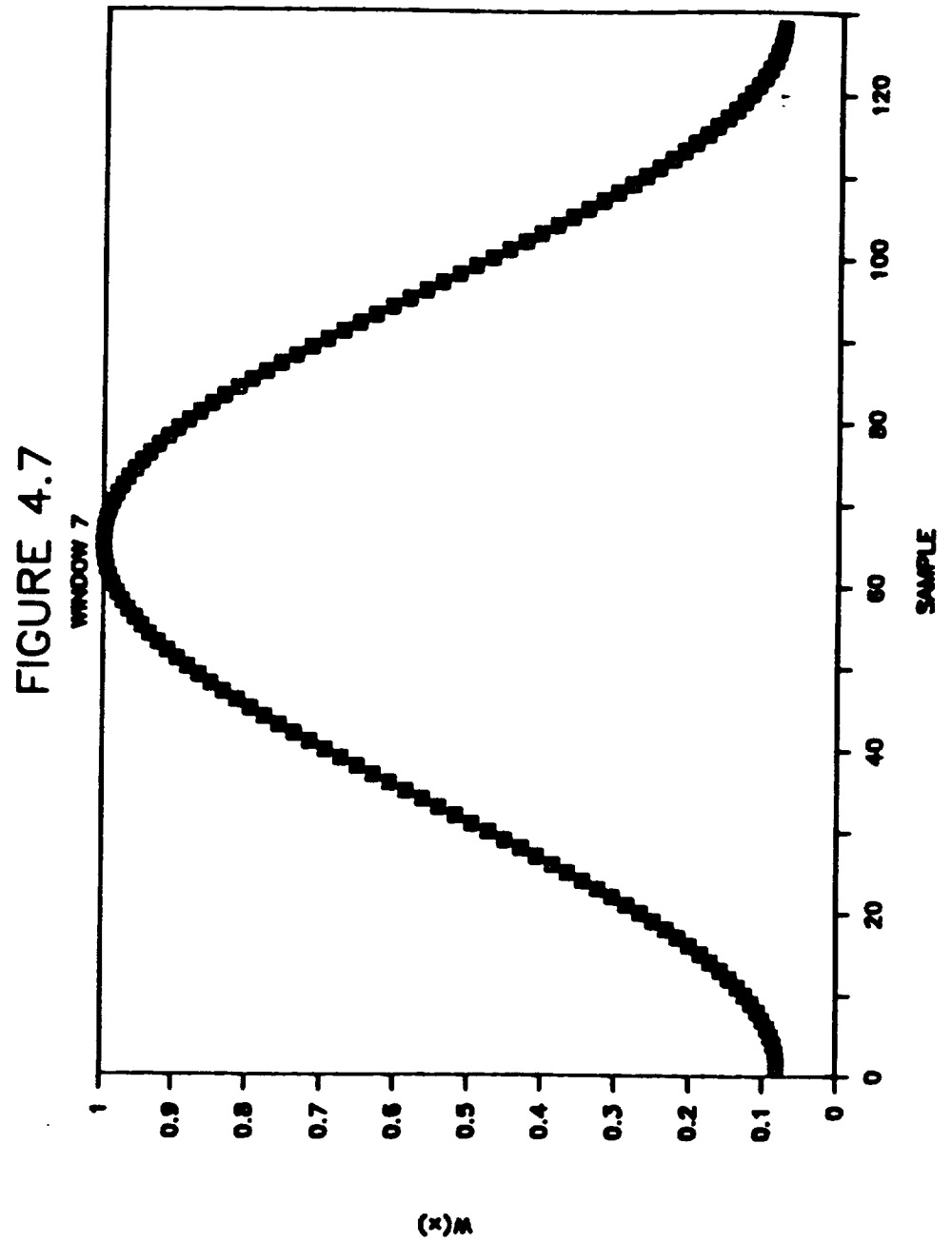
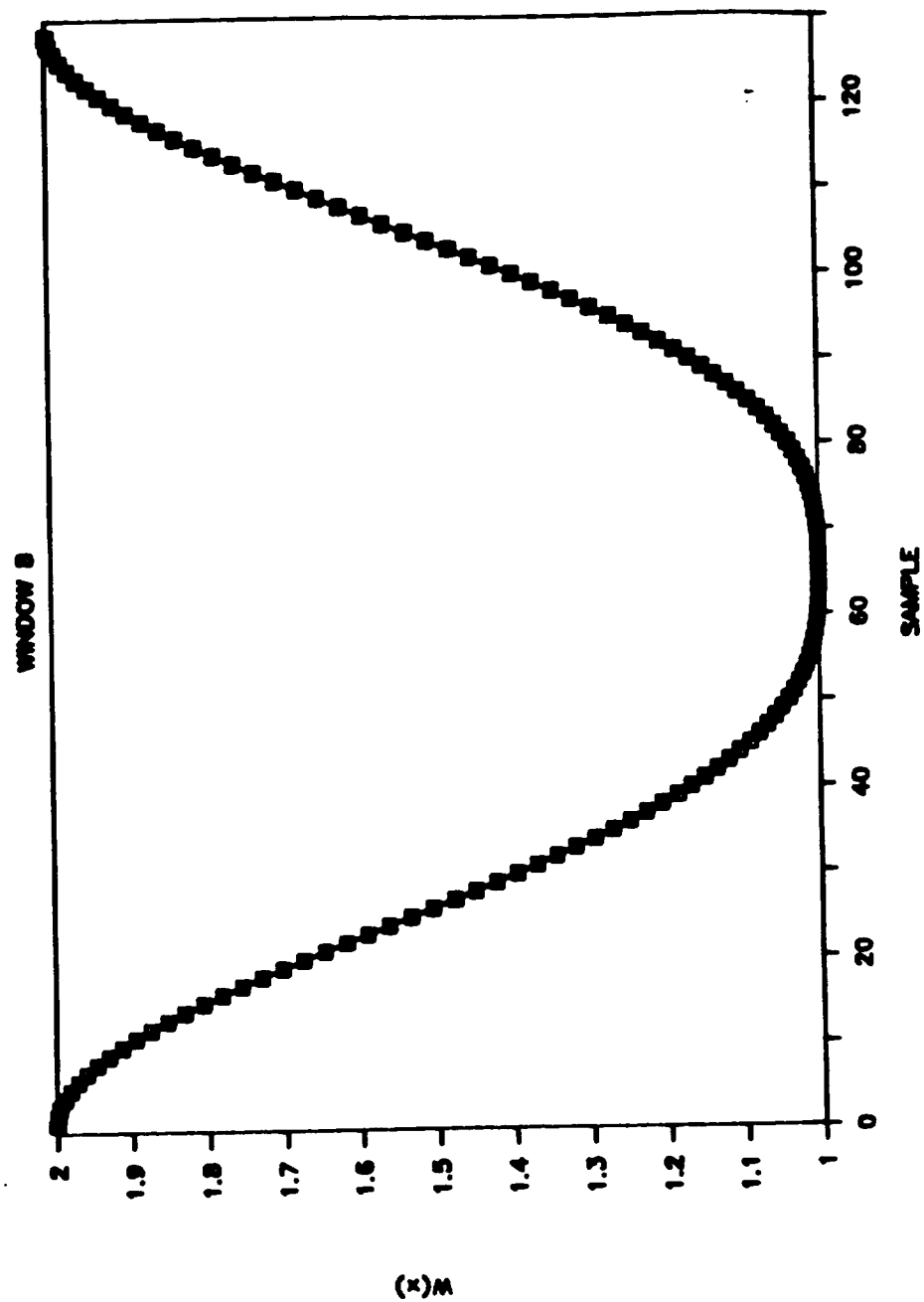


FIGURE 4.8



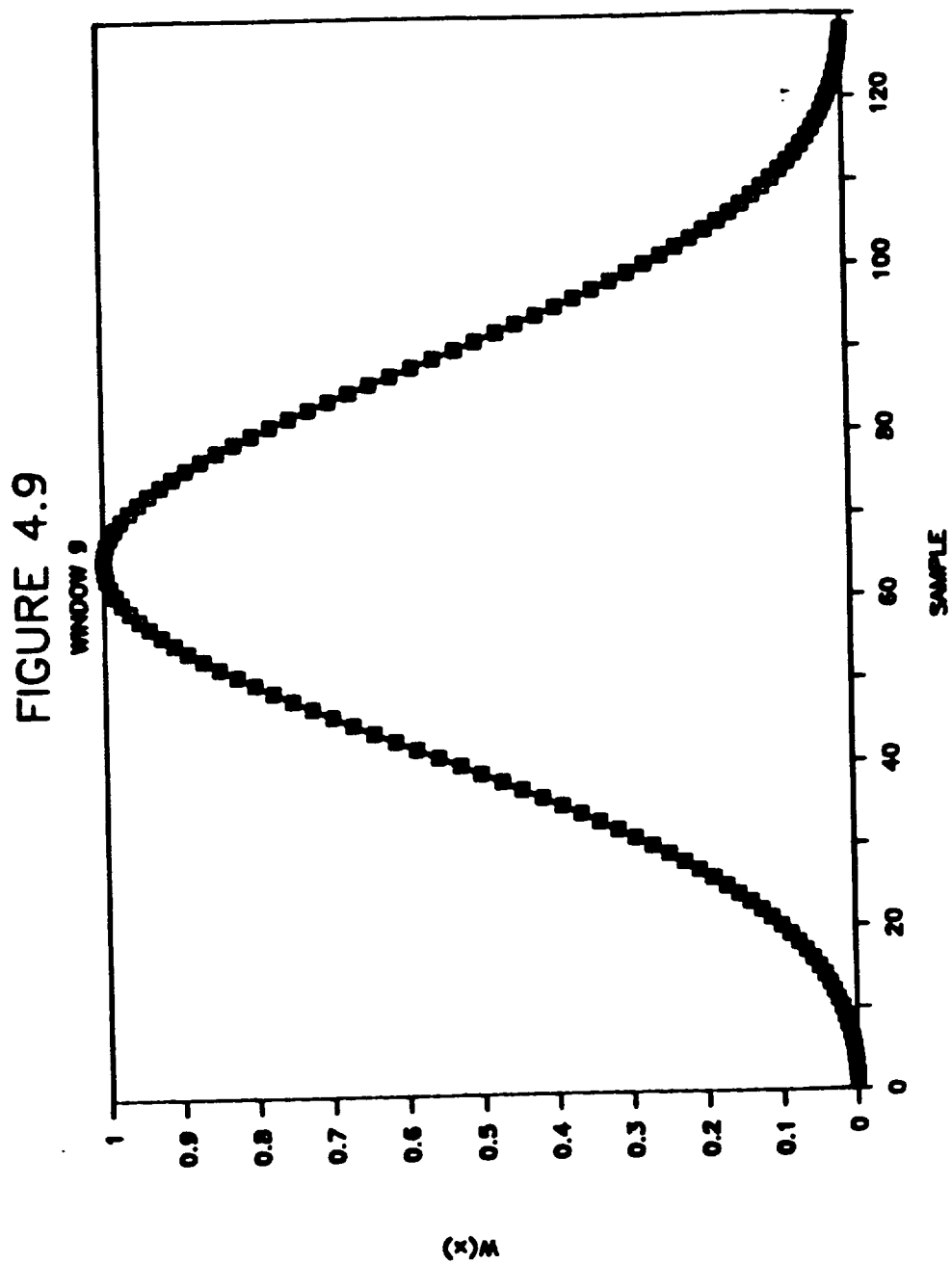
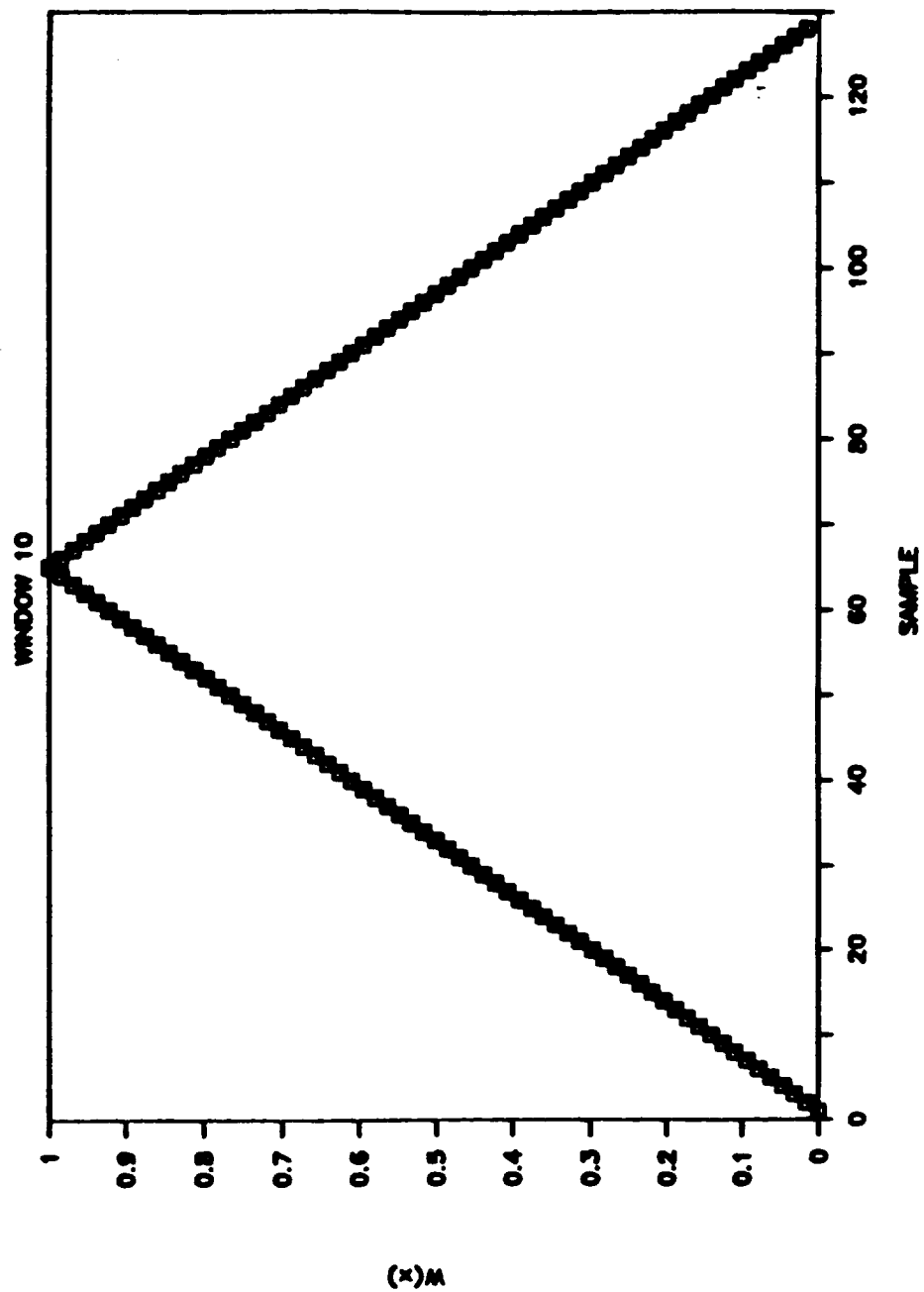


FIGURE 4.10



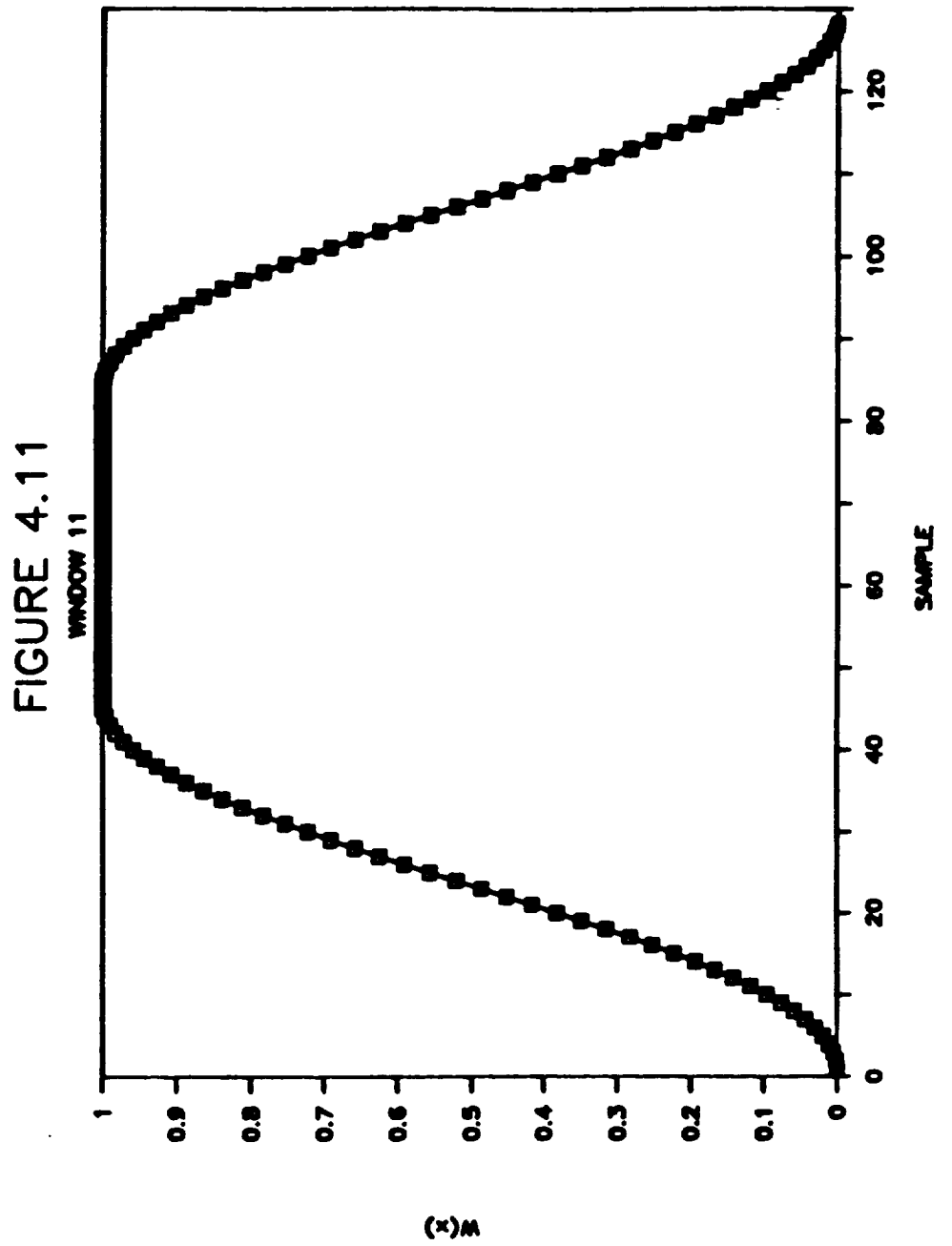


FIGURE 5.1

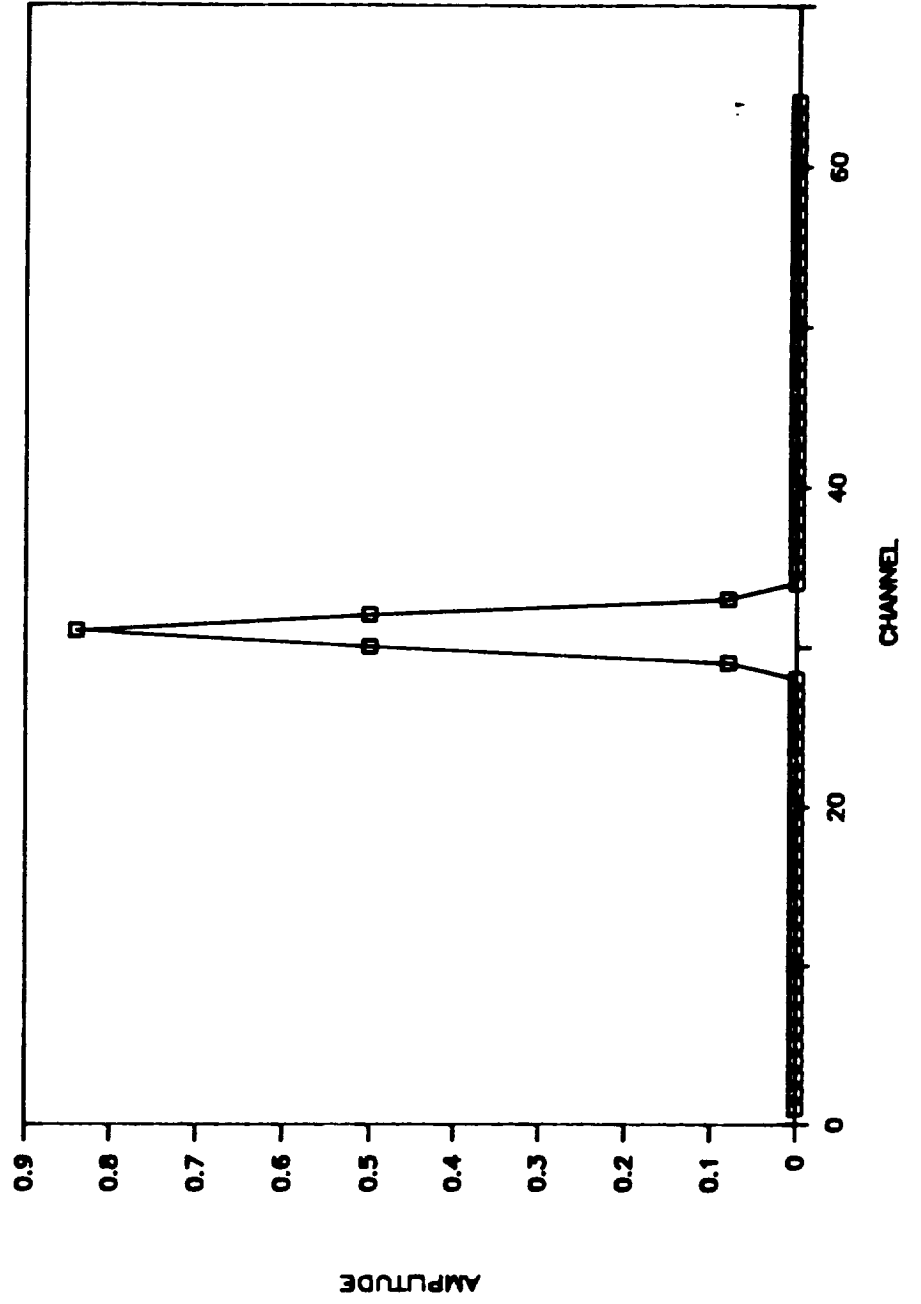


FIGURE 5.2

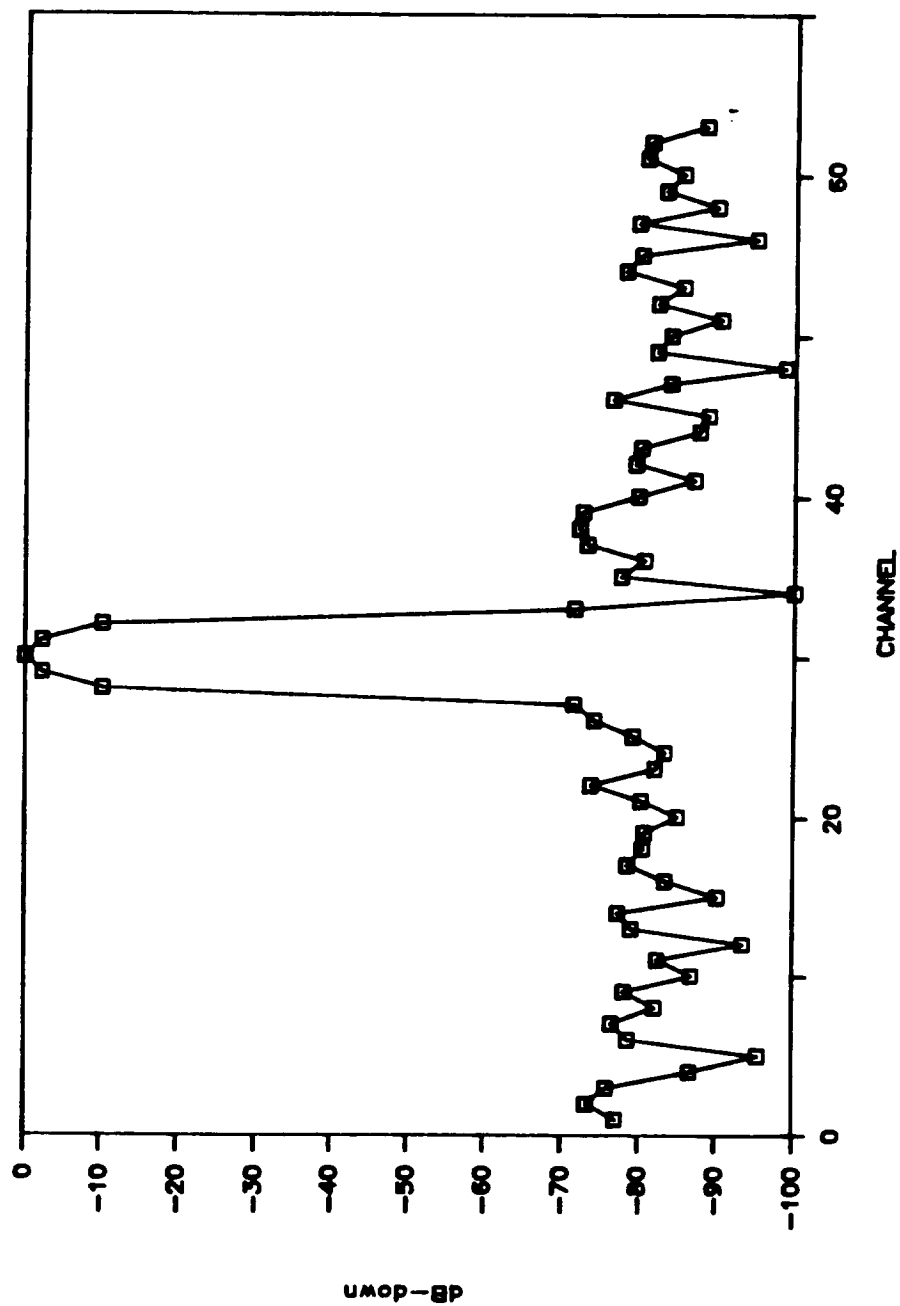




FIGURE 5.3

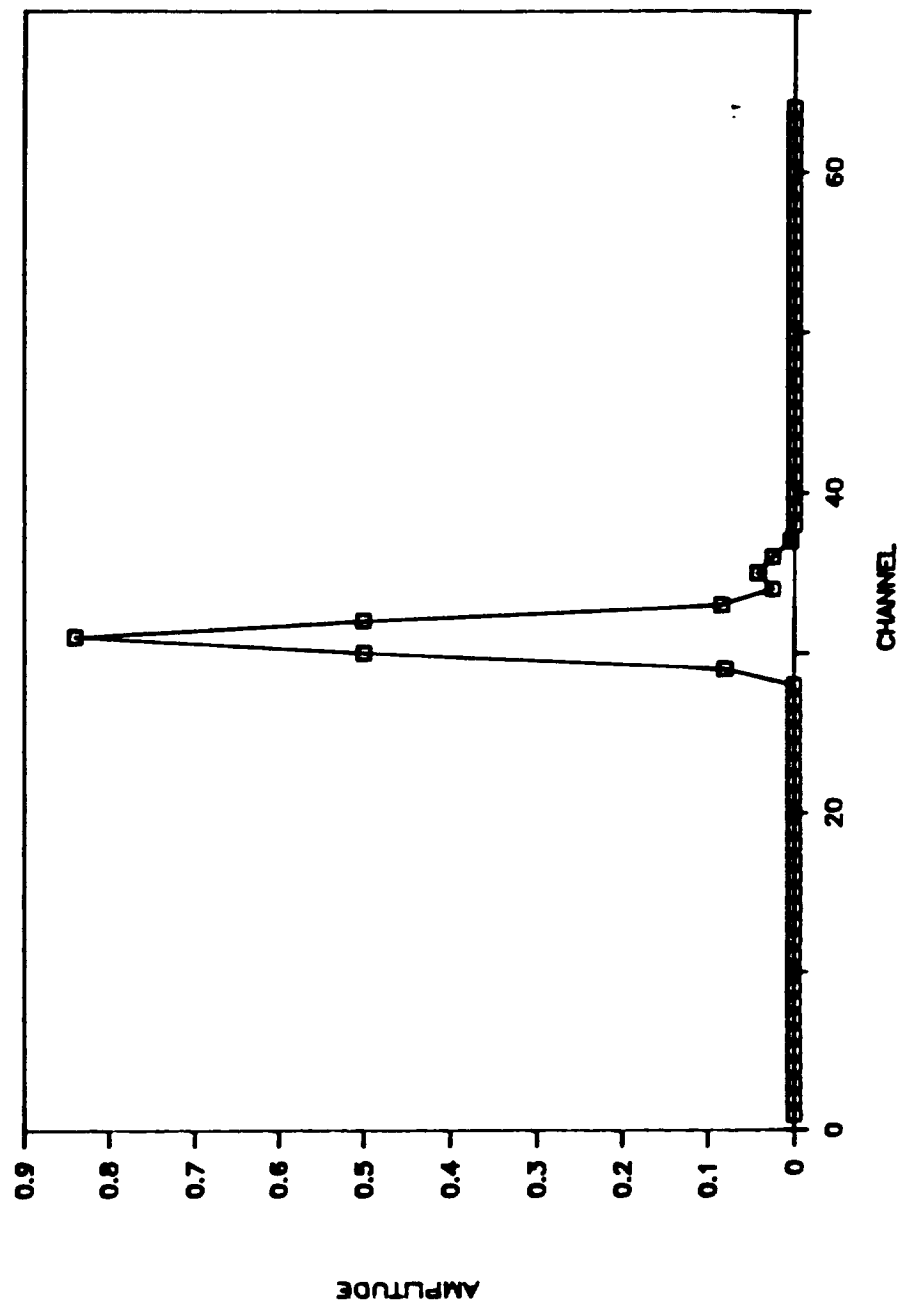
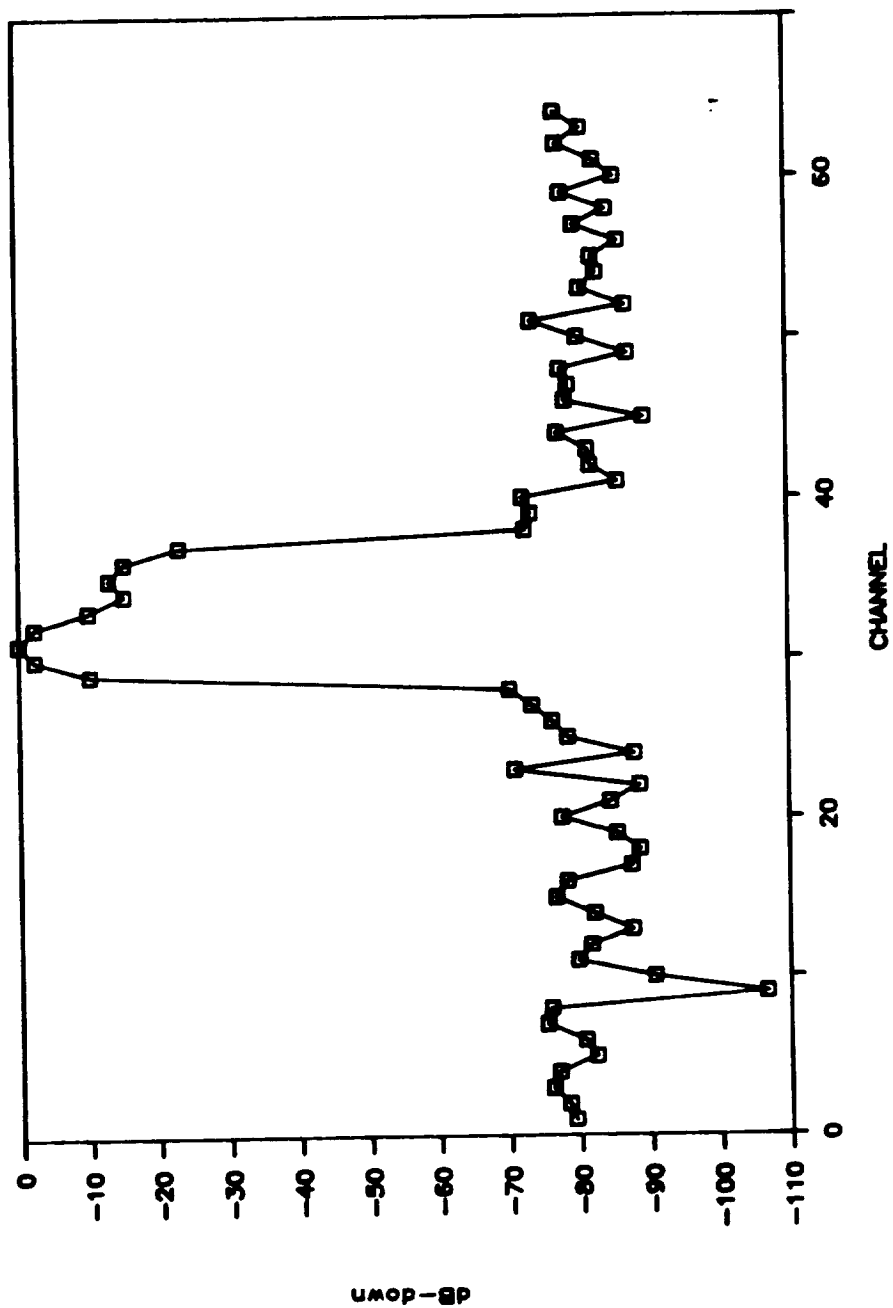


FIGURE 5.4



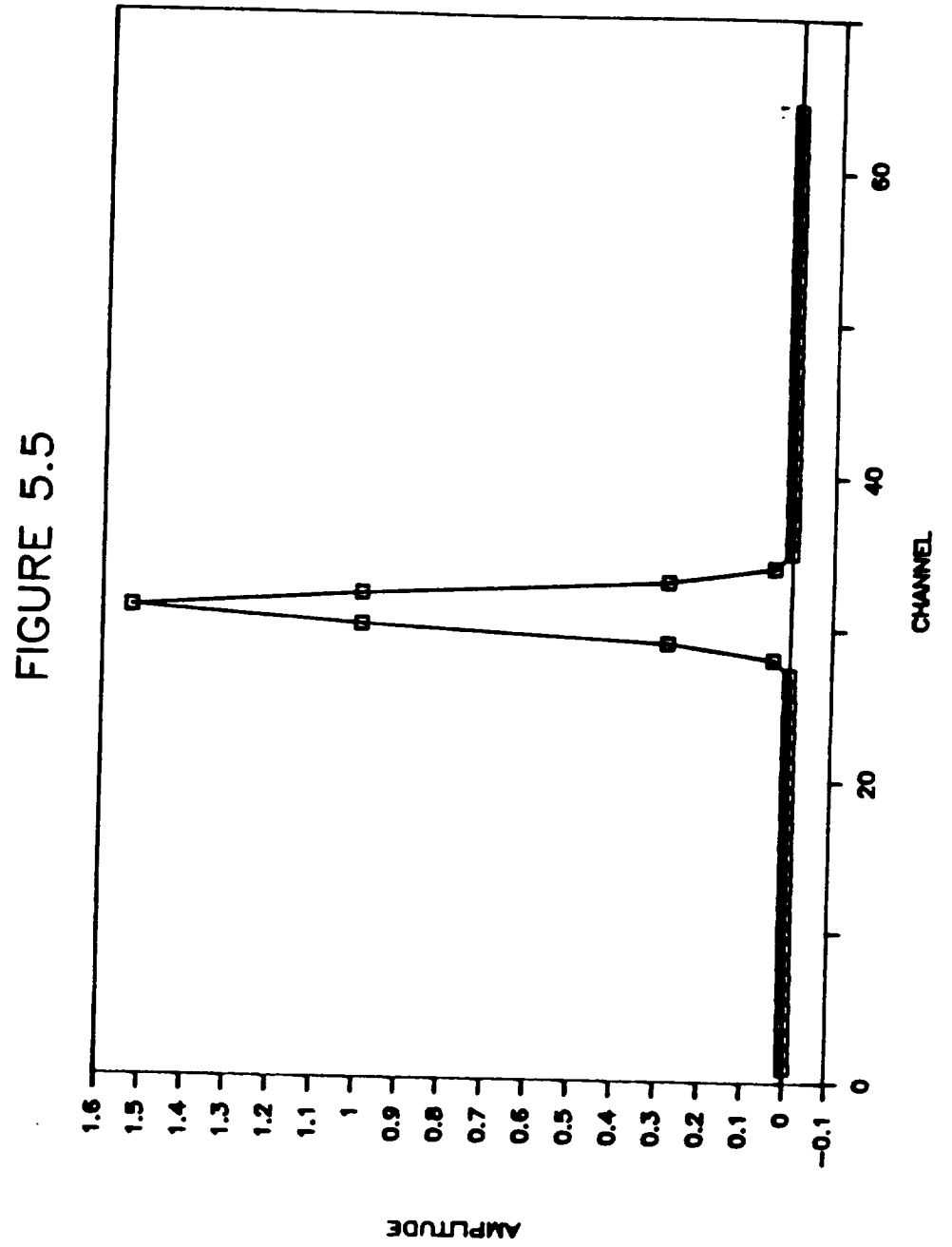


FIGURE 5.6

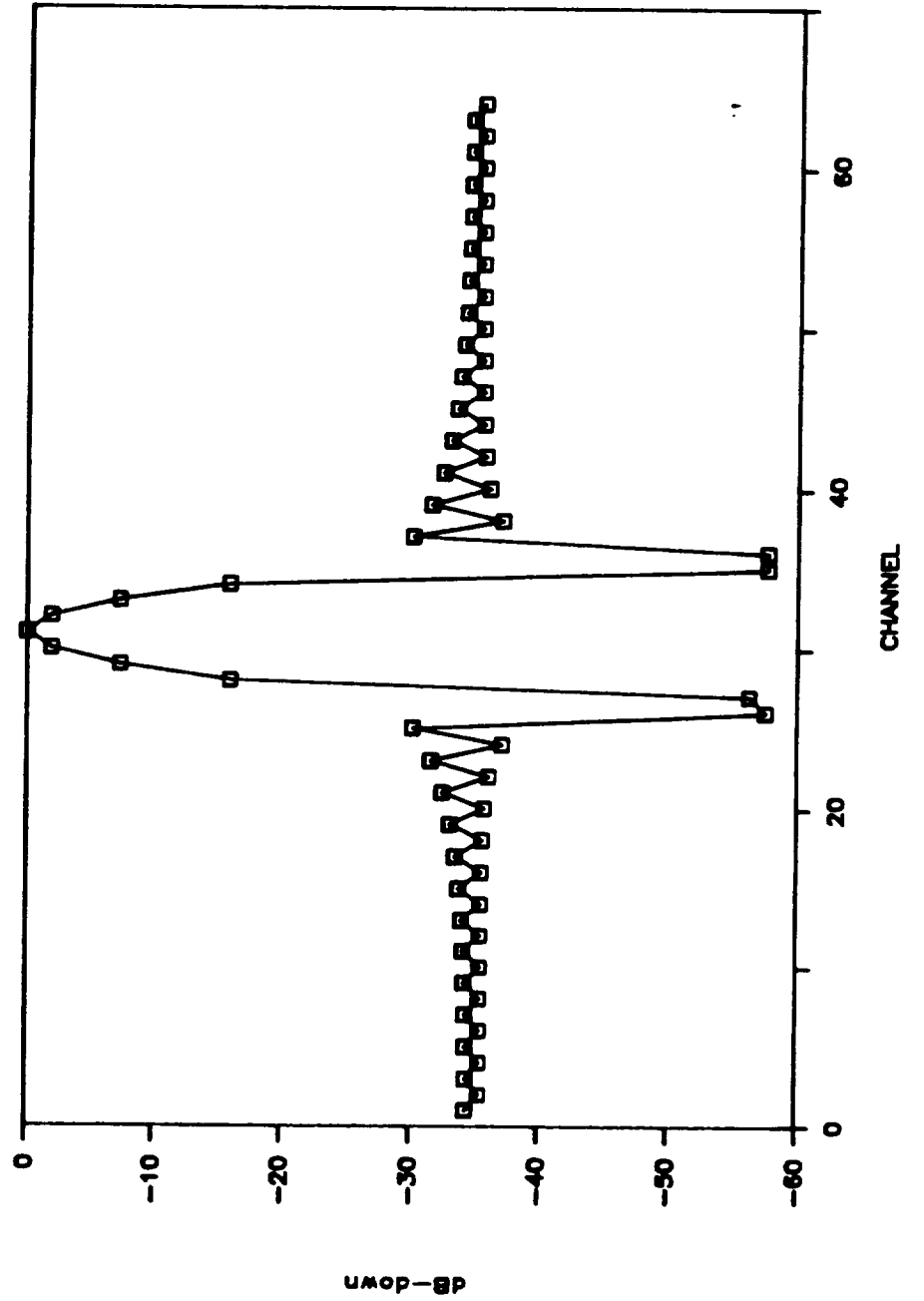


FIGURE 5.7

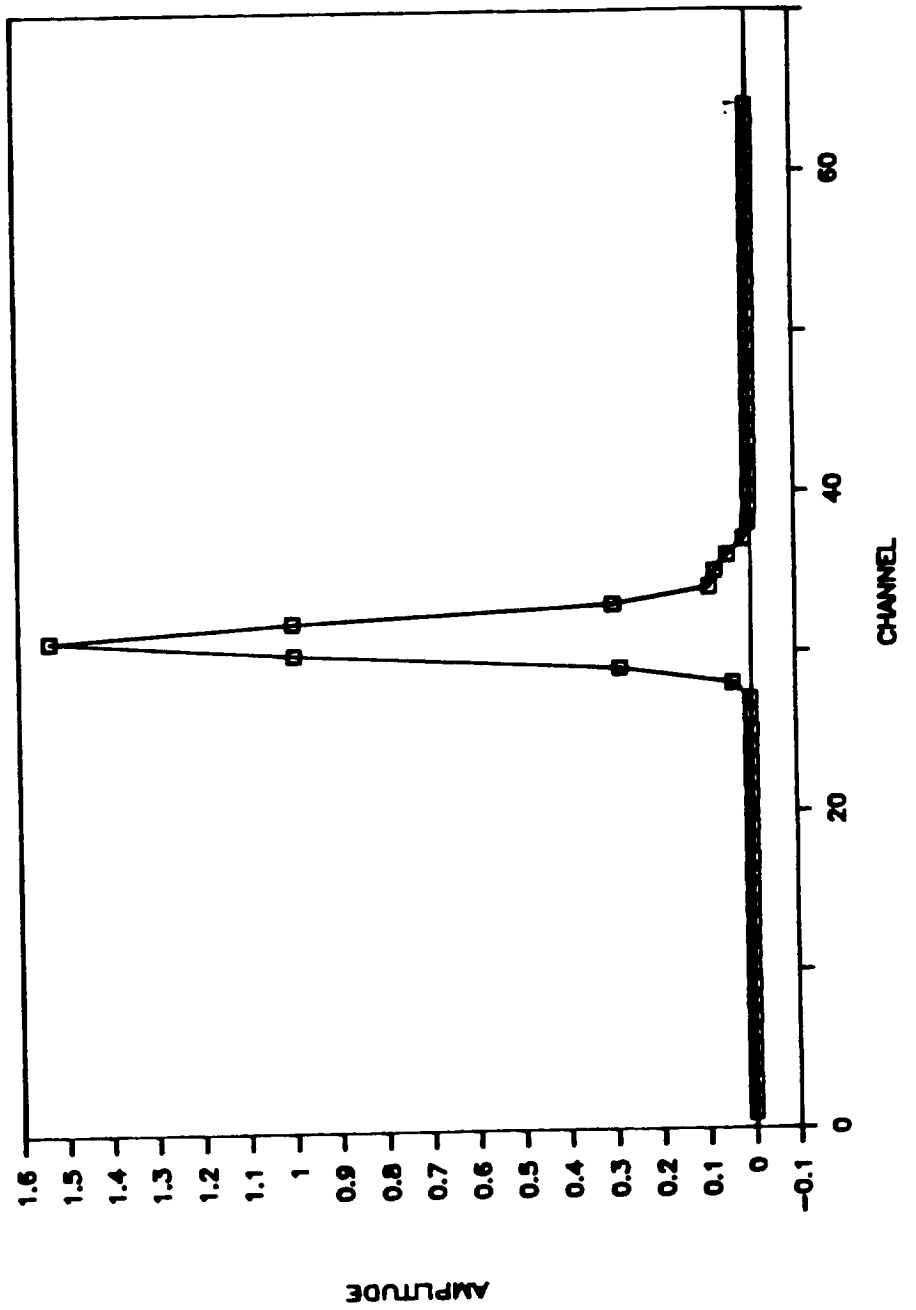


FIGURE 5.8

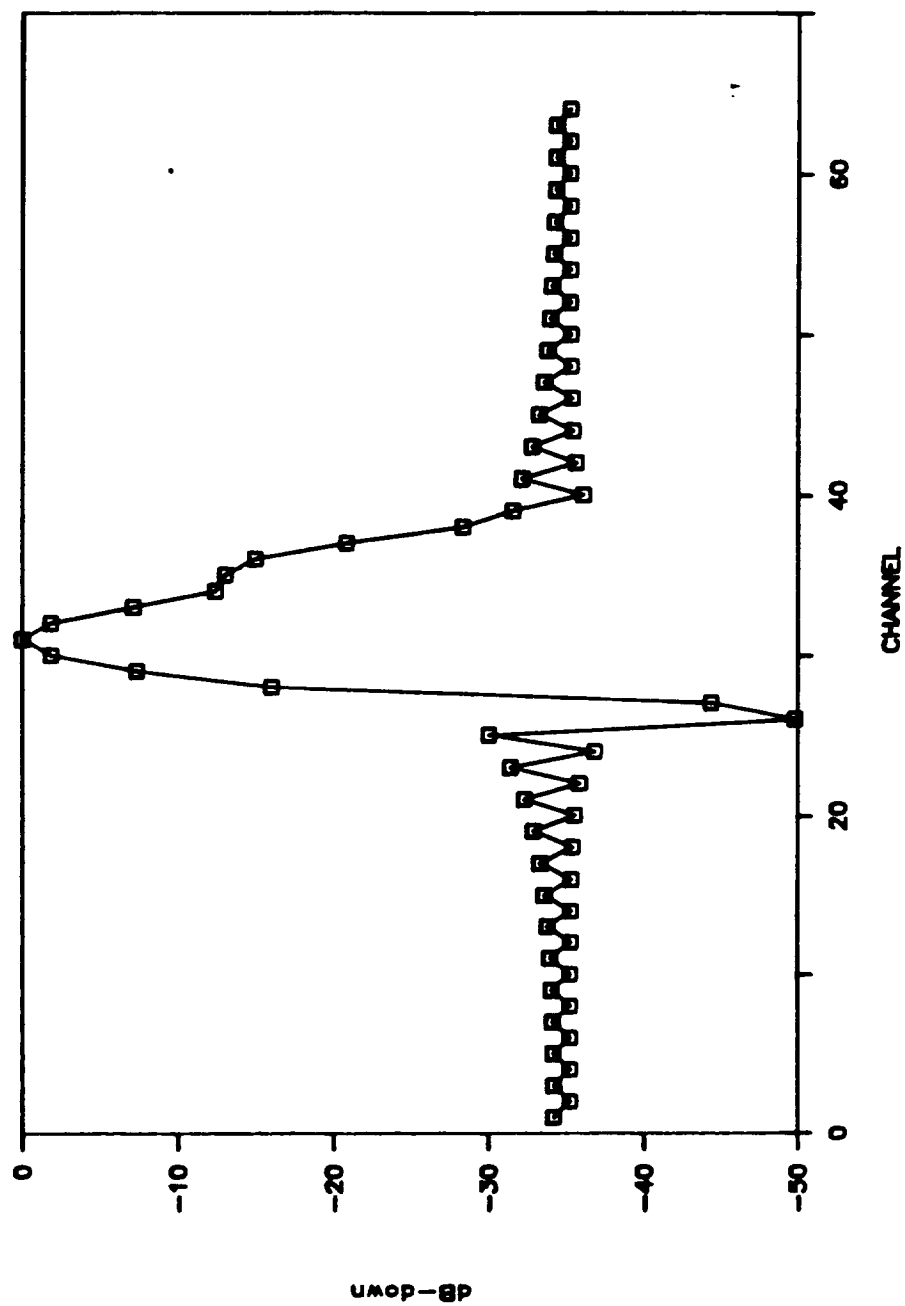


FIGURE 5.9

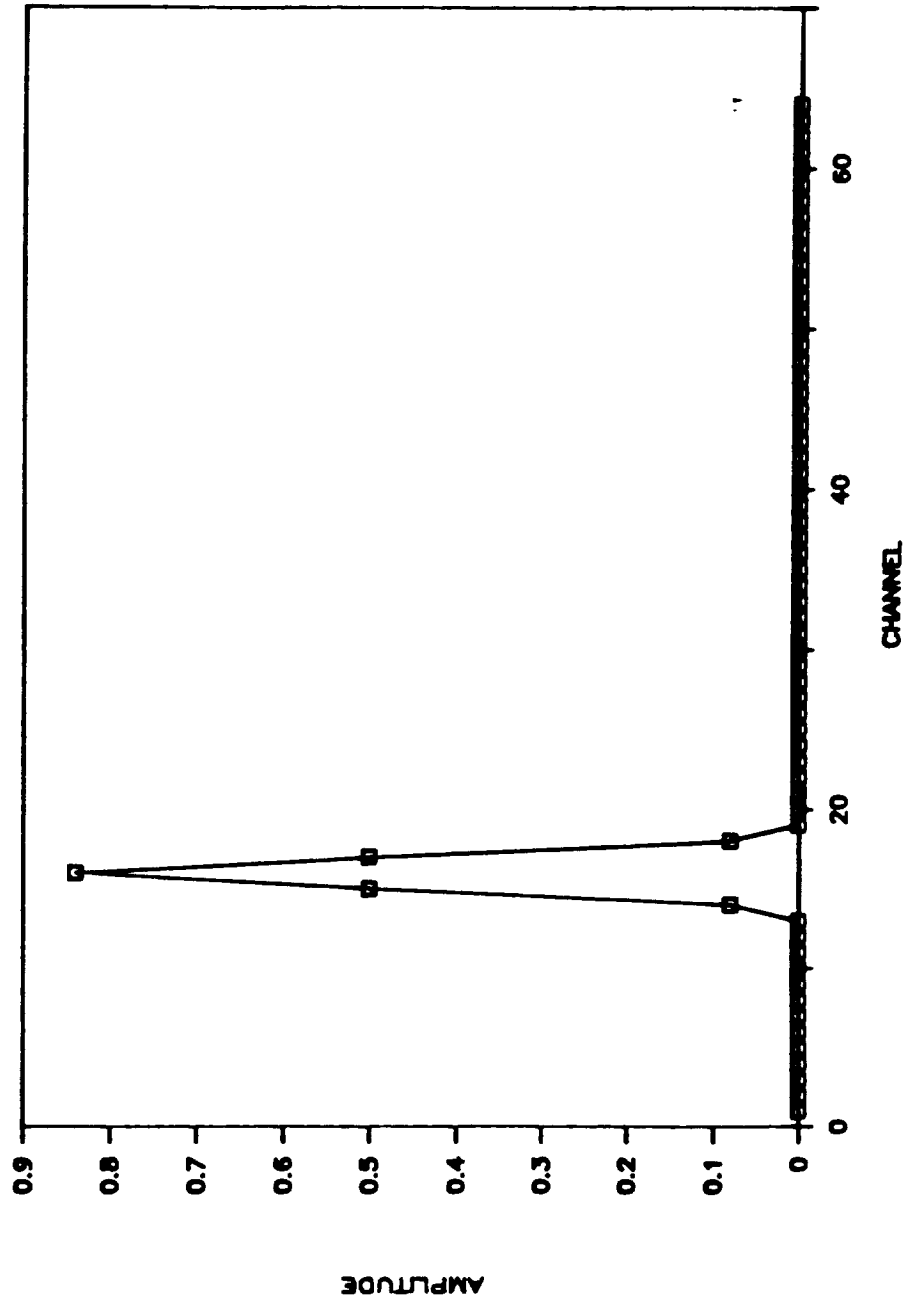


FIGURE 5.10

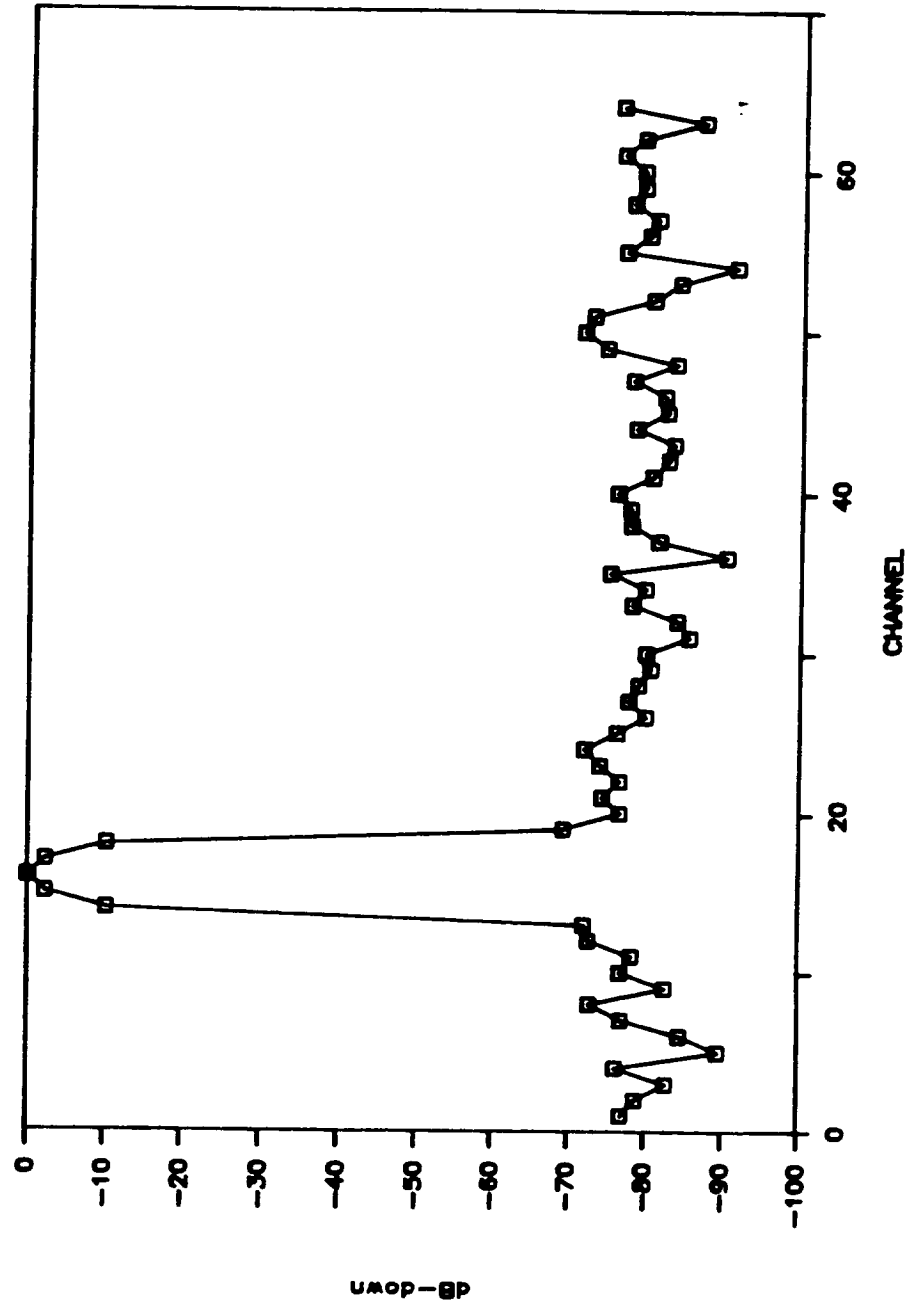




FIGURE 5.11

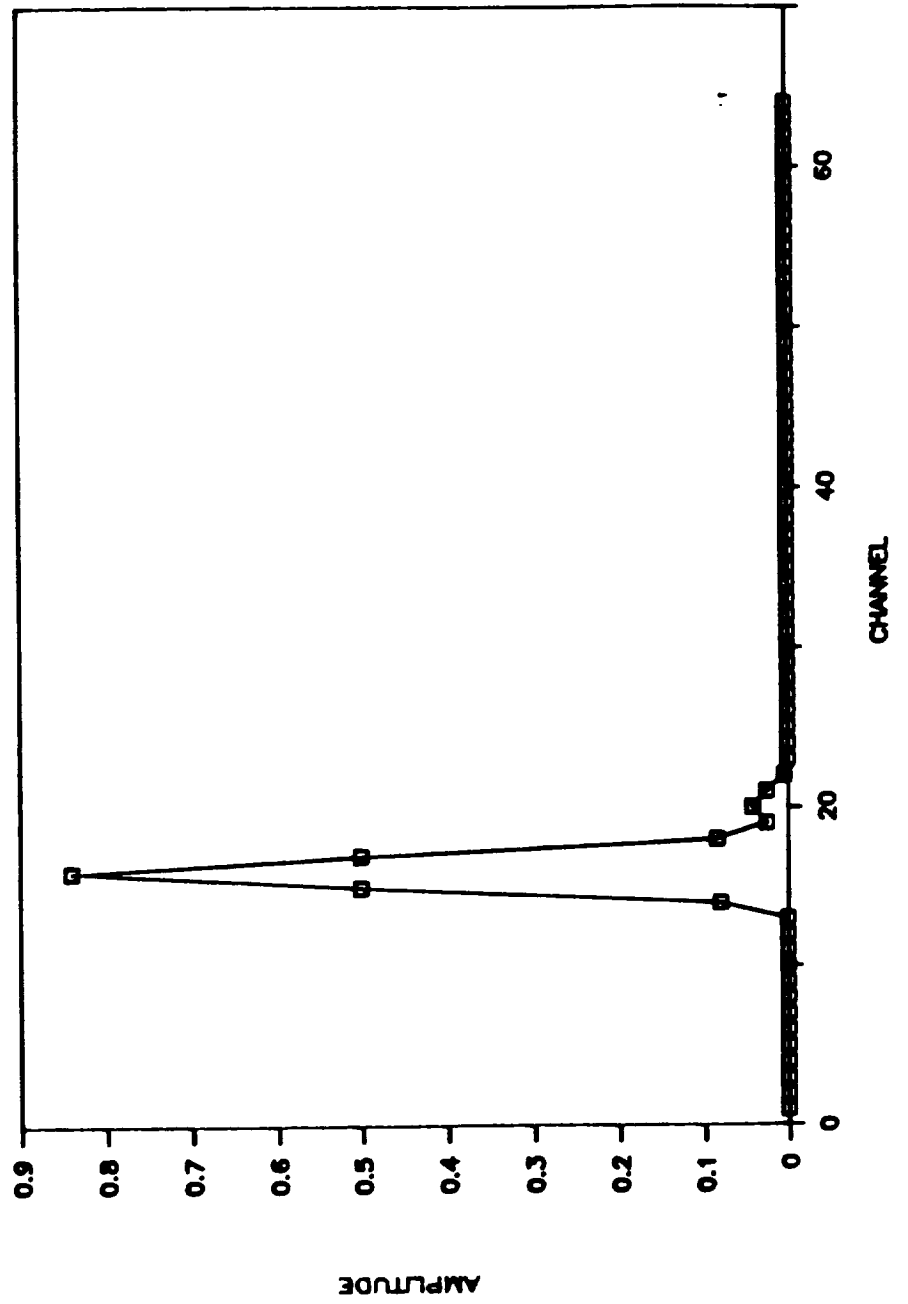


FIGURE 5.12

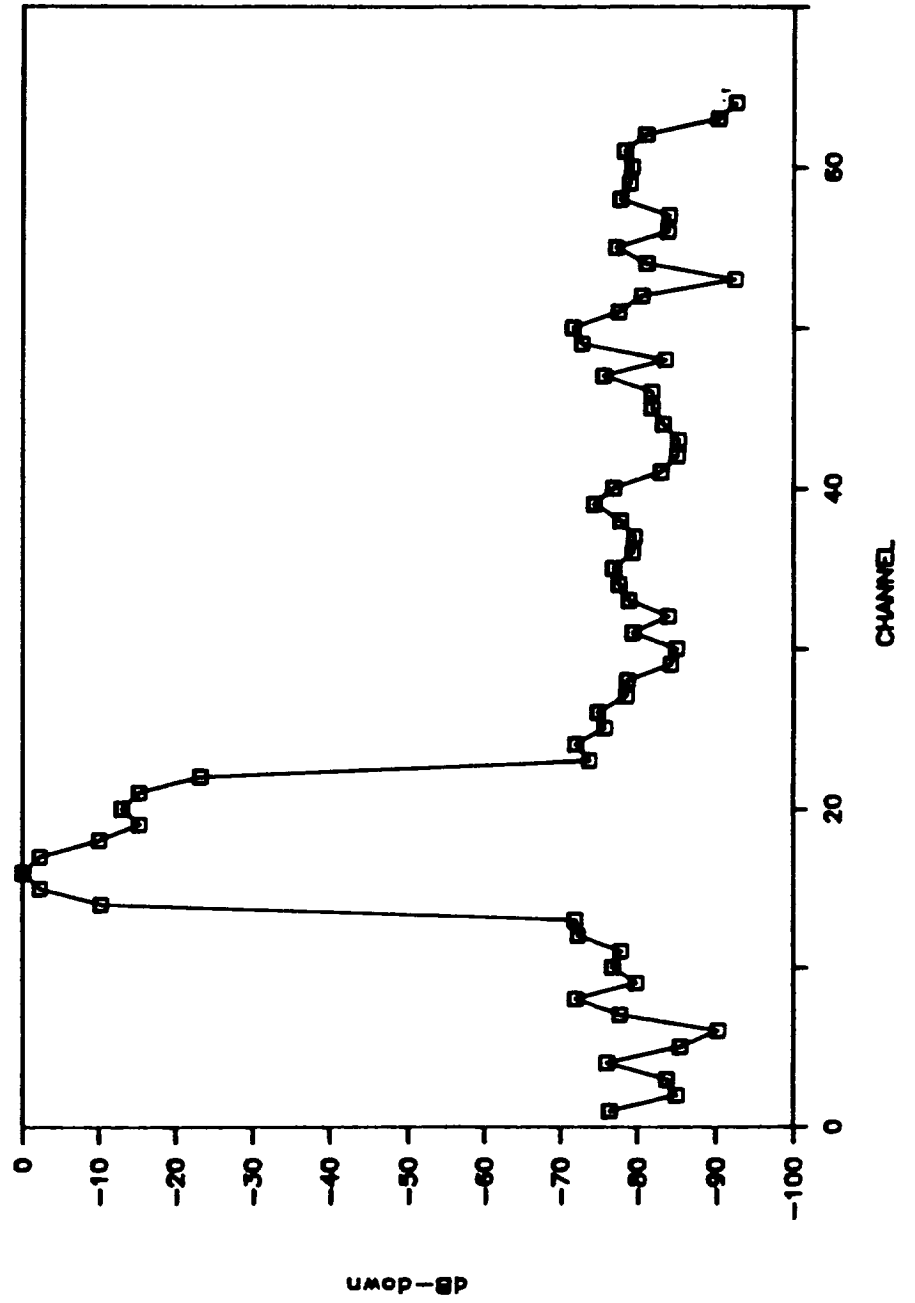


FIGURE 5.13

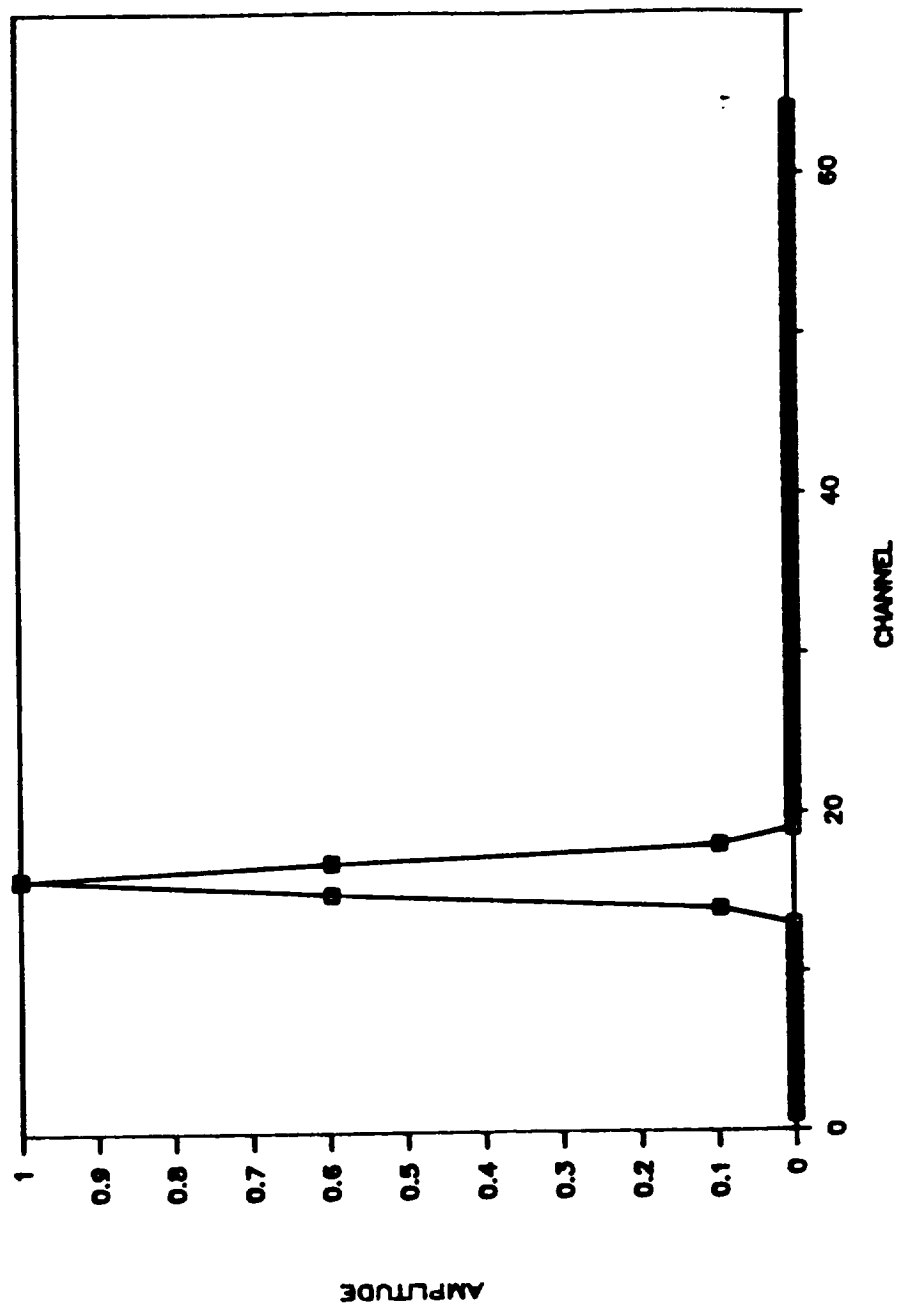


FIGURE 5.14

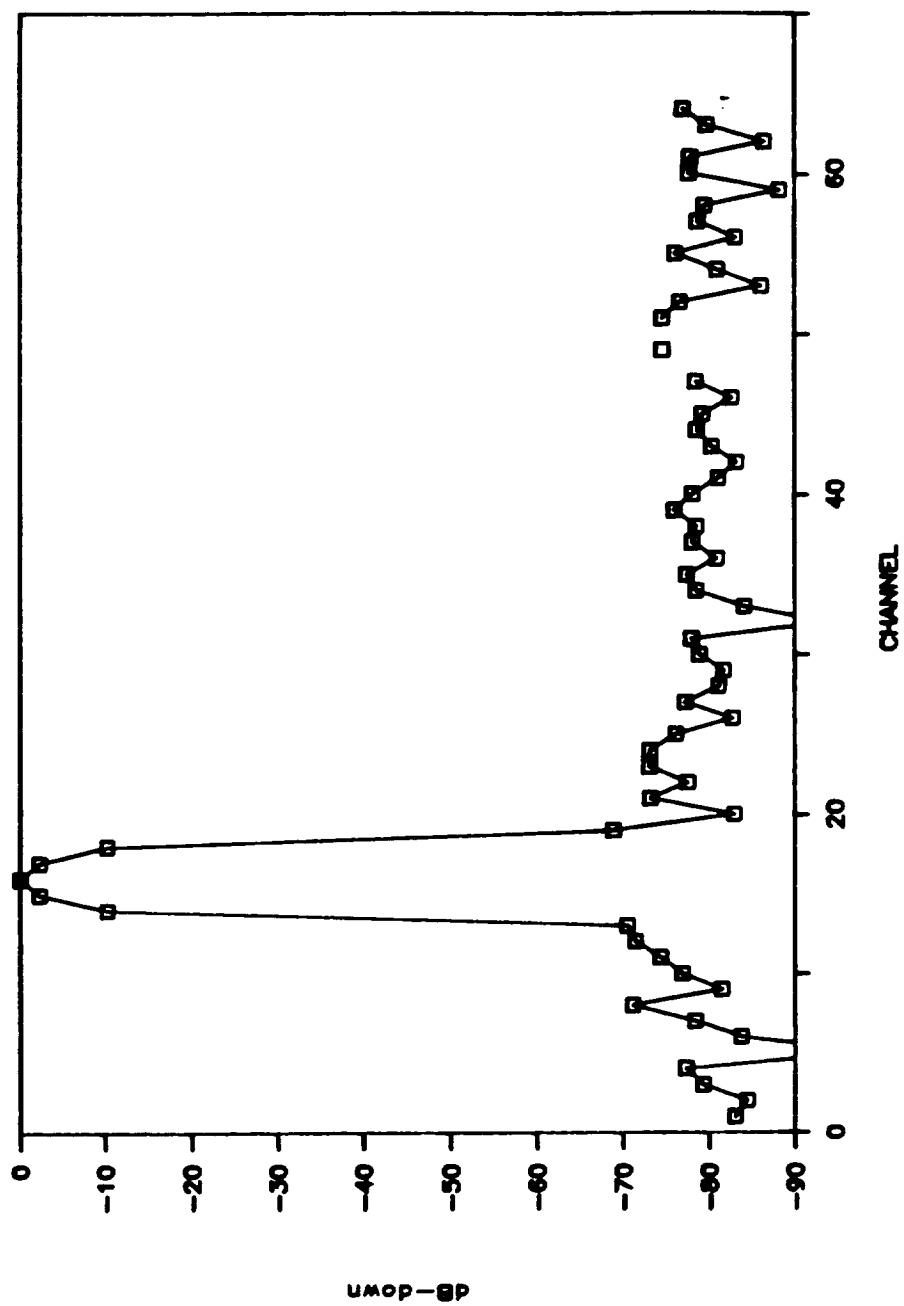


FIGURE 5.15

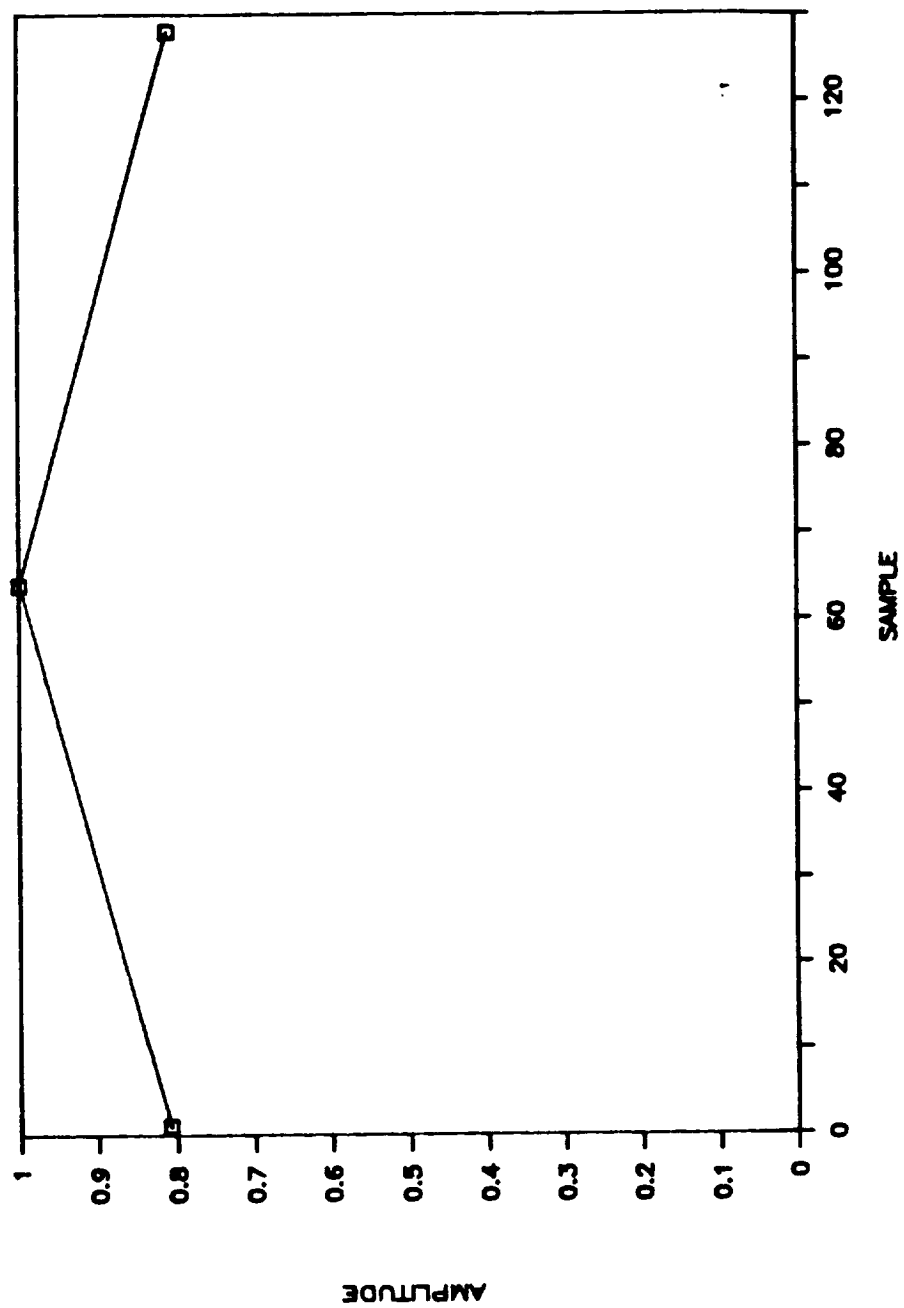


FIGURE 5.16

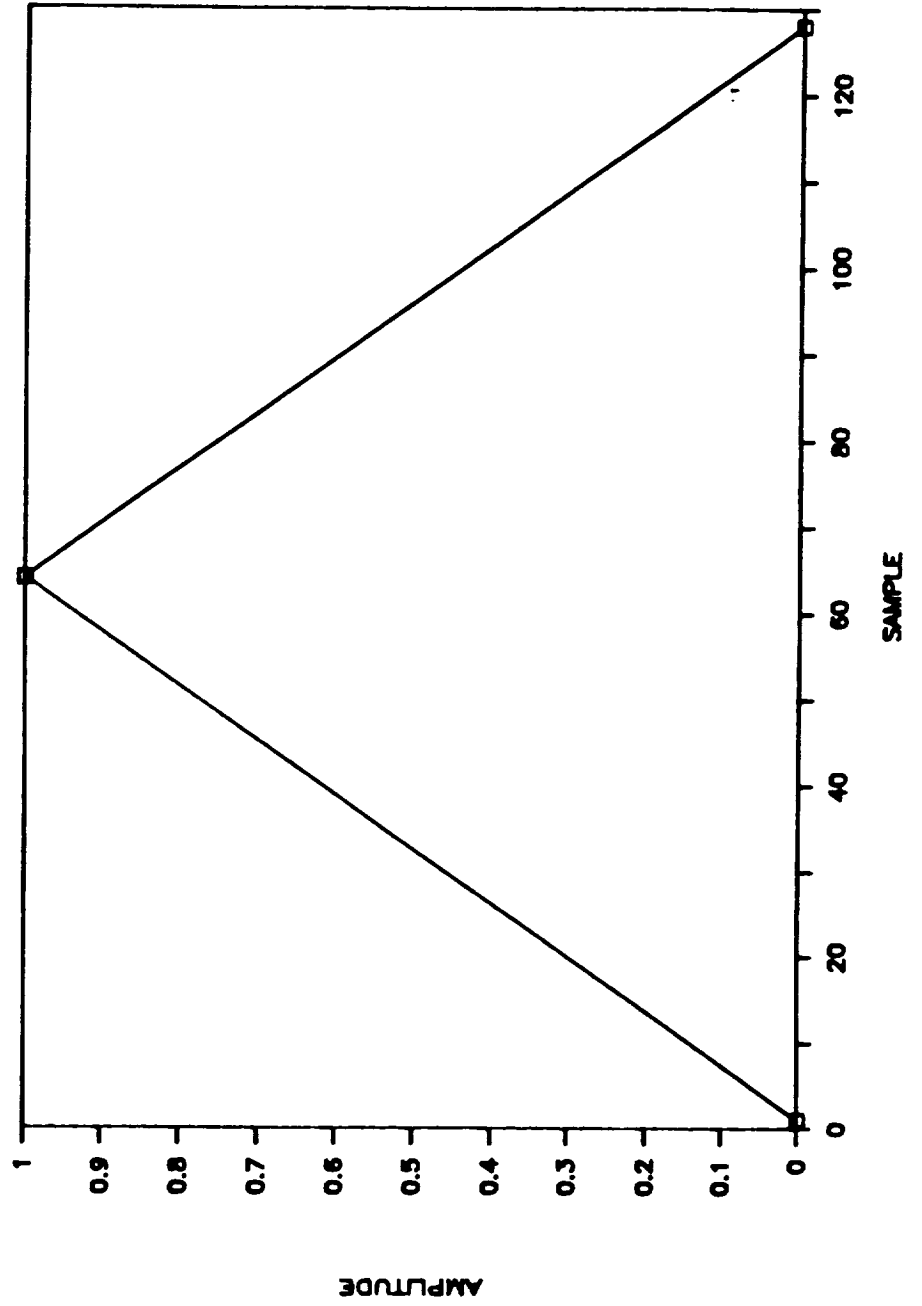


FIGURE 5.17

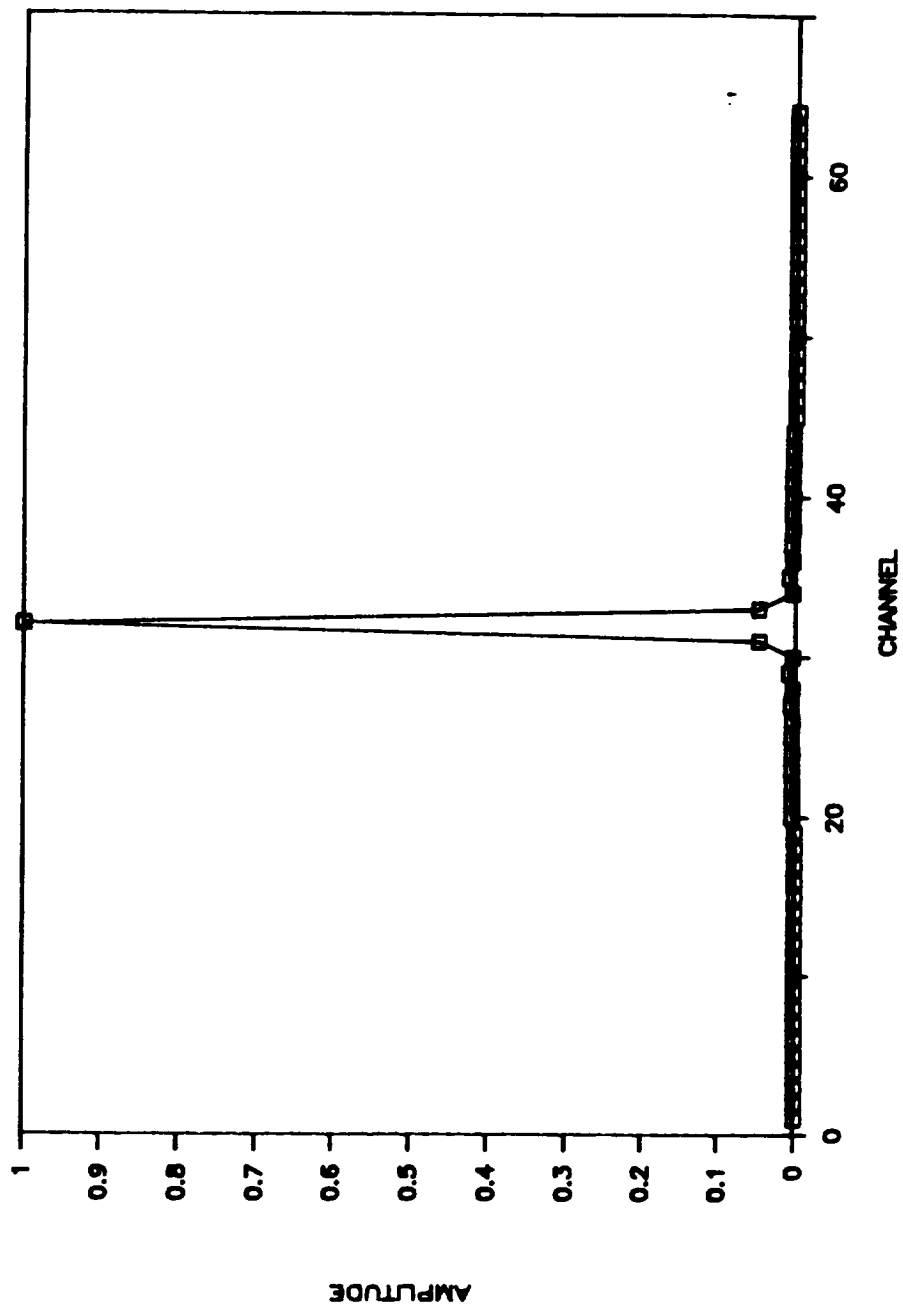


FIGURE 5.18

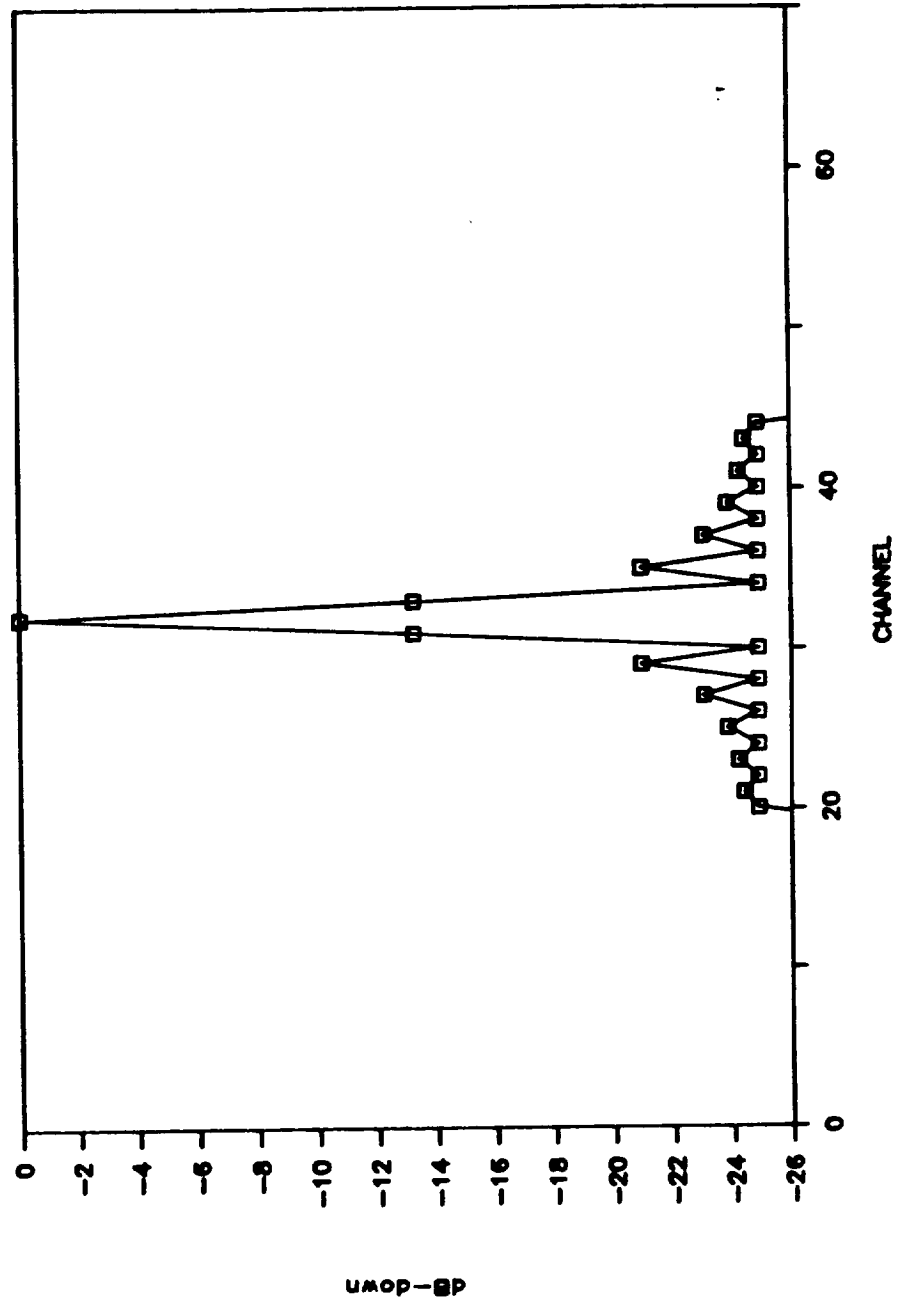




FIGURE 5.19

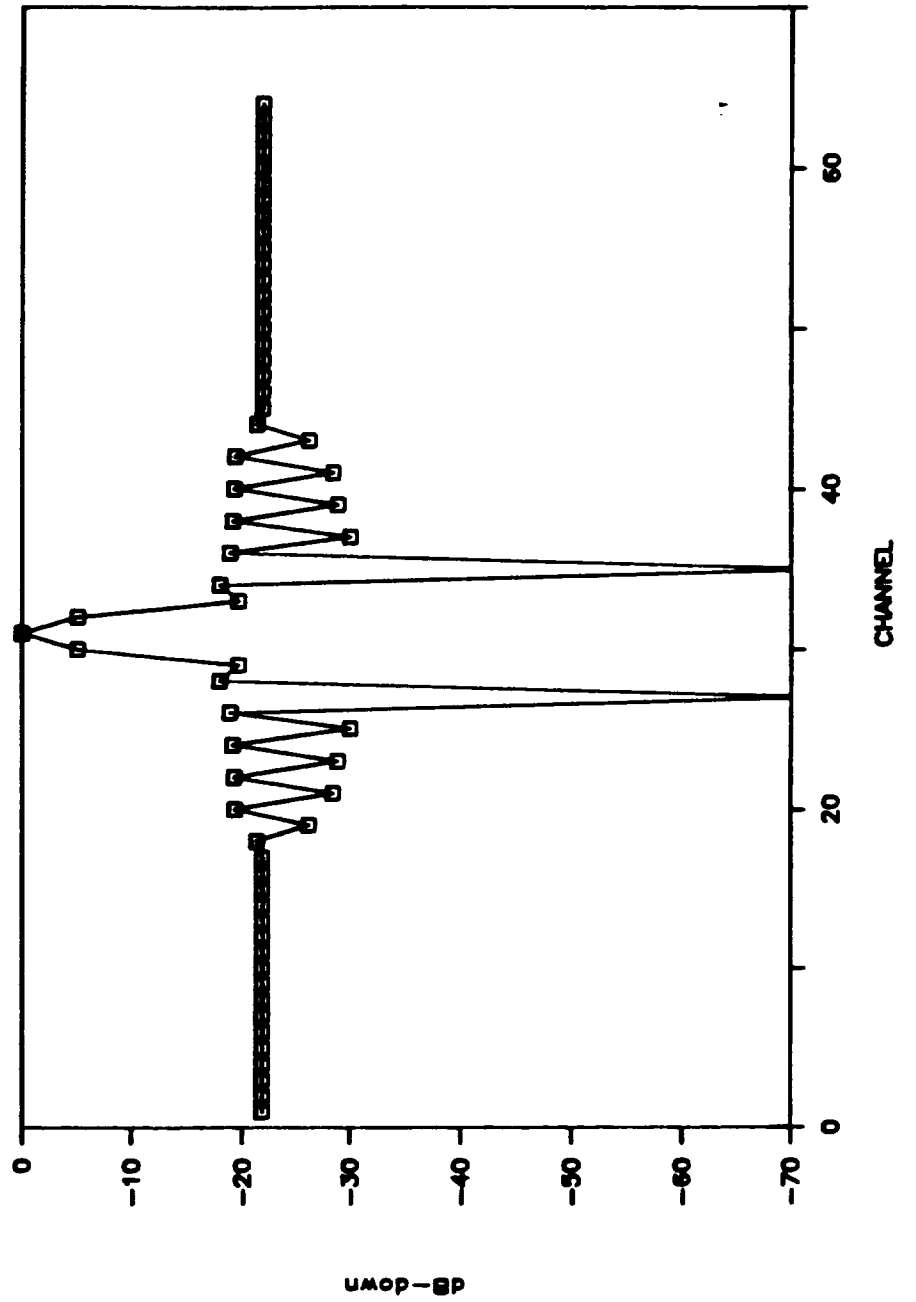


FIGURE 5.20

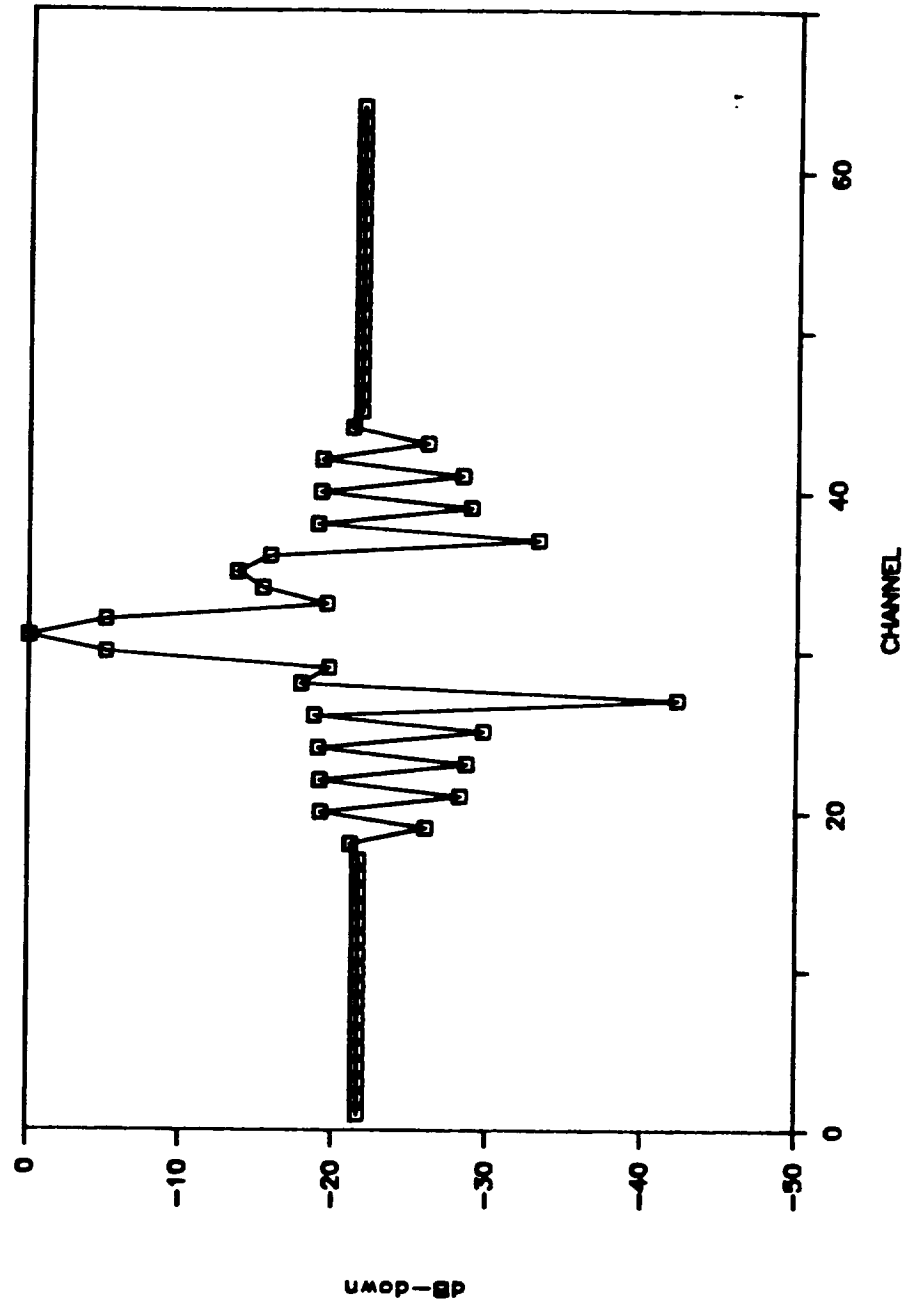


FIGURE 5.21

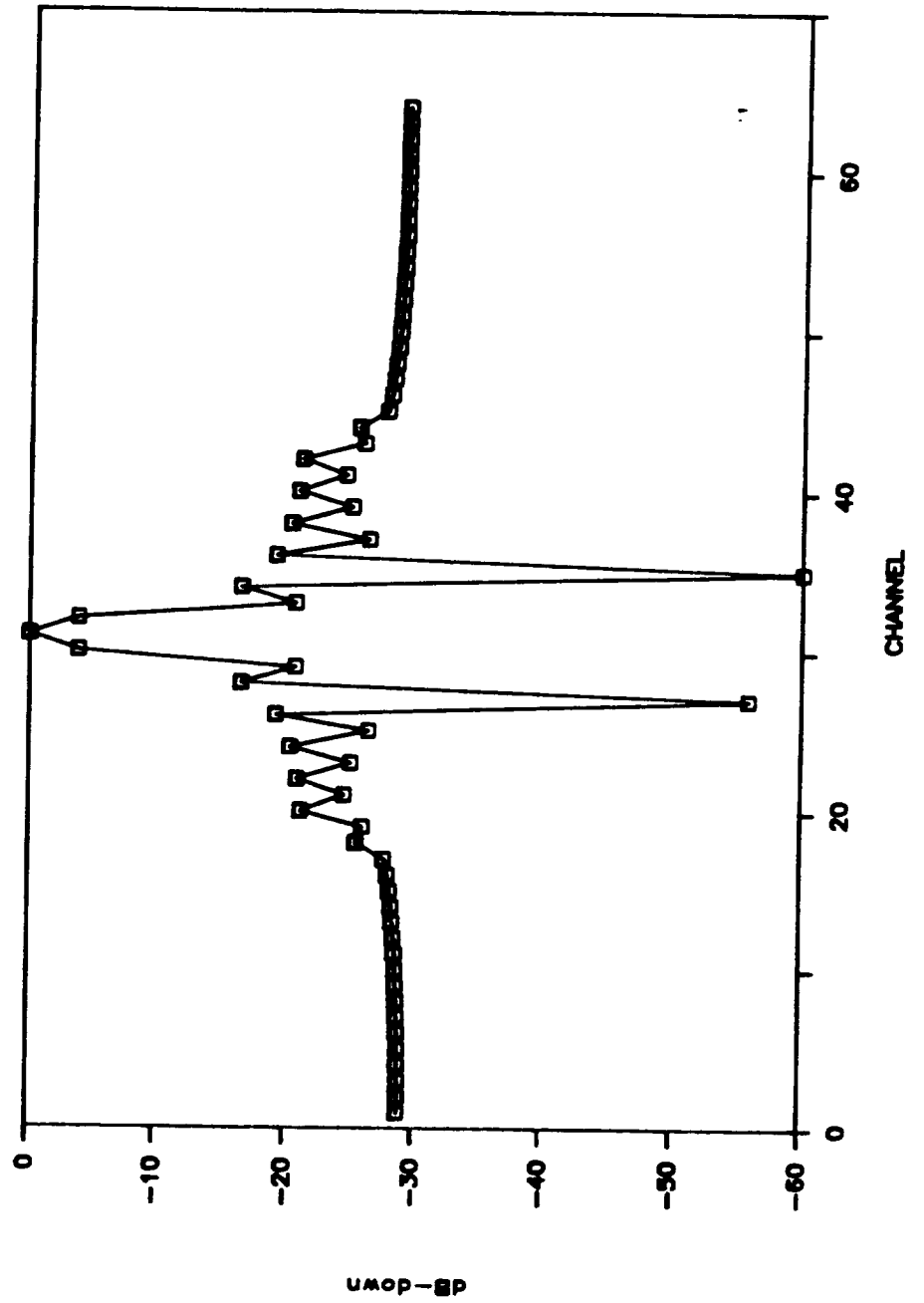


FIGURE 5.22

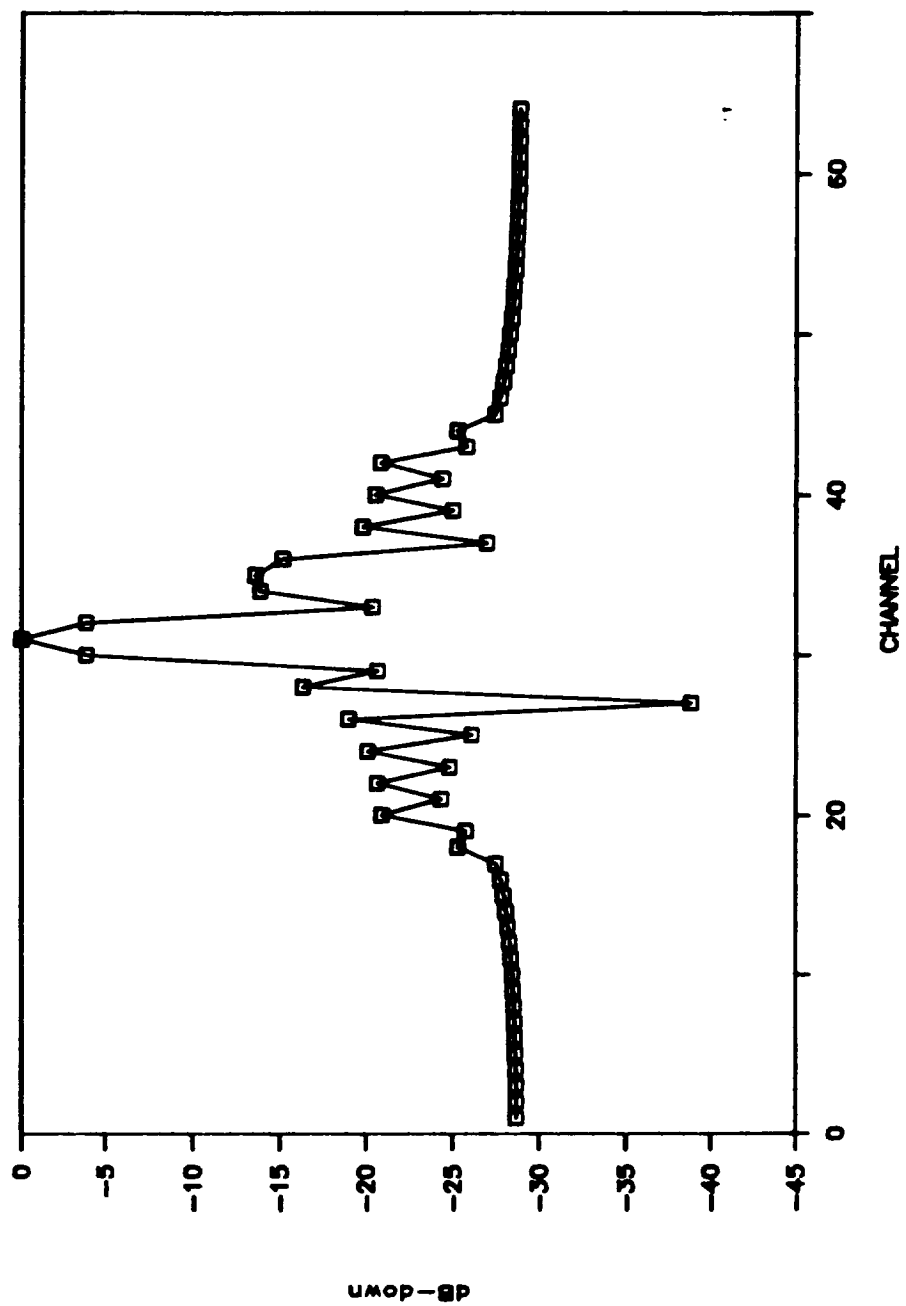


FIGURE 5.23

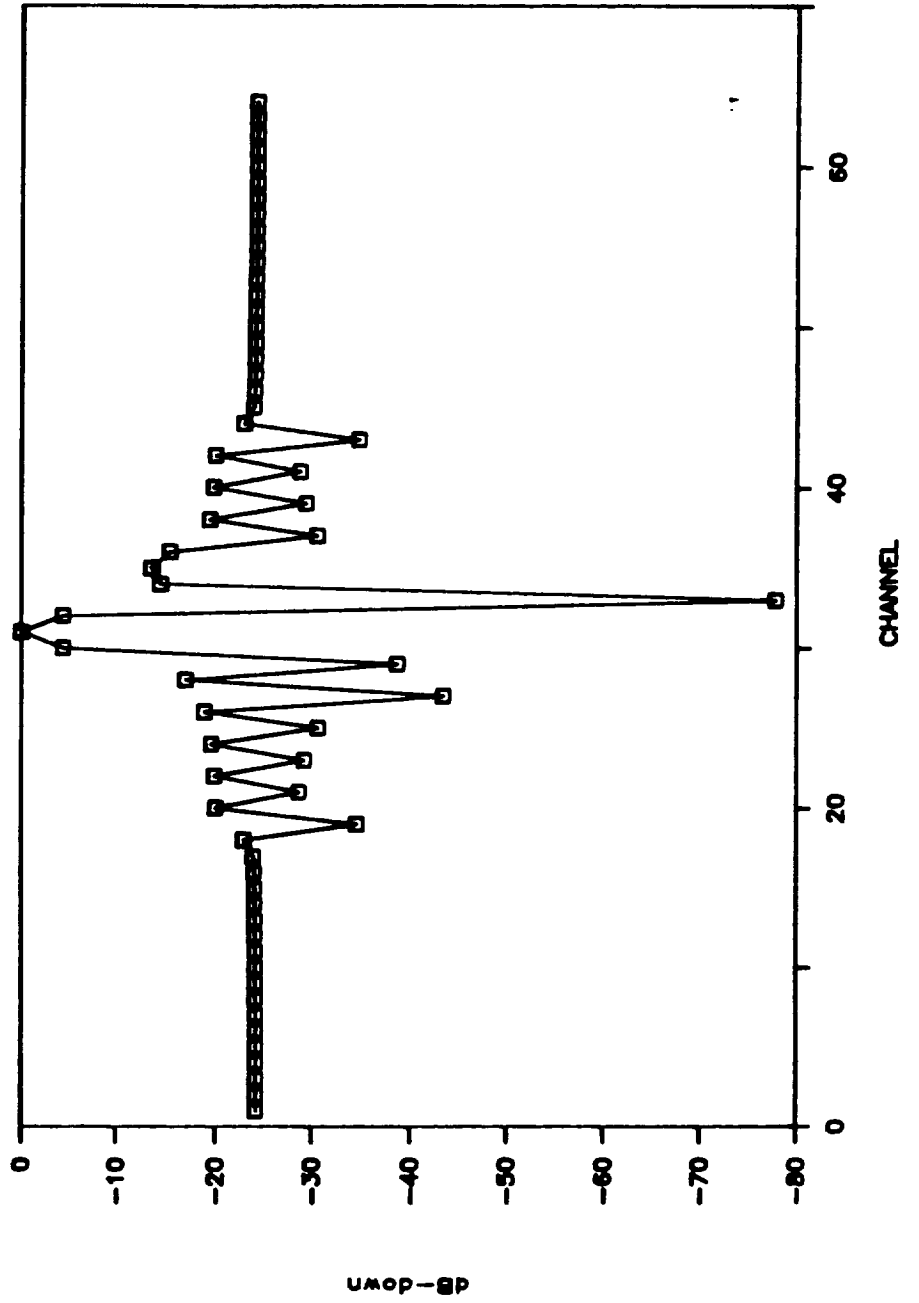


FIGURE 5.24

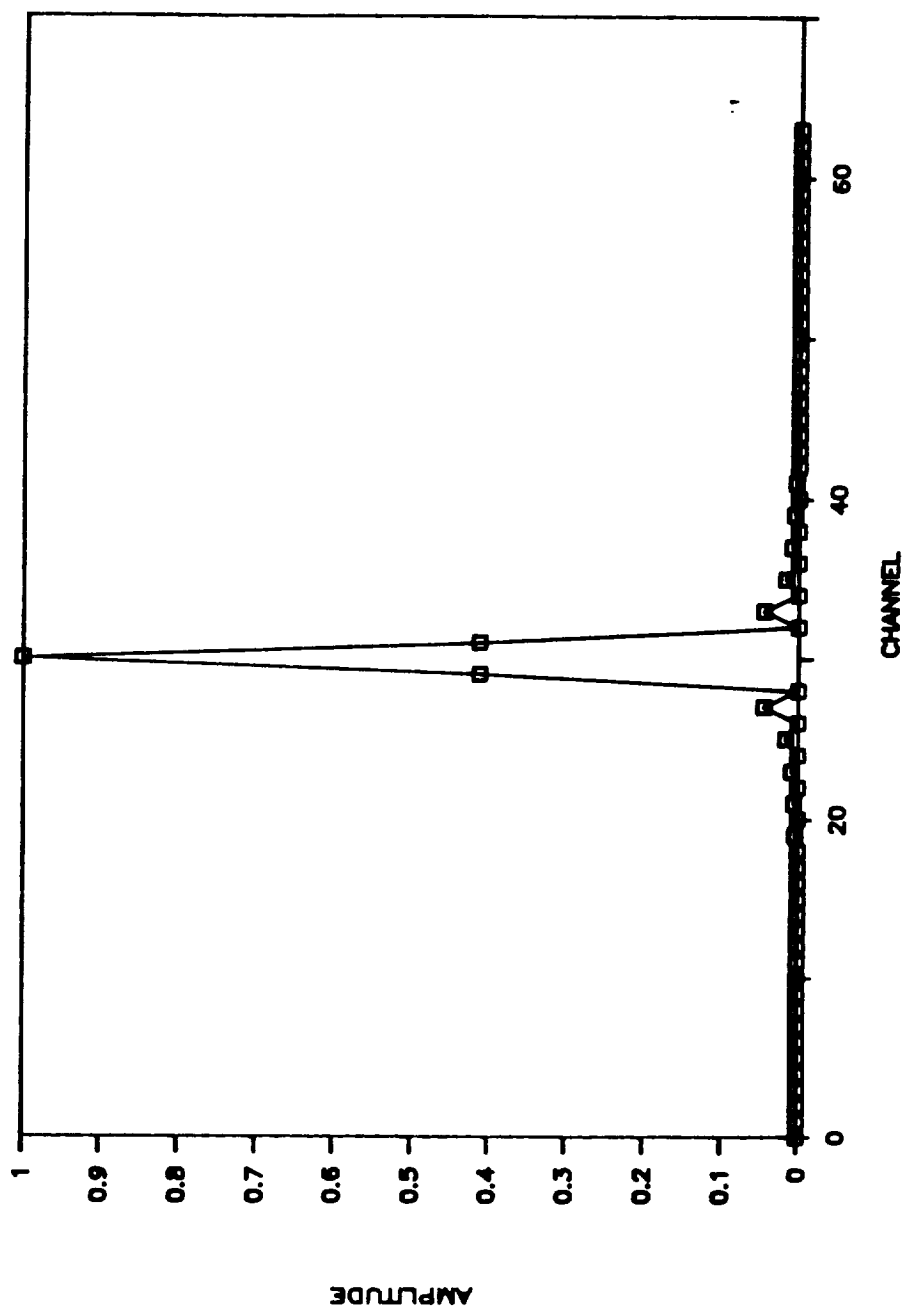


FIGURE 5.25

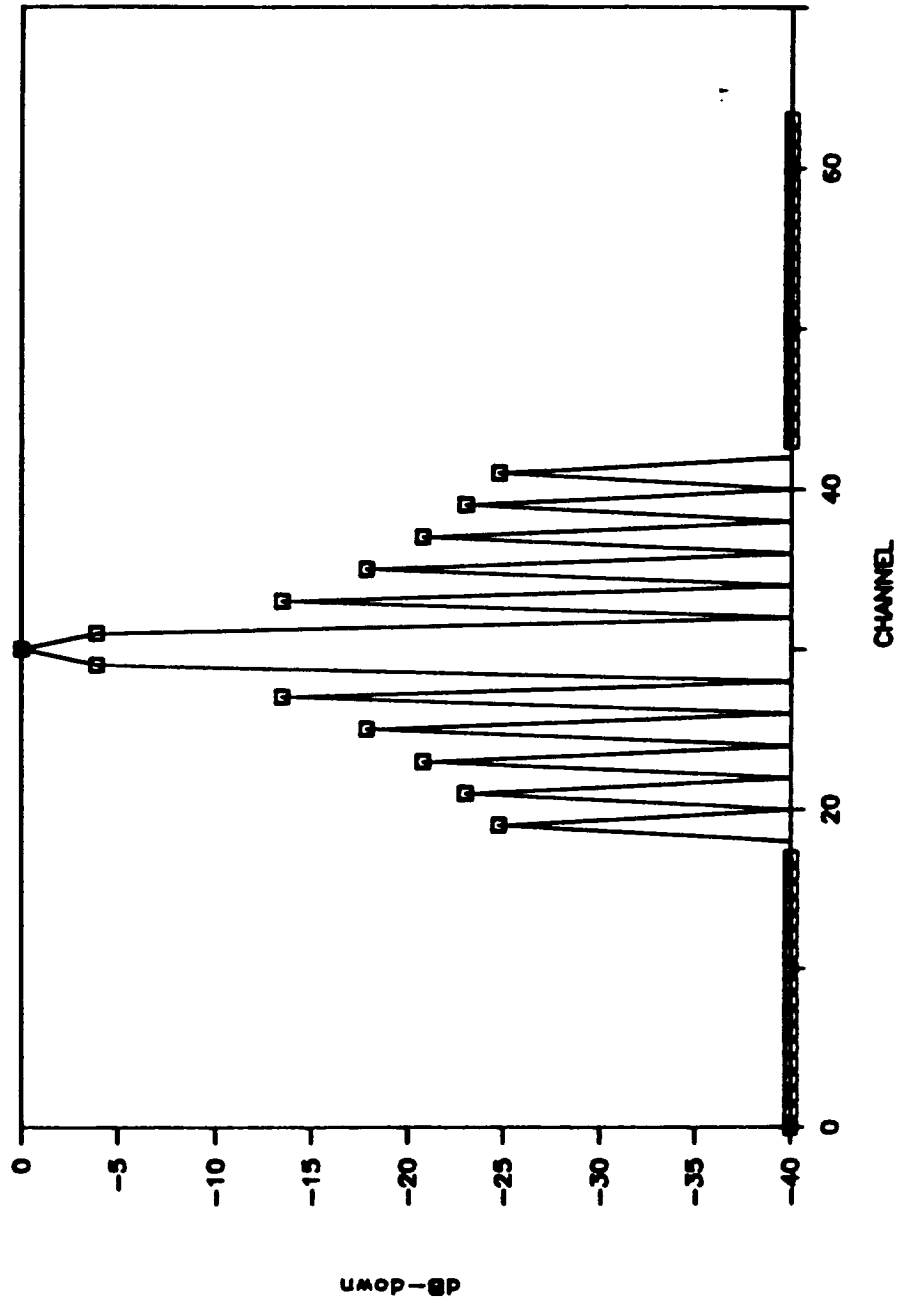


FIGURE 5.26

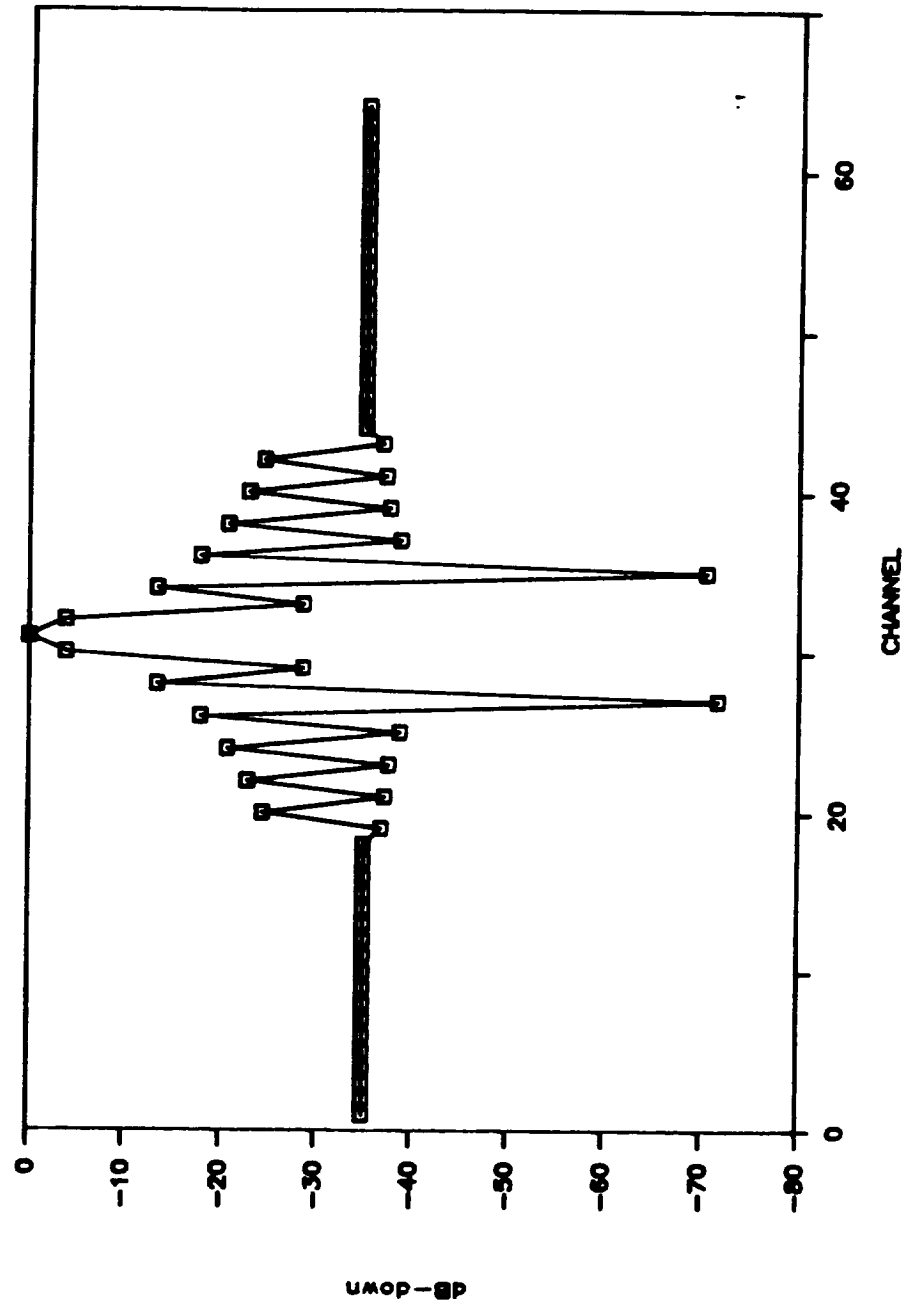




FIGURE 5.27

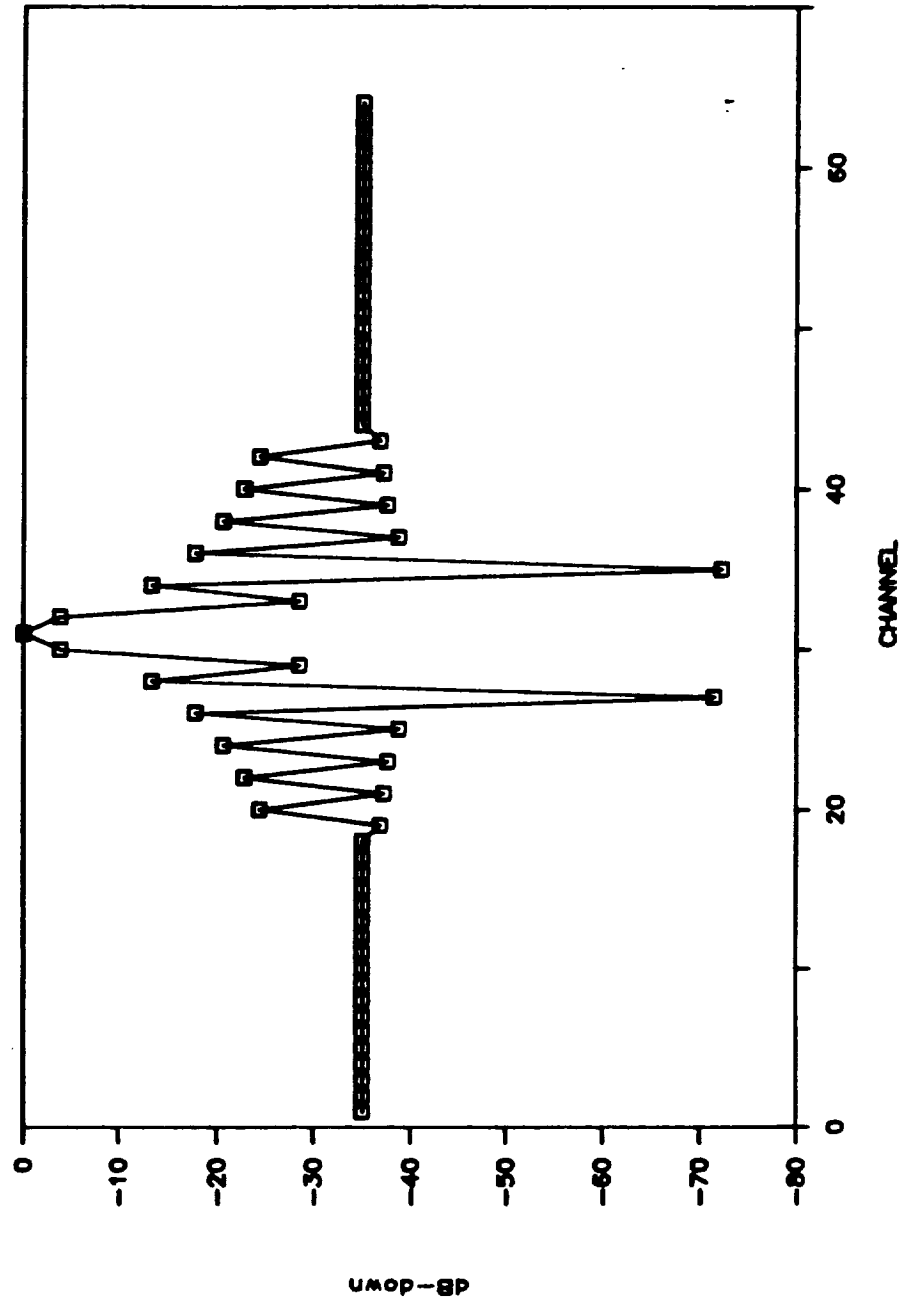


FIGURE 5.28

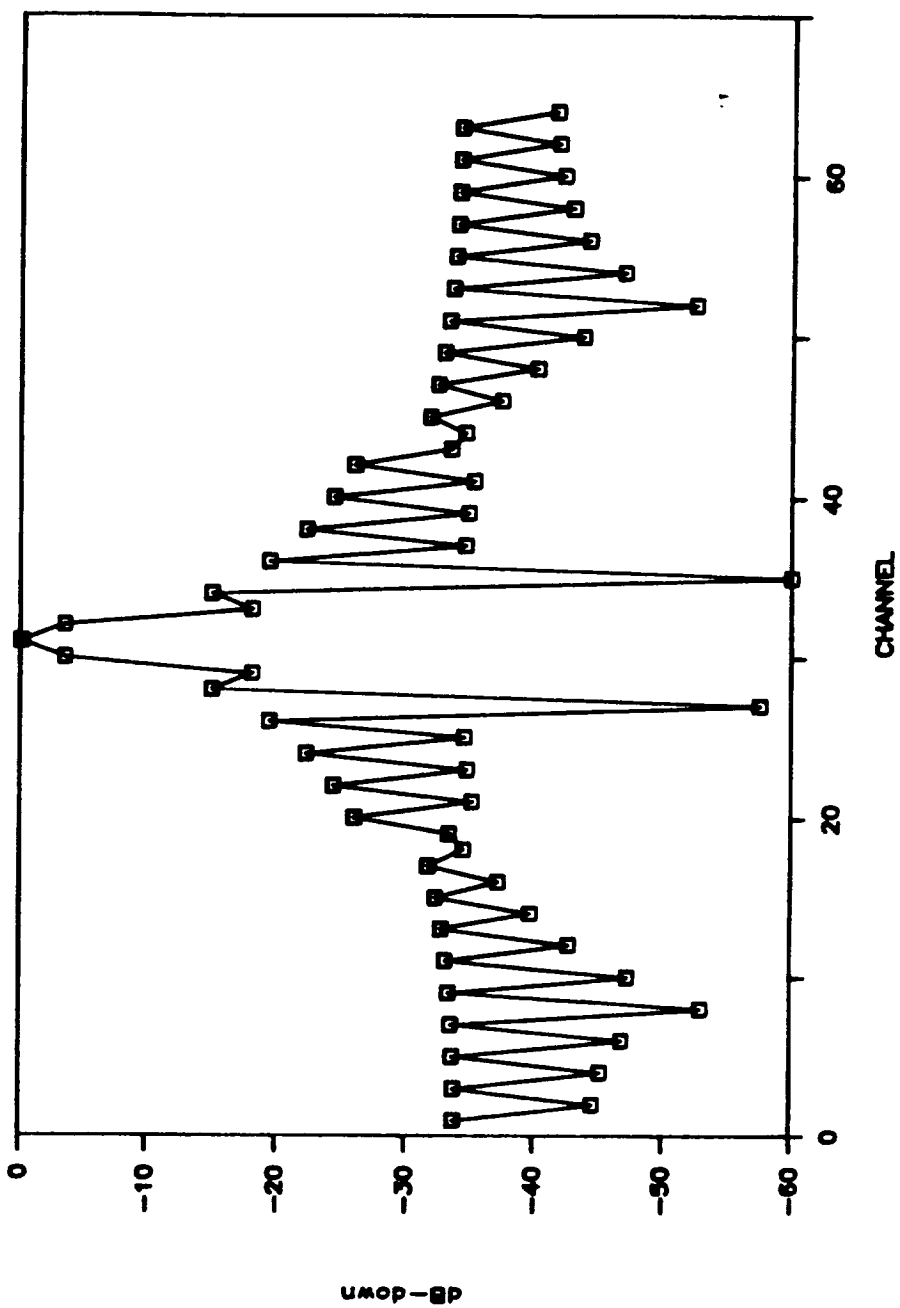


FIGURE 5.29

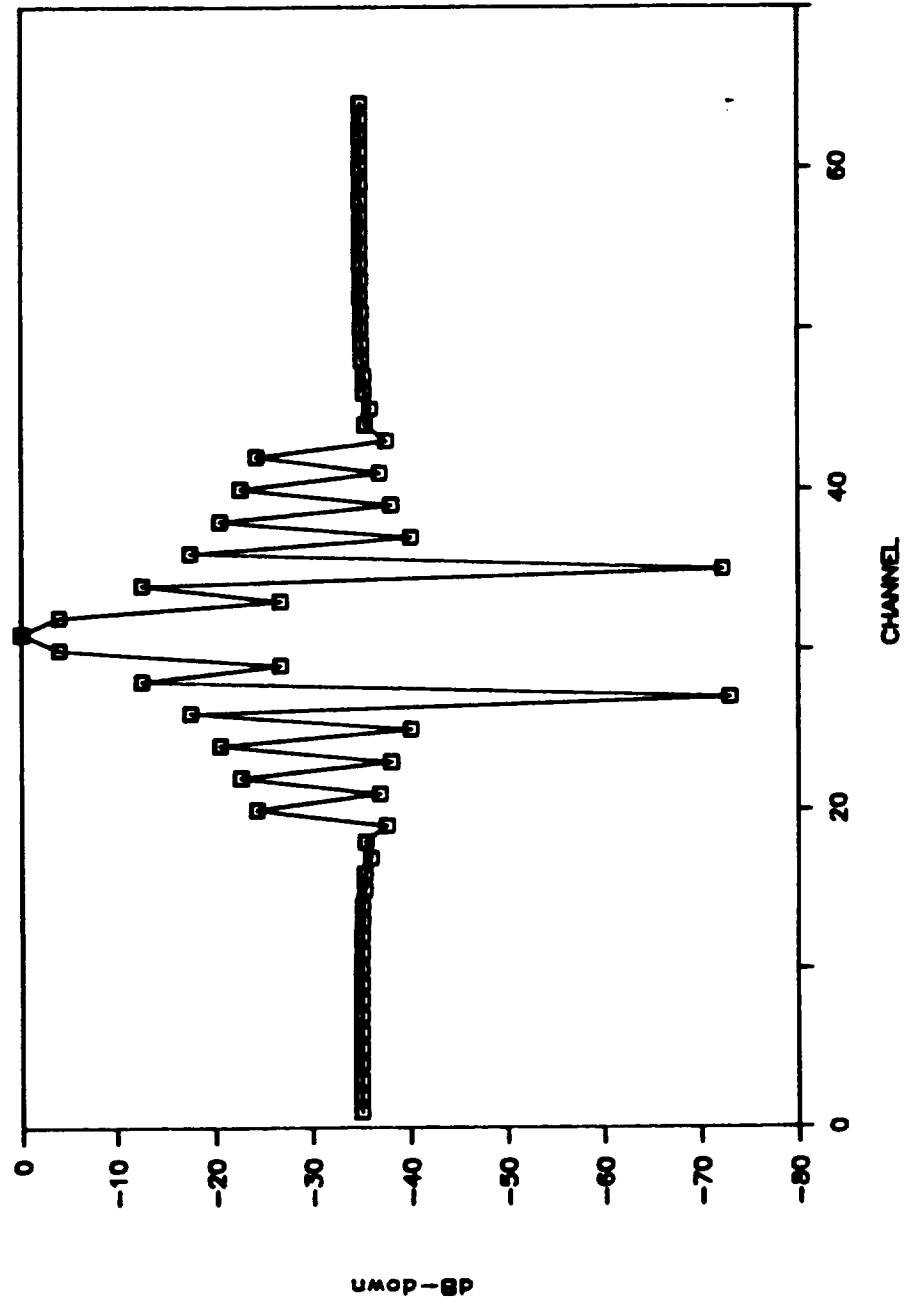


FIGURE 5.30

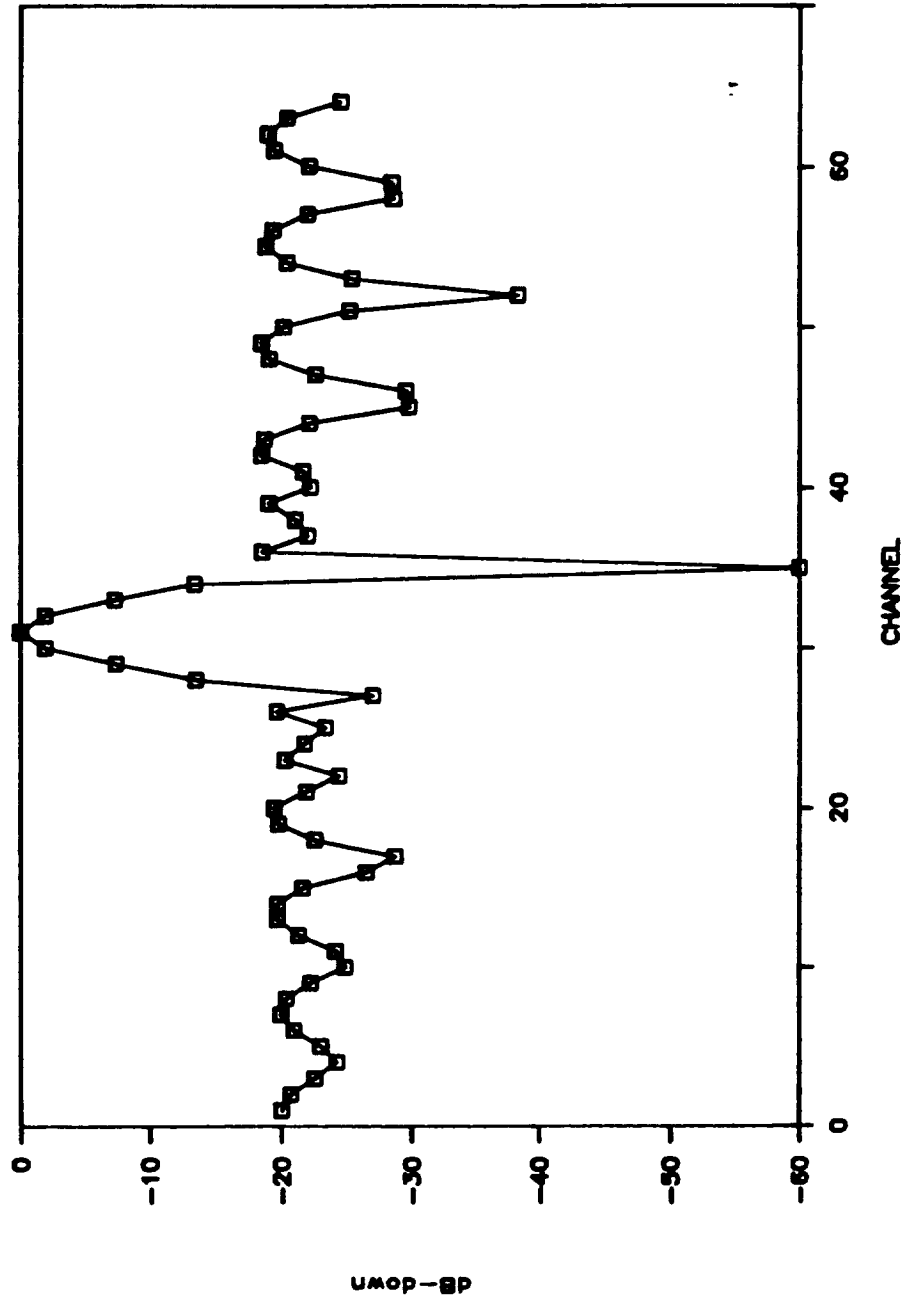


FIGURE 5.31

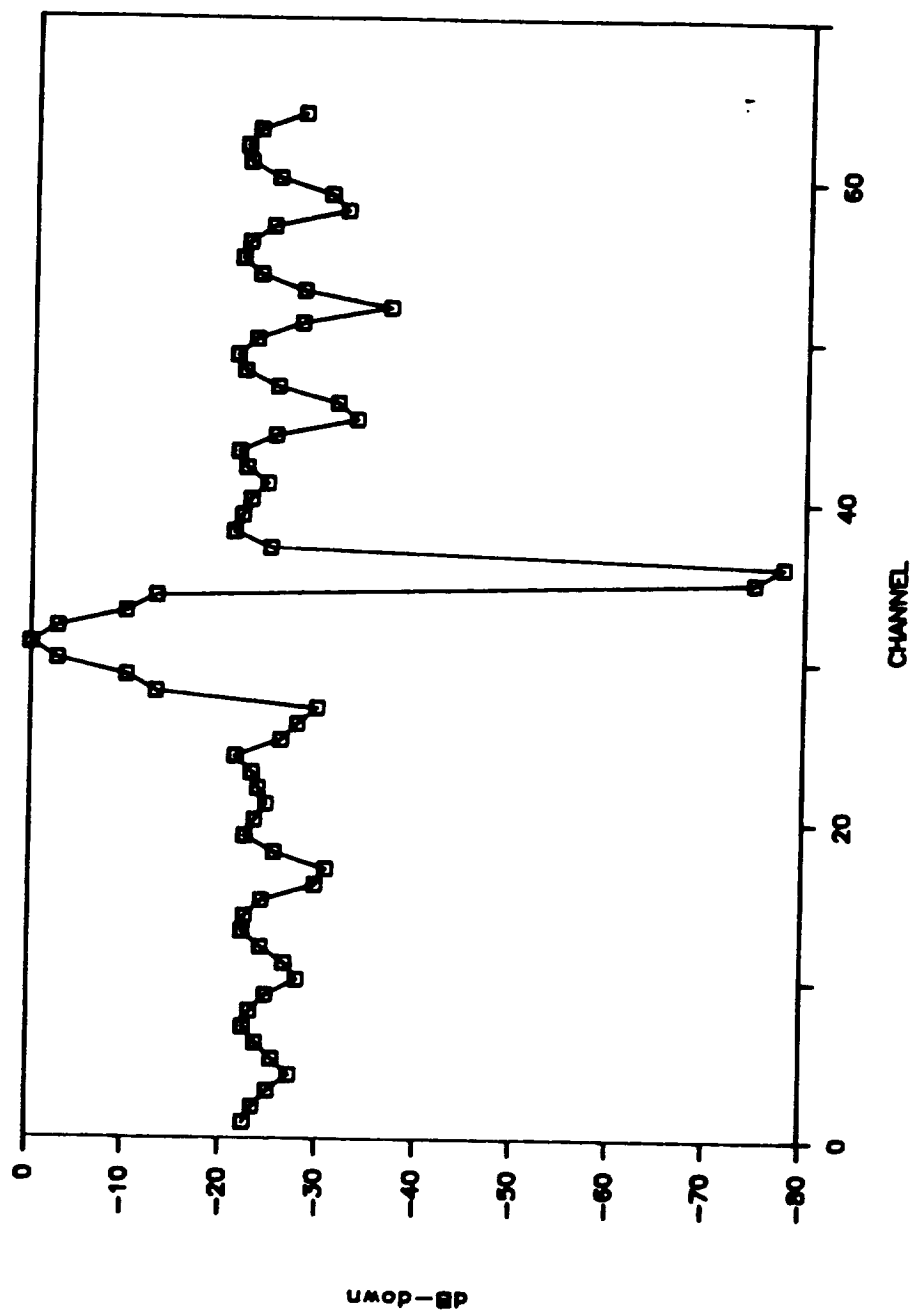


FIGURE 5.32

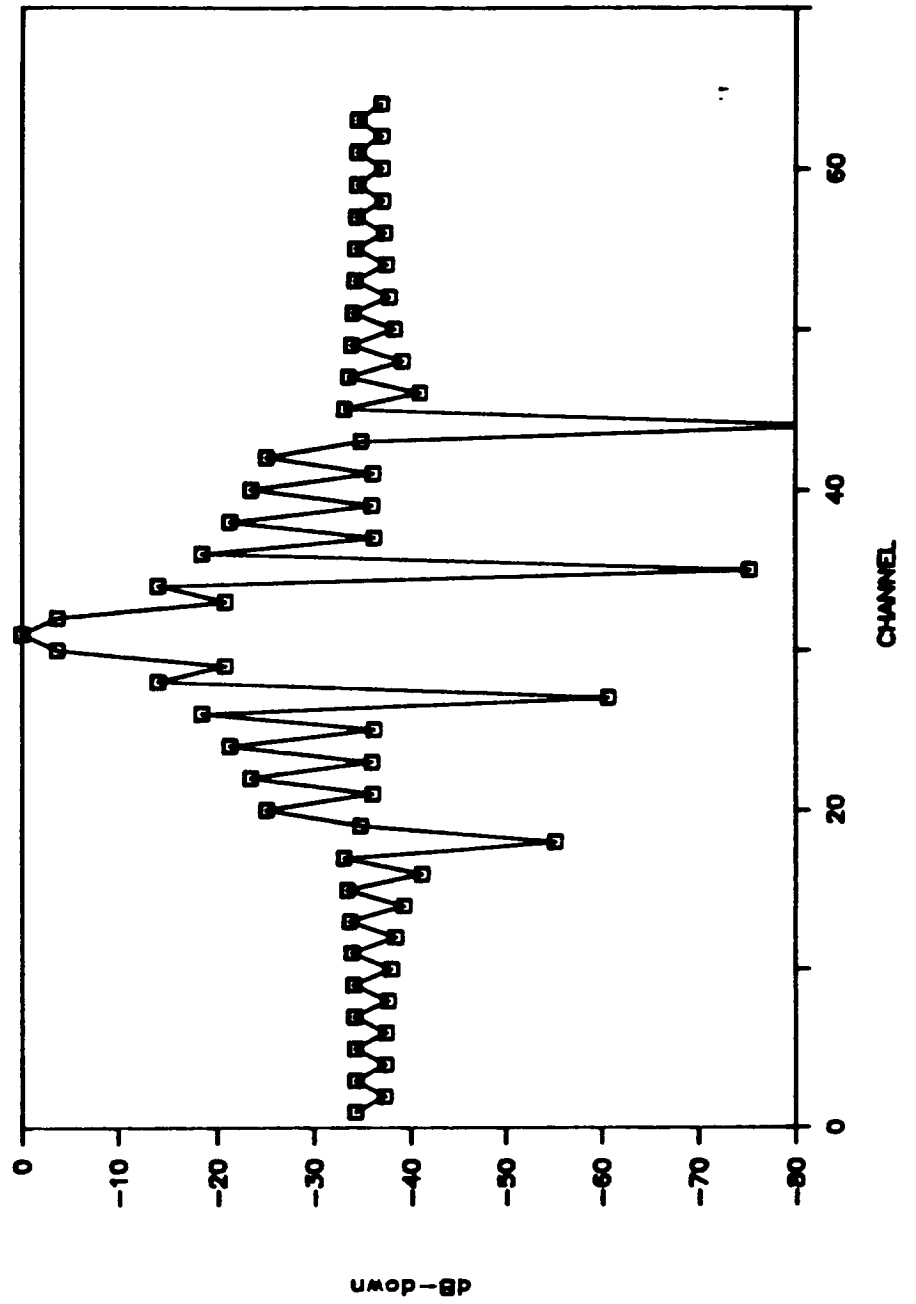


FIGURE 5.33

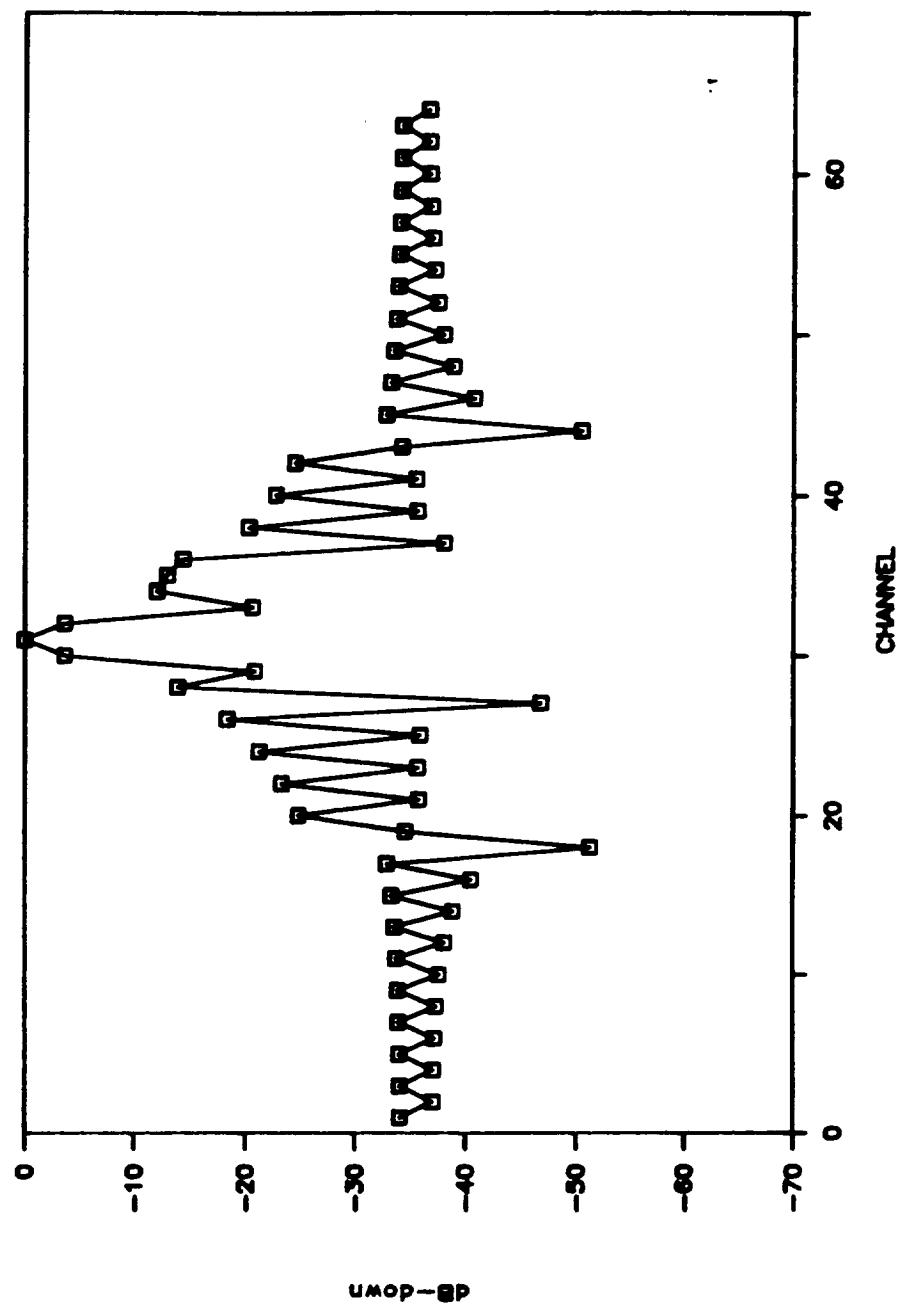


FIGURE 5.34

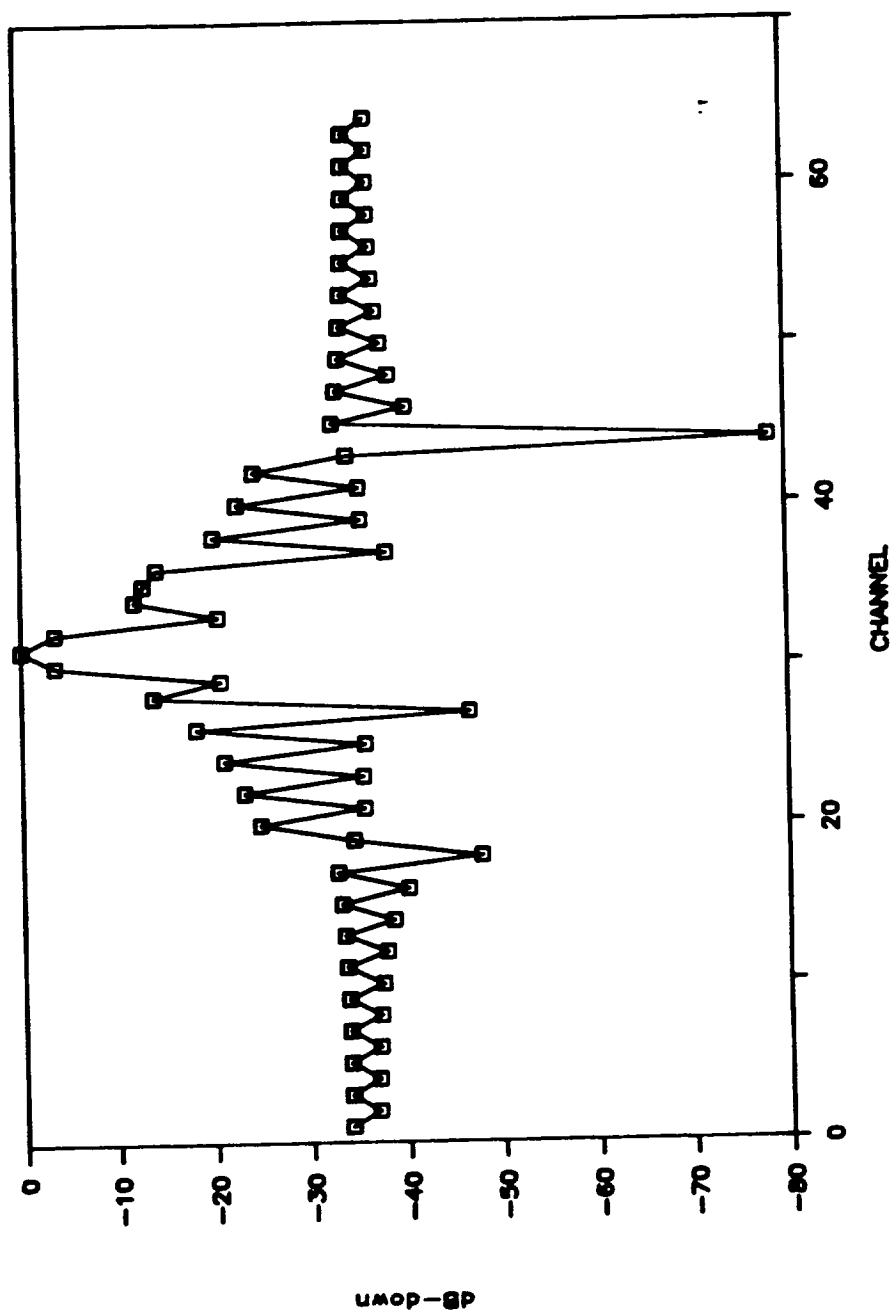




FIGURE 5.35

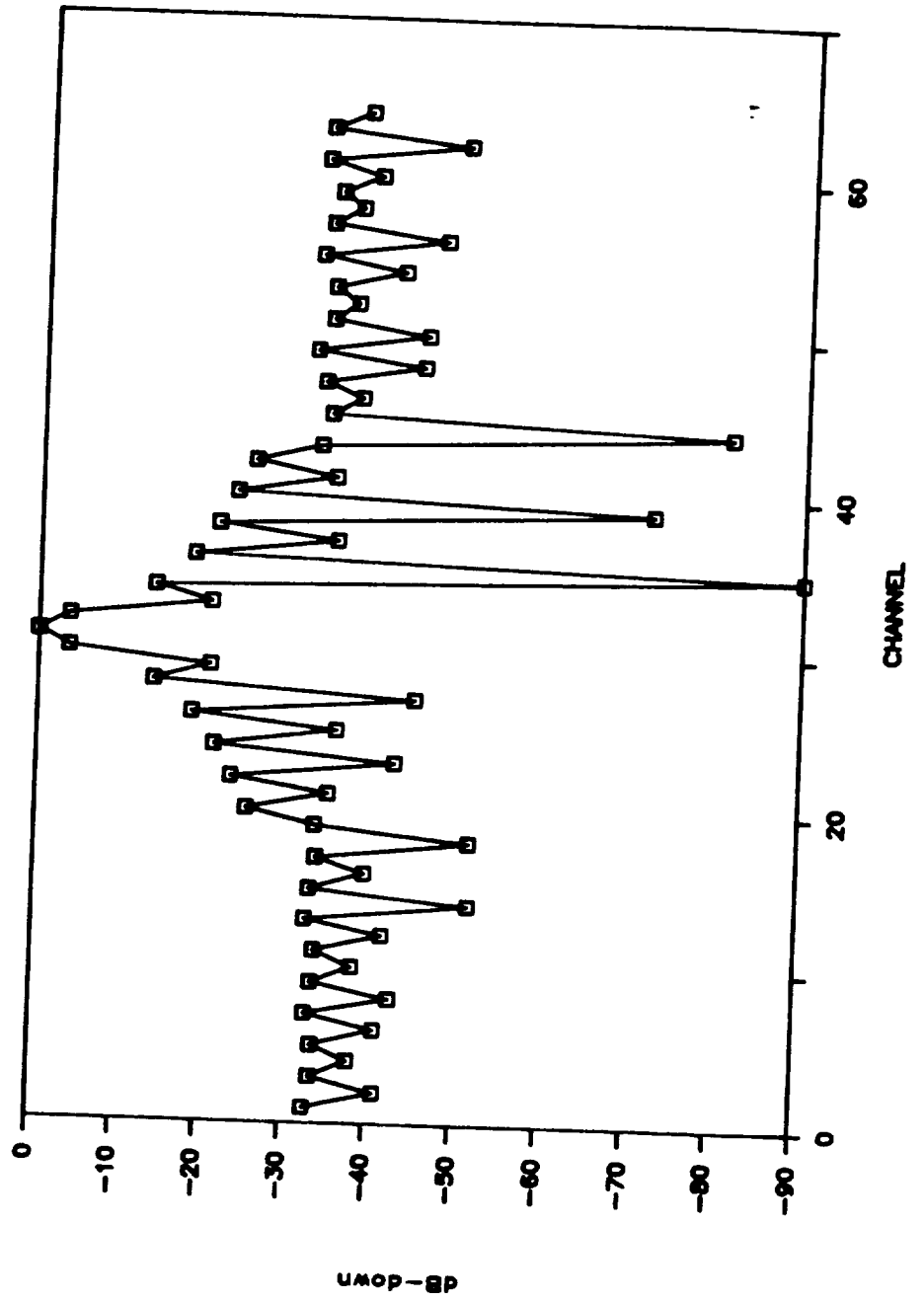


FIGURE 5.36

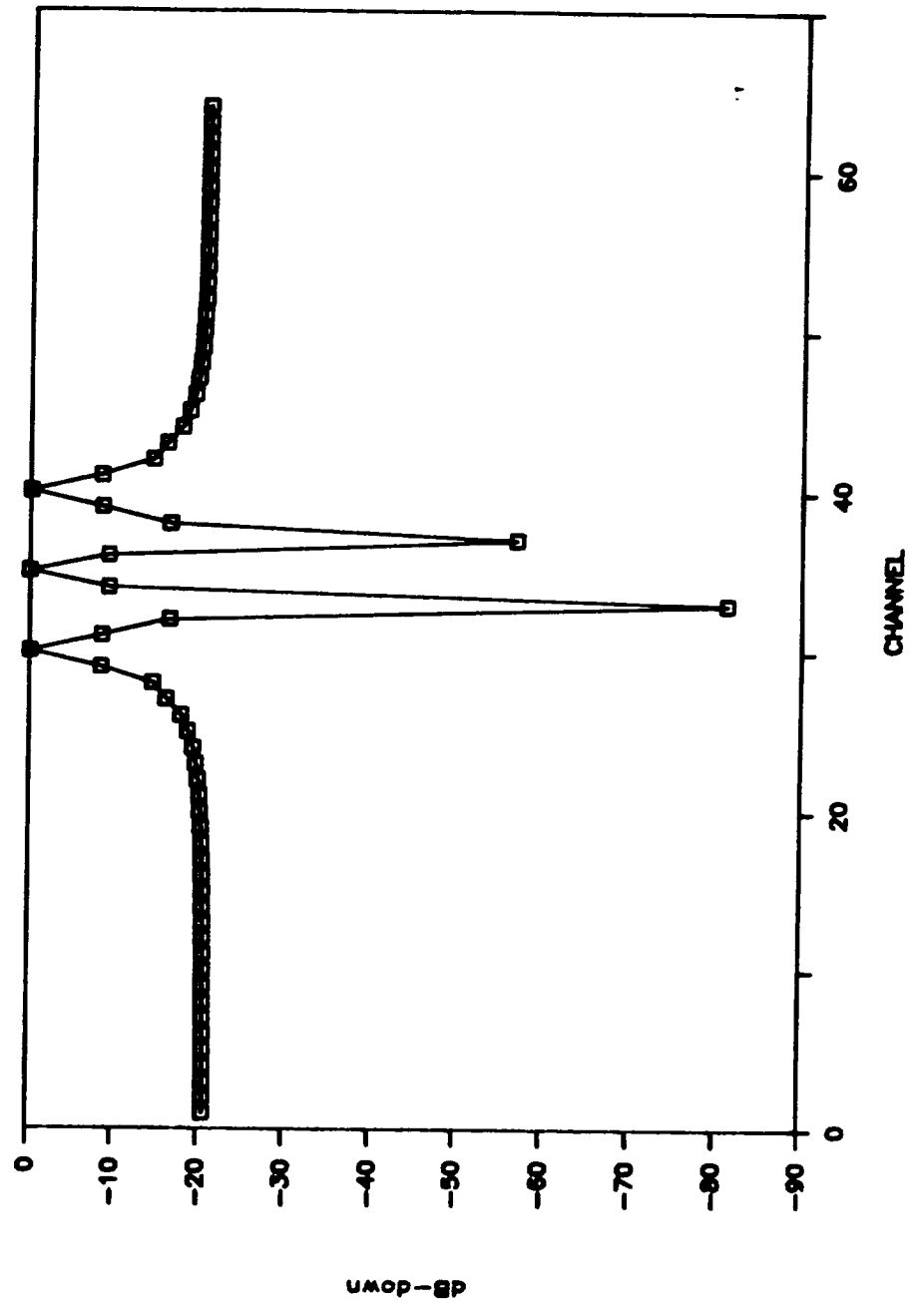
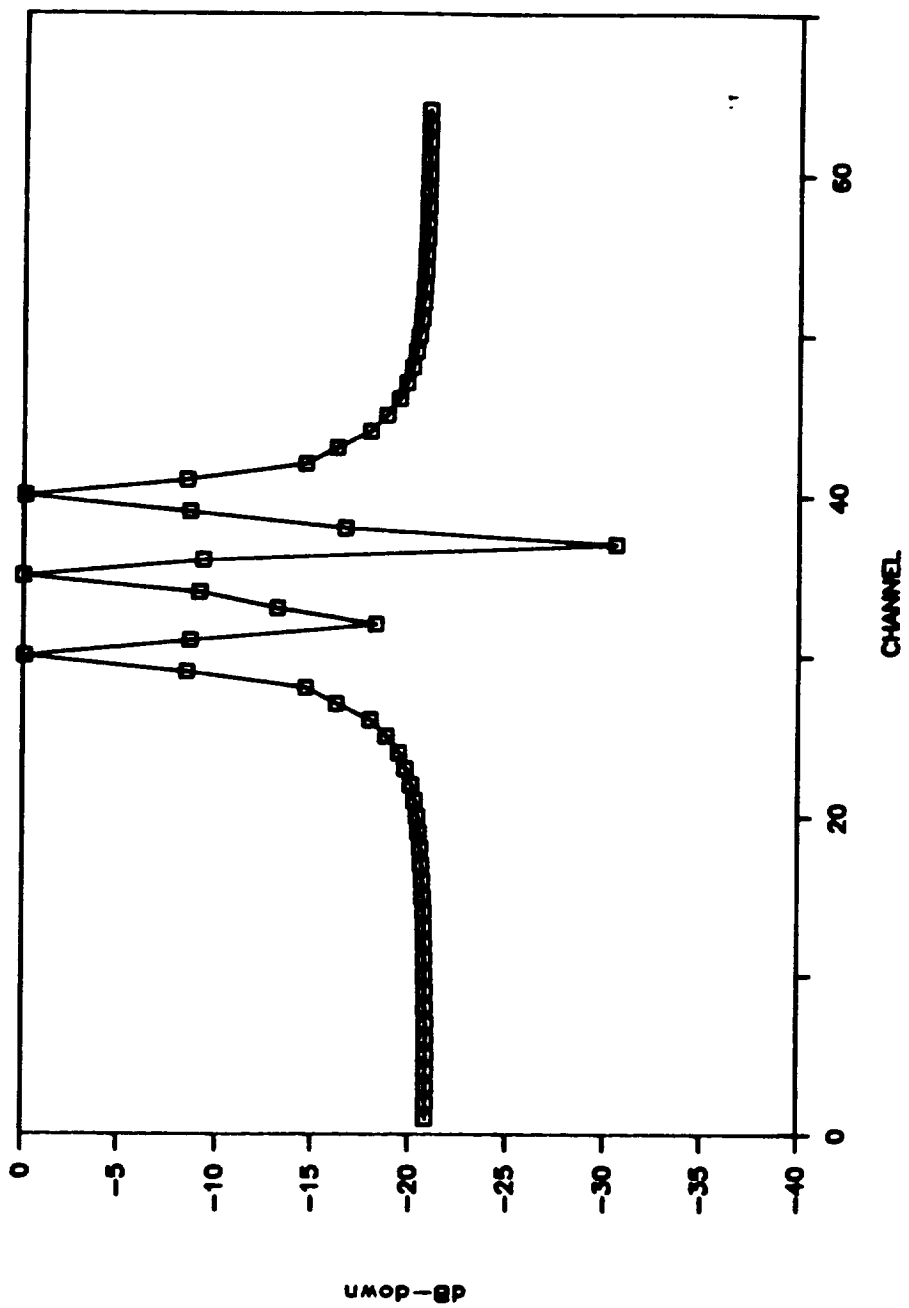


FIGURE 5.37



## BIBLIOGRAPHY

1. Blackman, R. B., and Tukey, J. W., "Measurement of Power Spectra", (Dover, New York, 1958).
2. Bracewell, R. N., "The Fourier Transform and Its Applications", (New York: McGraw-Hill, 1978).
3. Brigham, E. O., "The Fast Fourier Transform", (Englewood Cliffs, New Jersey: Prentice Hall Inc., 1974).
4. Geckinli, N. C., Yavuz, D., "Discrete Fourier Transform and Its Applications to Power Spectra Estimation", (Elsevier Scientific Publishing Company, New York, New York, 1983).
5. Harris, F. J., "On the Use of Windows for Harmonic Analysis With the Discrete Fourier Transform", IEEE V. 66, No. 1 (January 1978).
6. Kanasewich, E. R., "Time Sequence Analysis Geophysics", University of Alberta Press, (Edmonton, Alberta, Canada, 1981).
7. Nuttall, A. H., "Some Windows With Very Good Sidelobe Behavior", IEEE V. ASSP-29, No. 1 (February 1981).
8. Oppenheim, A. V., Schafer, R. W., "Digital Signal Processing", (Englewood Cliffs, New Jersey: Prentice-Hall Inc., 1975).
9. Priestly, M. B., "Spectral Analysis and Time Series", (Orlando, Florida: Academic Press, 1981).
10. Robinson, E. A., "Physical Application of Stationary Time-Series", (New York: McMillan Publishing, 1980).
11. Smith, H. M., "Creating Clear Channels by Minimizing Sidelobes in Power Spectral estimates Using Linear Combinations of Autocorrelation Windows", Master of Science Thesis, Dept. of Physics: University of New Orleans, New Orleans, Louisiana, 1985.

## APPENDIX 1

```

DIMENSION A(20), Q(20), W(257), F(513), FT(513), X(257)
PRINT 10
10  FORMAT(' ENTER NO. OF PARTITIONS  ')
    READ *, N
    PRINT 20
20  FORMAT(' ENTER NF  ')
    READ *, NF
    PI=3.1415927
    T=0.
    PRINT 30
30  FORMAT(' ENTER NO. OF WINDOWS  ')
    READ *, M
    DO 50 I=1,M
    PRINT *, 'WINDOW NUMBER ',I
    PRINT 43
43  FORMAT(' ENTER COEF.  ')
    READ *, A(I)
    PRINT 44
44  FORMAT(' ENTER SUBSCRIPTS  ')
50  READ *, Q(I)
51  NF=2
52  NF=NF*2
    PRINT *, 'NF=',NF
    IF(NF.LT.N) GO TO 52
    NF2=2*NF
    DO 99 K=1,NF
    W(K)=0.
    IF(K.GT.N) GO TO 99
    DO 90 II=1,M
    IF(T.EQ.0.) W(K)=1.
    IF(T.EQ.0.) GO TO 90
    IF(Q(II).GT.1.) GO TO 70
    IF(T.LE.NF) W(K)=W(K)+A(II)
70  W2=(1.-4.*(T**2))
    IF(Q(II).EQ.2.) W(K)=W(K)+A(II)*W2
    IF(Q(II).EQ.3.) W(K)=W(K)+A(II)*COS(PI*T)
    IF(Q(II).EQ.4.) W(K)=W(K)+A(II)*(SIN(2.*PI*T)/(2.*PI*T))
    IF(Q(II).EQ.5.) W(K)=W(K)+A(II)*(1.+2.*(ABS(T)))
    IF(Q(II).EQ.6.) W(K)=W(K)+A(II)*(.5+.5*COS(2.*PI*T))
    W1=1.
    IF(Q(II).EQ.7.) W(K)=W(K)+A(II)*(.54+.46*COS(2.*PI*T))
    IF(Q(II).EQ.1.) W(K)=W(K)+A(II)*W1
    WB=(1./PI)*ABS(SIN(2.*PI*T))+(1.-2.*ABS(T)*COS(2.*PI*T))

```

```

IF(Q(II).EQ.8.) W(K)=W(K)+A(II)*W8
W9=.42+.5*COS(2.*PI*T)+.08*COS(4.*PI*T)
IF(Q(II).EQ.9.) W(K)=W(K)+A(II)*W9
IF(T.GT.(.25)) GO TO 71
IF(Q(II).GT.10.) GO TO 89
W10=1.-(24.*ABS(T)**2)*(1.-2.*ABS(T))
IF(Q(II).EQ.10) W(K)=W(K)+W10
71 IF(Q(II).LT.10.) GO TO 90
IF(Q(II).GT.10.) GO TO 89
IF(T.GE.(.25)) W(K)=W(K)+A(II)*2*(1.-2.*ABS(T))**3
89 IF(Q(II).EQ.11.) W(K)=W(K)+A(II)*(1.-2.*(ABS(T)))
IF(T.GE.(.15)) GO TO 88
W(K)=W(K)+A(II)*W1
GO TO 90
88 W12=(.5+.5*COS((2*PI*(ABS(T)-.15))/7.7))
IF(Q(II).EQ.12.) W(K)=W(K)+A(II)*W12
90 CONTINUE
IF(K.EQ.1) GO TO 99
W(NF2-K+2)=W(K)
99 T=T+1./(TM*2)
DO 80 L=1,NF2
W(NF+1)=0.
FT(2*L)=0.
80 FT(2*L-1)=W(L)/(TM*2)
DO 101 K2=1,2*NF2
101 X(K2)=0.
X(37)=.0000975
X(39)=.0033475
X(41)=.0000965
X(43)=.0050195
X(45)=.0000955
X(47)=.0083305
X(49)=.0000945
X(51)=.0163905
X(53)=.0000935
X(55)=.0456595
X(57)=.0000915
X(59)=.4115925
X(61)=1.0
X(63)=X(59)
X(65)=X(57)
X(67)=X(55)
X(69)=X(53)
X(71)=X(51)
X(73)=X(49)

```

```

X(75)=X(47)
X(77)=X(45)
X(79)=X(43)
X(81)=X(41)
X(83)=X(39)
X(85)=X(37)
X(221)=X(37)
X(219)=X(39)
X(217)=X(41)
X(215)=X(43)
X(213)=X(45)
X(211)=X(47)
X(209)=X(49)
X(207)=X(51)
X(205)=X(53)
X(203)=X(55)
X(201)=X(57)
X(199)=X(59)
X(197)=X(61)
X(195)=X(63)
X(193)=X(65)
X(191)=X(67)
X(189)=X(69)
X(187)=X(71)
X(185)=X(73)
X(183)=X(75)
X(181)=X(77)
X(179)=X(79)
X(177)=X(81)
X(175)=X(83)
X(173)=X(85)
502  CONTINUE
      CALL FFT(NP2,1,X)
      DO 102 K3=1,NP2
        FT(2*K3)=0.
102    FT(2*K3-1)=W(K3)*X(2*K3-1)
      WRITE(75,405) (k,w(k),k=1,np2)
405    FORMAT(14,2X,F16.8)
      WRITE(76,*) (FT(K),K=1,2*NP2)
      CALL FFT(NP2,-1,FT)
      DO 401 IK=1,2*NP2
401    FT(IK)=FT(IK)/64.
205    FORMAT(F4.1,2X,E16.8)
      DO 206 IA=1,2*NP2-1,2
206    X(IA)=(IA+1)/2

```

```

WRITE(50,205) (X(IA),FT(IA),IA=1,127,2)
WRITE(51,*) (FT(IA),IA=2,2*NP2,2)
WRITE(59,*) ((1A+1)/2,IA=65,77,2),(FT(IA),1A=65,77,2)
PRINT 146
146 FORMAT(' REAL IN 50, IM IN 51')
201 STOP
END

SUBROUTINE FFT(NN,ISIGN,DATA)
DIMENSION DATA(600)
N=2*NN
J=1
DO 5 I=1,N,2
IF(I-J)1,2,2
1 TEMPR=DATA(J)
TEMP1=DATA(J+1)
DATA(J)=DATA(I)
DATA(J+1)=DATA(I+1)
DATA(I)=TEMPR
DATA(I+1)=TEMP1
2 M=N/2
3 IF(J-M)5,5,4
4 J=J-M
M=M/2
IF(M-2)5,3,3
5 J=J+M
MMAX=2
6 IF(MMAX-N)7,10,10
7 ISTEP=2*MMAX
THETA=6.2831853/FLOAT(ISIGN*MMAX)
SINTH=SIN(THETA/2.)
WSTPR=-2.*SINTH*SINTH
WSTPI=SIN(THETA)
WR=1
WI=0
DO 9 M=1, MMAX, 2
DO 8 I=M, N, ISTEP
J=I+MMAX
TEMPR=WR*DATA(J)-WI*DATA(J+1)
TEMP1=WR*DATA(J+1)+WI*DATA(J)
DATA(J)=DATA(I)-TEMPR
DATA(J+1)=DATA(I+1)-TEMP1
DATA(I)=DATA(I)+TEMPR
8 DATA(I+1)=DATA(I+1)+TEMP1
TEMPR=WR
WR=WR*WSTPR-WI*WSTPI+WR

```



```
9      WI=W1*WSTPR+TEMPR*WSTPI+W1  
        MMAX=ISTEP  
        GO TO 6  
10     RETURN  
      END
```

## VITA

The author, James Lester Kreamer, was born April 24, 1955. His undergraduate work was done at Southern Illinois University in Carbondale and Northern Illinois University in Dekalb, where he was awarded a Bachelor of Science Degree in Geology in December, 1980. He was employed by the U.S.G.S., Woods Hole. He is currently employed by Mobil Oil Corporation as a geophysicist and is a candidate for a Master of Science Degree from the University of New Orleans in Applied Physics.